

## Nuclear Constitution and the Interpretation of Fission Phenomena

DAVID LAWRENCE HILL\*

*Vanderbilt University, Nashville, Tennessee, and Los Alamos Scientific Laboratory, Los Alamos, New Mexico*

AND

JOHN ARCHIBALD WHEELER†

*Princeton University, Princeton, New Jersey, and Los Alamos Scientific Laboratory, Los Alamos, New Mexico*

(Received October 14, 1952)

An attempt is made to correlate in a unified picture the features of the empirical evidence on nuclear constitution, some of which appear to require for their explanation the liquid drop model as others require the independent particle picture. As an idealized and exploratory basis for an inclusive description, the extreme saturation assumption has been adopted: potential on a typical nucleon in the nuclear interior nearly independent of the position of the other nucleons, this potential falling off in a small distance at the nuclear surface. In the resulting *collective model* of the nucleus a distinction is made between the nucleonic state of the system—as defined by the states occupied by the individual nucleons—and the state of vibration and rotation of the nucleus as a whole. On quantum-mechanical grounds it is shown how the kinetic energy of this motion receives an explanation in terms of the degrees of freedom of the individual particles. As in the electronic-vibrational-rotational description of molecular constitution, so in the case of the nucleus it is reasonable to think of the sums of the energies of the individual particle states, plus the sum of the interaction energies, as defining a potential energy of deformation as a function of the shape of the system. Different states of the totality of individual particles give rise to different potential

energy surfaces. A given sheet touches one of the surfaces immediately above or below it only at certain isolated “funnels” as in the case of polyatomic molecules. For full validity of the collective model it is necessary that nonadiabatic transitions from one surface to another occur infrequently compared to the frequency of rotation and capillary oscillations, so that these collective motions have a well-defined existence. The mathematical consequences of the collective model have not been explored fully enough to tell whether this condition of self-consistency is fulfilled well or very roughly or not at all for any given excitation energy. The vibrational frequencies correspond in general terms to those predicted by the simple liquid drop model, with, however, certain characteristic quantum mechanical differences. Instances of the Franck-Condon principle have to be accepted, analogous to those in the molecular case. Discussed are some consequences of the collective model or of its liquid drop simplification for energy levels, compatibility of strong neutron capture with individual particle effects in binding, quadrupole moments, alpha-decay, fission thresholds, photofission, spontaneous fission, asymmetry in nuclear fission, hydrodynamics of the division process, fission alpha-particles, and fragment excitation.

### I. THE LIQUID DROP AND THE INDEPENDENT PARTICLE

**F**ISSION is unusual among nuclear processes. The division of a many-particle system into two equal fragments is beyond explanation in terms of the movement of a single nucleon, or any small number of nucleons. In evidence is the collective behavior of the nucleus as a whole. This behavior has been idealized in the liquid drop model. The nuclear substance is compared with a nearly incompressible fluid, of almost uniform volume density of electrification, with an approximately constant energy of binding per particle, except as modified (1) by the electrostatic energy of interaction of the different portions of the fluid and (2) by the deficit of binding of the incompletely surrounded particles at the surface—a deficit proportional to the extent of the surface, and therefore responsible for the phenomenon of a surface tension, as in ordinary liquids.<sup>1,2</sup> Such a system is susceptible to deformation (Fig. 1<sup>3</sup>). The stabilizing effect of the surface tension overbalances the potentially disruptive influence of the electrostatic repulsions even for heavy nuclei in their

normal nearly spherical configurations. Consequently a small disturbance will lead to oscillations about the equilibrium shape. However, a marked dumbbell-like distortion will decrease the perimeter available for the action of surface tension proportionately more than it cuts down the electrostatic repulsion of the two halves of the system.<sup>4</sup> Consequently sufficient deformation of a heavy nucleus will cause instability. Then a still greater extension will occur, with electrostatic energy being set free faster than the consumption of energy in the increase of the surface. The movement thus accelerates. Ultimately the nucleus breaks into two or more parts. Thus the act of fission has several stages:<sup>5</sup> (1) raising the nucleus to the given level of excitation by radiation or impact of a material particle; (2) concentration of sufficient of this energy in a capillary oscillation to lead to a critical deformation (Figs. 2 and 3); (3) subsequent automatic growth of this deformation (Fig. 4); (4) scission into distorted fragments; (5) separation of these fragments; (6) de-excitation of the new nuclei.

While fission demonstrates that nucleons can undergo collective modes of motion, evidence has recently been growing<sup>6-9</sup> that nucleons also behave as if they possess individual and nearly independent states of binding—

\* Holder for part of this work at Princeton University of a Socony Vacuum Fellowship, which is gratefully acknowledged.

† Holder for part of this work of a John Simon Guggenheim Fellowship, for which hearty appreciation is expressed.

<sup>1</sup> N. Bohr, *Nature* **137**, 344, 351 (1936).

<sup>2</sup> N. Bohr and F. Kalckar, *Kgl. Danske Videnskab. Selskab, Mat.-fys. Medd.* **14**, No. 10 (1937).

<sup>3</sup> All figures in this paper, together with related discussions, have been placed in the Appendix.

<sup>4</sup> L. Meitner and O. R. Frisch, *Nature* **143**, 239 (1939).

<sup>5</sup> N. Bohr and J. A. Wheeler, *Phys. Rev.* **56**, 426 (1939).

<sup>6</sup> M. G. Mayer, *Phys. Rev.* **78**, 16, 22 (1950).

<sup>7</sup> Haxel, Jensen, and Suess, *Z. Physik* **128**, 295 (1950).

<sup>8</sup> L. W. Nordheim, *Phys. Rev.* **75**, 1894 (1949).

<sup>9</sup> E. Feenberg and K. C. Hammack, *Phys. Rev.* **75**, 1877 (1949).

evidence from spins and magnetic moments, and from the shell structure in nuclear binding energies. We are forced to conclude that two such apparently dissimilar views as the liquid drop picture and the independent particle model are necessarily incomplete parts of a larger unity. Consequently, it must be possible to see and understand the collective aspects of nuclear behavior starting with what we can reasonably say about the properties of individual nucleons. If we justify in this way hydrostatic-theoretic calculations of the general trend with atomic number and atomic weight of the critical energy required for fission, we must at the same time expect that deviations have to be expected about these average values from nucleus to nucleus because of the individual character of nucleon states.

That neither the liquid drop model nor the model of individual nucleons moving in a field of spherical symmetry are separately adequate shows very clearly in the evidence on nuclear quadrupole moments (Figs. 5, and 29). Both pictures fail to account for asymmetries in the distribution of nuclear electric charge nearly so large as many of the typical observed values.<sup>10,11</sup> However, one must recognize that the pressure of a few individual nucleons against the nuclear surface will deform the collective assemblage of nuclear charge (Fig. 6). In this way one estimates quadrupole moments of the observed order of magnitude, as first pointed out by Rainwater.<sup>12</sup>

The lesson of the quadrupole moments is the strength of interaction of nucleons with each other by way of the surface compared to the strength of their direct interactions with each other. In support of this conclusion is the empirical evidence on nuclear binding energies. The energy of a nucleon which has an adequate complement of neighbors within a distance of order  $10^{-13}$  cm is evidently little affected by the presence or absence of more nucleons outside this distance. Neither does this difference much affect the average spacing of the closer neighbors. How this saturation character of nuclear forces comes about is as little understood as the origin of these interactions.<sup>13,14</sup> Nor is it clear why spins, magnetic moments, and finer details of the nuclear binding energies should be consistent with the picture of individual nucleons travelling nearly independently through an average potential. Nevertheless, the evidence requires us to take seriously and to explore the consequences of the idealization in which each particle moves in a potential well, of depth approximately constant throughout the nuclear interior, abruptly falling off within a distance of the order  $r_0$  near the surface.

Finer details of nuclear shell structure have suggested

<sup>10</sup> Walter Gordy, Phys. Rev. **76**, 139 (1949).

<sup>11</sup> Townes, Foley, and Low, Phys. Rev. **76**, 1415 (1949).

<sup>12</sup> J. Rainwater, Phys. Rev. **79**, 432 (1950).

<sup>13</sup> L. Rosenfeld, *Nuclear Forces* (Interscience Publishers, Inc., New York, 1948).

<sup>14</sup> V. F. Weisskopf, Helv. Phys. Acta **23**, 187 (1950); Science **113**, 101 (1951).

the hypothesis that the individual nucleons are subject not only to the nuclear potential field but also to a spin-orbit coupling.<sup>6</sup> Without in any way questioning this fruitful proposal, we can legitimately overlook the existence of such a coupling in a first survey of the relation between the independent particle picture and a more nearly unified description of the nucleus.

## II. THE COLLECTIVE MODEL

We shall explore the *collective model* of the nucleus, based upon the following assumptions.

### Features Regarded as Reasonable in Any Model

- (1) Roughly constant density; one particle per volume  $(4\pi/3)r_0^3$ , with  $r_0 \sim 1.4 \times 10^{-13}$  cm =  $e^2/2mc^2$ .
- (2) Maximum kinetic energy,  $F$ , per nucleon consequently nearly independent of mass number; roughly 24 Mev.
- (3) Distribution of charge over volume uniform to perhaps 25 percent or better.
- (4) Nucleon binding energies generally between 5 and 10 Mev; average potential energy of order of  $-30$  Mev.
- (5) Saturation character of nuclear forces.

### Special Assumptions

(1) Extreme saturation: forces regarded as giving a potential for a typical nucleon in the nuclear interior nearly independent of the position of the other nucleons, this potential falling off in a small distance at the nuclear surface. Contrast this idealization with the opposite extreme model of an impenetrable liquid drop, with forces conceived as sharply dependent on positions of nearby nucleons, whether the particle in question is in the interior or at the surface. In that picture the direct coupling between the particles is envisaged as so large that individual nucleon states have absolutely no well-defined existence. The observations which suggest the notion of nearly independent particle orbits refer mostly to ground states and low, excited states. There circumstances are at work specially favorable to suppress the consequences of nucleon-nucleon interactions which deviate from the saturation average. There appear to be no strong arguments for or against such over-the-background interactions of quite significant strength. Nevertheless, the essential idealization of the collective model is to *neglect* these direct couplings in comparison with the indirect couplings which take place through the intermediation of the movable potential wall. In this respect the picture is a first approximation whose distance from the truth will only be found by full exploration of its consequences. The theory of the collective model is in too early a stage to make a detailed confrontation with experiment.

(2) The state of the whole system is assumed to be specified in first approximation by the states of motion of the individual nucleons—or, as will be seen, by a

particular one out of many potential energy curves—and by appropriate quantum numbers for the rotation of the system and its collective vibration on the potential energy curve in question. In actuality exchange of energy will take place with a finite probability between vibration and individual particle excitations, via couplings of both modes of motion with the wall. These exchanges are not accidental side issues of the collective model—they are the vital part of reaction kinetics. But if they are frequent, compared to the oscillation rate, then the division of energy into a collective part and an individual particle part will not be well defined, and the collective model will lose its sense. We must therefore ask, is the model self-consistent? We have not yet been able to carry through a detailed comparison of the energy exchange rate with the vibration frequency. Rough estimates below suggest the possibility of a borderline situation, with the two rates comparable, and the division into general vibrational and proper nucleonic motion smudged out in part. It is too soon to exclude the possibility that the two rates compare more favorably; or that the numbers go the other way, in which case the usefulness of the collective model will be strictly limited. Unaffected would be general conclusions about the influence of quadrupole moments upon alpha decay, about fluctuations from element to element in height of fission barriers, etc., but most of the anticipated quantitative applications of the model would become nearly hopeless. We have hope enough about the approximate self-consistency of assumption B2 to have gone some distance in investigating in this report certain mathematical details of the collective model and its applications.

#### Nuclei vs Atoms and Molecules

The idealization that we now contemplate for the behavior of nucleons in the nucleus recalls in many ways the motion of electrons in an atomic field. There is a similar justification to speak of individual quantum states and transition probabilities. One is invited to consider the same possibilities for calculation of a self-consistent nuclear potential. Yet there is one important difference of principle. In the electronic case the field of force is dominated by the nucleus. Percentage-wise the field on one electron in a many-electron atom changes little as a second electron sweeps through its orbit. Thus the potential is reasonably thought of as static.

In the nuclear case the *value* of the potential in the interior may perhaps be idealized as unaffected by the orbit of any individual nucleon, and as constant in space and time; but the *boundaries* of that potential as seen by one particle are very greatly affected by the motion of a small number of the other entities. To this extent the potential field has to be considered as fluctuating or oscillating.

Moreover, there is necessarily a kind of momentary self-perpetuation in such displacements of the local

surface from its time average position. New particles coming up are turned back at the same place; in so far as they in turn have an effect on the potential, they keep the effective surface approximately where it already was.

There might be some point to overlooking fluctuations in the position of the nuclear surface if our concern were limited to the ground states of nuclei, where the amplitude of the movements is of the order  $r_0$ .<sup>5</sup> However, it is necessary to consider also states of excitation and fission processes where the amplitude of motion is comparable to the nuclear extension itself. How are we then to describe the quantum mechanics of a system of many independent particles with the characteristic new feature of collective modes of motion?

Illuminating is a comparison of the collective model of the nucleus with a typical molecule. In that case the electrons move rapidly in a field of force whose own alterations—by changes in the internuclear separation—go on at a frequency 10 to 100 times slower. Thus each electron adjusts itself for the most part adiabatically to the potential of the moment. The total energy of the electronic system at each instant provides on the other hand a storehouse of potential energy. On this supply internuclear motion can draw for kinetic energy, and into the pool it again returns energy as the molecular oscillation comes to rest at one or other limit of its amplitude. Similarly the characteristic time of radial motion of a nucleon of average kinetic energy,  $T = 15$  Mev, is

$$\begin{aligned}
 t_{\text{nucleon}} &\doteq \oint \left[ \frac{2T}{M} - \frac{l(l+1)\hbar^2}{M^2 r^2} \right]^{-\frac{1}{2}} dr \\
 &= \frac{2R}{(2T/M)^{\frac{1}{2}}} \left[ 1 - \frac{l(l+1)\hbar^2}{2MTR^2} \right]^{\frac{1}{2}} \\
 &< \frac{2R}{(2T/M)^{\frac{1}{2}}} \equiv \frac{2R}{v} = \frac{2A^{\frac{1}{2}} r_0}{0.18c} \\
 &= 0.3 \times 10^{-21} \text{ sec for } U^{236}, \quad (1)
 \end{aligned}$$

an interval 15 times smaller than the estimated period,

$$\begin{aligned}
 t_2 &= 2\pi\hbar/\hbar\omega_2 \\
 &\doteq 2\pi \times 0.658 \times 10^{-21} \text{ Mev sec}/0.8 \text{ Mev} \\
 &= 5 \times 10^{-21} \text{ sec}, \quad (2)
 \end{aligned}$$

of the lowest mode of capillary oscillation of the same nucleus. Therefore, in the nuclear case also, the states of the particles will be expected to follow the changing configuration of the nuclear boundary with little probability of a nonadiabatic jump from one state to another, provided that the deformation in question is a simple one.

#### Response of Nucleons to Surface

In the case of a complicated distortion of the surface, the particle will require a longer time to feel out the

whole surface, and the adiabaticity condition will not be so readily satisfied. For a surface deformation of order  $n$ , it is reasonable to require that  $(n/2)t_{\text{nucleon}}$  exceed the period  $t_n$  of  $n$ th order disturbances, a condition which plainly cannot be satisfied for disturbances of very high order ( $n > \sim 6$ ). Such disturbances therefore have no well defined significance in the collective model.

A natural limit to the finest irregularities to which the nucleon can respond is clearly the square of the reduced de Broglie wavelength,  $\lambda = \lambda/2\pi$ , of the particle. The time required to make this response will be of the order (number of encounters to touch all regions of the surface  $S$ ) (time between encounters)  $\sim (S/\lambda^2)(R/v) \sim (V/\lambda^3)(\hbar/E) \sim \hbar/\Delta E$ , where  $V$  is the accessible volume,  $E$  is the kinetic energy of the nucleon, and  $\Delta E$  is the typical spacing (Fig. 11) between individual particle levels in a region of the given size. Such a spacing is so small, and the corresponding time therefore so long compared to oscillation periods, that the adiabaticity condition will not allow any discussion of very fine grain irregularities. If two particles are involved, and they interact strongly with each other, then the time required by the two-particle system for response to fine grained surface deformations will be increased by the factor  $V/\lambda^3$ , the number of distinguishable positions for the second particle within the nucleon volume  $V$ . As the number of strongly interacting particles grows larger, the factor in question goes up: by a term  $V/\lambda^3$  for distinguishable particles, less rapidly for particles which satisfy the Pauli principle; but the increase is always such that the time in question is  $\hbar$  divided by the spacing of levels of the total system. Obviously such times would be far too long to allow any adiabatic response to surface oscillations. In other words, the collective model can be justified only if the individual particles interact with each other in a strongly saturated manner, free of dependence on the location of any one particle in the nuclear interior.

As we are accustomed to the idea of molecular potential energy curves as a function of internuclear separation, so we arrive at the notion of nuclear potential energy curve as a function of surface deformation. As there are in the case of a polyatomic molecule several independent coordinates, so in the nuclear case a number of parameters will be required to specify the shape of the surface (Fig. 1). We deal with a potential energy surface. As the minima of the various surfaces do not coincide in the molecular case, neither will they in the nuclear case. The equilibrium quadrupole moment will differ from state to state, according to the special features of the push exerted on the surface by the nucleons in excess of closed shells. The energy of the system will consist of proper nucleonic energy, plus vibrational energy, plus rotation energy.

### Kinetic Energy of Collective Motion

In the molecular case the vibrational kinetic energy comes into evidence in the motion of the nuclei. But

in the nuclear case, what mass is it whose motion gives account of the vibrational kinetic energy? The nucleons? Is not their energy of motion already included in the ordinate of the oscillational potential energy curve itself? That vibrational potential energy is defined by adding up the potential and kinetic energies of all the individual nucleon states calculated for the static configuration of a deformed nucleus. However, such a calculation by its very nature overlooks the slow change in the shape of the nucleus. That alteration in form necessarily implies a bulk transport of mass from one place in space to another. With such a current of matter there is inevitably associated a kinetic energy of the nucleonic system over and above the energy reckoned for the individual nucleons in a static potential well. This additional kinetic energy has to be interpreted as the oscillational energy of motion of the system.

In the quantum-mechanical description (Figs. 7 and 8) the fluid motion comes into evidence in the transport of the nodes of the wave function of the bound nucleon from place to place in harmony with the motion of the surface. In the simpler situations the nodal surfaces move like lines of ink bodily carried along with the irrotational flow of an imaginary liquid. The wave function  $\psi$  of the nucleon at any moment of the slow wall deformation differs from the value  $u$ , which it would have for stationary walls of the same shape by a factor which in this approximate description of the nodal motion may be taken to be  $\exp(-iM\phi/\hbar)$ , where  $\phi$  is the velocity potential of the liquid movement in question. From this circumstance it follows that the kinetic energy of the nucleon is greater than the value it would have had in the absence of wall motion by an amount proportional to the square of the wall velocity. The coefficient of proportionality is identical with that expected for a classical irrotational fluid subject to the same wall constraints.

Particularly interesting among surface changes is one which leaves the shape of the wall unaltered: a pure rotation of the boundary. In this case the amount of matter transported from place to place is set by the size of the departures from sphericity, not by the total mass content of the figure. The effective moment of inertia of the system is likewise far less than would correspond to the picture of rigid rotations. The corresponding rotational levels lie far higher. All of these consequences of a proper quantum picture of nuclear rotations have been pointed out by A. Bohr,<sup>15,16</sup> who has also shown their importance for the analysis of nuclear spins and magnetic moments.

The lower rotational excitations, though far larger than the few tens of kev values which would follow for a rigid nucleus, are still lower than most of the quanta

<sup>15</sup> A. Bohr, Phys. Rev. **81**, 134 (1950).

<sup>16</sup> A. Bohr, Kgl. Danske Videnskab. Selskab, Mat.-fys. Medd. **26**, No. 14 (1952); A. Bohr and B. R. Mottelson, Phys. Rev. **89**, 316 (1953).

of vibrational energy. For this reason it is appropriate to follow the manner of speaking employed in molecular physics and to employ the term "potential energy surface" for the case where the rotational angular momentum either vanishes or is treated as negligible. Higher angular momenta produce modifications in the potential energy surface of the kind familiar from molecular spectroscopy.<sup>17</sup> These rotation-induced modifications in the potential surface will give rise to a number of complicated and interesting effects. They will be disregarded in this paper, however, in comparison with the vibrational and nucleonic-excitational phenomena.

Under certain circumstances the deformation of the surface will displace the nodal surfaces in a manner which is no longer even approximately described by transport in irrotational fluid flow. Then a vortical motion of the carrier fluid must be envisaged. The effect upon the nucleonic wave function (see Fig. 10) may be considered as the quantum analog of the swirls which can be set up in classical fluids. In so far as such effects show up only in one nucleon state out of many, the kinetic energy of the whole system under deformation will not differ greatly from the value expected on the simple liquid drop picture.

### Quantum Description of Collective Motion

Granted that the kinetic energy of the droplet model can be brought into evidence in the collective picture of the nucleus when the wall motion is regarded as given, how is the wall motion itself ever to appear as part of a proper quantum-mechanical description of the  $N$  particle system rather than something imposed from outside? Is not the full quota of degrees of freedom already accounted for without the wall motion? How then can the surface oscillation be described by degrees of freedom which are not there? Physically, we answer, the fluctuations in wall position and the collective character they imply for the  $N$  particle system are an unavoidable consequence of the strong coupling of particles at the nuclear surface. Mathematically we can describe the situation in the following terms. Were the wall position described by externally fixed parameters of the type of  $\alpha$ , then the wave function of the system—apart from unimportant details—would have the character of the determinant:

$$\Psi_{\text{stationary}} = \begin{vmatrix} u(1, x_1; \alpha) & \cdots & \cdots & \cdots & \cdots & \cdots & u(1, x_N; \alpha) \\ \vdots & & & & & & \vdots \\ \vdots & & & & & & \vdots \\ \vdots & & & & & & \vdots \\ \vdots & & & & & & \vdots \\ u(N, x_1; \alpha) & & & & & & u(N, x_N; \alpha) \end{vmatrix}, \quad (3)$$

where the  $u(n, x_j; \alpha)$  represent the individual particle wave functions in a potential well of the given shape.

<sup>17</sup> G. Herzberg, *Molecular Spectra and Molecular Structure* (D. Van Nostrand Company, Inc., New York, 1950).

With a changing but still externally controlled deformation,  $\alpha$  becomes a function of time and the determinant on the right has to be multiplied by the factor,

$$\exp\{-i(M/\hbar)[\phi(x_1) + \cdots + \phi(x_N)]\}, \quad (4)$$

in order to obtain the approximate wave function for the nucleonic system. Here  $\phi$  (expressed in  $\text{cm}^2/\text{sec}$ ) is the velocity potential of the irrotational motion of the imaginary carrier fluid. Conversely, when the nucleons are regarded as determining the potential energy of deformation for the coordinate  $\alpha$ , then the vibrational state of the system—if that could be thought of as having an independent existence—would have the value  $h_n(\alpha)$  appropriate to a quasi-harmonic oscillator. To write the wave function of the whole system as the product of determinant, of velocity potential factor, and of harmonic oscillator function, is illegitimate because there would be too many independent variables in the product for an  $N$  particle system. However, integration of this product with respect to  $\alpha$  yields a wave function

$$\Phi(x_1, \cdots, x_N) = \int \Psi(x_1, \cdots, x_N; \alpha) \times \exp\{-i(M/\hbar) \sum_j \phi(x_j)\} h_n(\alpha) d\alpha, \quad (5)$$

which depends only on the coordinates of the particles themselves.<sup>17a</sup> This function, nevertheless, provides a physically reasonable description of the collective motion in question. (a) It has the proper antisymmetry. (b) It is large in the vicinity of the classical turning points of the oscillation in the sense that presence of one of the particles in a region a little outside the average position of the nuclear surface is associated preferentially with a probability for other particles to be a similar distance outside the average surface; and a similar probability to see one missing at a given distance outside the average surface is associated with an increased likelihood for other nucleons to be absent there; and these correlation probabilities are greatest when the distances in question are comparable with the amplitudes of the corresponding classical surface vibrations. (c) Two of

<sup>17a</sup> The  $\alpha$ -factor in the velocity potential in the exponent (Figs. 7 and 8) is of course to be replaced before integration over  $\alpha$  by its operator value,  $(\hbar/iM\alpha)(\partial/\partial\alpha)$ . Alternatively, if we use for  $h_n(\alpha)$  its J.W.K.B. approximate value, then the exponential operator acting on this oscillator function gives two additive terms. In one of the terms the  $\alpha$ -factor in the exponent is given the value

$$+ \{2[E - V(\alpha)]/M\alpha\}^{\frac{1}{2}},$$

and the exponential function is multiplied into that part of  $h_n(\alpha)$  which represents a wave running to the right; similarly for the other term, where  $\alpha$  is given the opposite sign. Although the wave function of (5) is formulated on the basis of physical reasoning, one can of course alternatively regard  $h_n(\alpha)$  as a quite undetermined function, which is to be so chosen as to make  $\Phi$  the "best possible wave function" in the sense of the Ritz variation principle. How this method of approach can be used to derive from first principles a wave equation for  $h_n(\alpha)$  is a problem identical in principle with the formulation of the method of "resonating group structure" [J. A. Wheeler, *Phys. Rev.* **52**, 1107 (1937)]. In particular, it is not at all necessary that the potential  $V(\alpha)$  be quasi-elastic nor that  $h_n(\alpha)$  be a harmonic oscillator wave function.

the individual determinants which are combined by integration are very nearly orthogonal to each other (Fig. 9) when the displacements  $\alpha_1$  and  $\alpha_2$  to which they correspond differ in normal surface coordinate by an amount of the order  $r_0/N$ , where  $N$  is the number of particles of identical character and  $4(4\pi r_0^3/3)$  is the volume available to one of these particles. In physical terms there is a very high correlation between the probability distribution of the particles and the values of the "hidden" deformation variable  $\alpha$ . This near-orthogonality of the piece-wise functions makes it a reasonable approximation to treat the alpha-variable almost as an independent coordinate.

The deformation coordinate is indeed expressible in terms of the particle variables; the collective model does not contemplate a quite inadmissible increase in the total number of degrees of freedom. How then can we justify a count of the states of the system in which we tally up not only the indices of the individual particle states but also reckon in all the quantum states of the surface oscillators? The system of functions is already complete when the oscillator quantum numbers have specified values. To sum subsequently over vibrational quantum numbers too is to get the same complete set many times over. The solution to this counting paradox is of course that no such extended summations are either intended mathematically or sensible physically. Only the few lowest modes of oscillation have a well-defined physical existence. Moreover, the rate of interchange of energy between vibrational and nucleonic motion depends on the choice of potential energy surface and becomes the greater the higher the degree of excitation of the nucleons in that state. Thus there is a limit of energy beyond which no vibrations of any kind make sense. The problem in the collective model is not that we have too many states but too few. The failure of the description above some tens of Mev has to be accepted physically. A nucleus endowed with sufficient excitation is capable of breaking apart into many individual particles, as evidenced by cosmic-ray stars. The collective model is valid only for not too high excitations.

Conventional expansions of nuclear wave functions in terms of individual particle states in a spherical potential are quite unadapted to describe states of collective oscillation and rotation. Staggering would be the number of kinds of multiple excitations of nucleons required to describe a combination of vibration and nucleonic excitation.

### III. THE DEFORMATION POTENTIAL

#### Definition and Survey Formula

Key to the collective description is the concept of potential energy of deformation: sum of the kinetic and potential energies of the individual nucleons moving inside a nuclear surface of fixed shape. For a first survey of the energy surfaces it is reasonable to make the

following simplifications: (a) Neglect spin-orbit coupling. (b) Treat the internuclear force as having such an extreme saturation character that the potential energy of a particle is constant within the nuclear matter and at the surface suffers a sudden and abrupt rise. The actual wave functions will penetrate into the region of negative kinetic energy to a distance of order  $r_0$ . In dealing with wave functions for bound nucleons it is often convenient to idealize the potential discontinuity at the wall as infinitely high. Then the calculated nucleonic wave function does not penetrate at all outside the wall. This effect—and its consequences in shifting nodal surfaces inside the potential well and displacing energy proper values—can be corrected in a reasonable approximation by an appropriate slight adjustment in the values adopted for nuclear dimensions. For each particle put down then a contribution to the total energy equal to (i) the appropriate eigenvalue of  $\nabla^2\psi_n + (2ME_n/\hbar^2)\psi_n = 0$ , subject to the boundary condition, diminished by (ii) a standard quantity  $B_0$ , of the order of 14 Mev, representing the saturation binding per nucleon. (c) Represent the deficit from saturation binding of the particles at the nuclear surface by a term in the total nucleonic energy of the system which is proportional to the surface area,  $S$ . The constant of proportionality we denote by  $O(\text{potential})$ —not the total surface tension<sup>18</sup>  $O = O_p + O_k \sim 14 \text{ Mev}/4\pi r_0^2$ , of the nuclear matter, but that part of this quantity which has to do with specific nuclear forces. The other part,  $O_k$ , of the usual surface tension has to do with the total kinetic energy of a system of particles bound in a potential, in so far as that total depends upon the *surface*, as distinct from the *volume*, of the potential well. This kinetic part is already included in (b). Whatever differences there are in the dependence of kinetic energy upon deformation magnitude between statistical analysis as typified in the constant  $O_k$  and detailed analysis via summation of eigenvalues  $E_n$ , the latter is to be considered the more nearly definitive. As to the dependence of specifically nucleonic *potential* energy upon deformation, it would likewise be more nearly accurate—if it were practicable—(i) to evaluate the expectation value of the interaction energy with respect to a determinantal wave function built up out of individual eigenfunctions  $\psi_n$  than (ii) to use for  $A$  nucleons the expression  $-AB_0 + O_p S$  as statistical means to estimate this nucleonic interaction energy. The difference between (i) and (ii) is the less the more nearly the forces between nucleons have the extreme saturation character which is assumed in the idealized collective model. (d) The electric energy of interaction between protons could likewise be evaluated via the determinantal wave function of the system, but again it is a reasonably consistent approximation to represent the Coulomb interactions in terms of the electrical

<sup>18</sup> W. J. Swiatecki, Phys. Rev. **83**, 178 (1951); C. F. von Weizsäcker, Z. Physik **96**, 431 (1935); E. Feenberg, Phys. Rev. **60**, 204 (1941).

energy of a uniformly charged fluid contained within the given boundaries:

$$V_e = \rho_e^2 \iint d(\text{vol})_1 d(\text{vol})_2 / 2r_{12}.$$

It would be possible to consider—although we do not do so here—a refinement of this analysis, in which (i) slightly different boundaries are ascribed to the regions in which the neutrons and the protons move,<sup>19</sup> (ii) there are two different potential wells inside which the two kinds of particles move, (iii) neither potential well is of constant depth, (iv) the potential gradient is in such a direction to make the number of protons in the outer half of the nucleus, and the number of neutrons in the inner half, slightly greater than would correspond to a uniform proton-neutron ratio,<sup>20</sup> and (v) oscillations of the neutrons en masse relative to the protons become possible, as discussed by Goldhaber and Teller, and Jensen and Steinwedel,<sup>21</sup> especially in reference to the maximum observed in the nuclear photoabsorption cross section between 10 Mev and 20 Mev.

In summary, the collective model envisages a deformational potential energy function,  $V(\alpha_2, \alpha_3, \dots; n_1, \dots)$ , which depends (a) upon the coordinates  $\alpha_2, \alpha_3$ , etc., which specify the shape of the nuclear surface, and (b) upon the quantum numbers  $n_1, \dots$  of the occupied nucleonic states. This potential energy is taken to have the form

$$V(\alpha, n) = -AB_0 + O_p S(\alpha) + \sum E_n(\alpha) + V_e(\alpha). \quad (6)$$

### Level Density

Interest attaches to the deformation potential both in its dependence upon deformation for a fixed state  $n = (n_1, \dots)$  of the whole nucleonic system, and its variation with quantum state for a specified configuration,  $\alpha$ , of the wall. The variation of potential with wall configuration specifies an energy surface in  $(V, \alpha)$  space. Upon this potential surface the representative point of the system may be considered to move like a marble. This surface ordinarily possesses at least one minimum—a point of equilibrium for the collective oscillations of the nucleonic system. The location of the minimum specifies the normal equilibrium deformation of the nucleus. A first rough impression of the curvature of the potential surface about the minimum is given by identifying  $V(\alpha, n)$ —up to an additive constant and a shift in the origin of  $\alpha$ -space—with the expression  $V_{\text{liquid drop}}(\alpha) = (O_p + O_k)S(\alpha) + V_e(\alpha)$ . For a fixed value of the distortion coordinates,  $\alpha$ , there are many different

<sup>19</sup> J. H. D. Jensen and P. Jensen, *Z. Naturforsch.* **5a**, 343 (1950).

<sup>20</sup> E. P. Wigner, *Nuclear Masses and Binding Energies*, p. 27, part IV of University of Pennsylvania Bicentennial Conference Publication, *Nuclear Physics* (University of Pennsylvania Press, Philadelphia, 1941); E. Feenberg, *Revs. Modern Phys.* **19**, 239 (1947); W. J. Swiatecki, *Proc. Phys. Soc. (London)* **A64**, 226 (1951).

<sup>21</sup> M. Goldhaber and E. Teller, *Phys. Rev.* **74**, 1046 (1948); H. Steinwedel and J. H. D. Jensen, *Phys. Rev.* **79**, 1019 (1950); *Z. Naturforsch.* **5a**, 413<sup>2</sup>(1950).

values of  $V$ , according as the nucleons are placed in one or another set of individual particle states. The spacing of successive potential surfaces therefore goes qualitatively much like the pattern of levels of a spherical  $A$  particle nucleus, with the same statistical relationship between the density of proper values of the totalized energy, and the density of individual particle proper values:<sup>22</sup> (a) The lowest level of the whole system is found by filling up the individual particle levels, starting at the bottom, until all  $A$  particles are accommodated: kinetic energy of the order of  $F \sim 24$  Mev for the highest single particle state; for all particles together,  $\sum E_n \sim \frac{3}{2} AF$ . (b) The first few excited states of the whole system have spacings of the same order as the average spacings,  $\Delta E_F$ , of the levels of a single particle at excitation  $F$ . (c) For excitations  $E_N = \sum E_N$  larger than several times  $\Delta E_F$ , yet very much smaller than  $AF$ , (by which excitation the collective model will already long since have failed) the density of system levels increases roughly exponentially (neglecting power factors) with an exponent  $\pi(8E_N/3\Delta E_F)^{\frac{1}{2}}$ . Consequently the number of potential energy surfaces of the nucleus, like the corresponding number for the case of a polyatomic molecule, increases more and more rapidly with the excitation, nucleonic in the one case, electronic in the other.

The density,  $dZ/dE$ , of states of the collective nuclear model at relevant energies will increase with energy even faster than the density of potential surfaces,  $dZ_N/dE$ , because there are many ways in which the total energy  $E = E_N + E_{\text{vib}}$  can be partitioned between individual particle excitation and collective oscillation:

$$dZ/dE = \int_0^E \left( \frac{dZ_N}{dE} \right)_{E_N} \left( \frac{dZ_{\text{vib}}}{dE} \right)_{E-E_N} dE_N. \quad (7)$$

The density of capillary oscillational levels increases with energy, as Wergeland<sup>23</sup> has shown, at a rate also dominated by an exponential factor, this factor depending upon energy in roughly the same way as the factor for the density of nucleonic levels. However, instead of *comparing* the two expressions for level density, we *combine* them by the indicated integration. The result is to increase the exponent in the level density by a factor in the neighborhood of  $2^{\frac{1}{2}}$  for those

<sup>22</sup> N. Bohr and F. Kalckar, *Kgl. Danske Videnskab. Selskab, Mat.-fys. Medd.* **14**, 10 (1937); V. F. Weisskopf, *Phys. Rev.* **52**, 295 (1937); L. Landau, *Physik. Z. Sowjetunion* **11**, 556 (1937); H. A. Bethe, *Phys. Rev.* **50**, 332 (1936); J. Bardeen, *Phys. Rev.* **51**, 799 (1937); J. Bardeen and E. Feenberg, *Phys. Rev.* **54**, 809 (1938); C. Van Lier, and G. E. Uhlenbeck, *Physica* **4**, 531 (1937); L. Motz and E. Feenberg, *Phys. Rev.* **54**, 1055 (1938); K. Husimi, *Proc. Phys.-Math. Soc. Japan* **20**, 912 (1938); V. F. Weisskopf and D. H. Ewing, *Phys. Rev.* **57**, 472 and 935 (1940); I. N. Sneddon and B. F. Touschek, *Proc. Cambridge Phil. Soc.* **44**, 391 (1948); J. M. Blatt and V. F. Weisskopf, *Theoretical Nuclear Physics* (John Wiley and Sons, Inc., New York, 1952), Chap. VIII, Sec. 6.

<sup>23</sup> H. Wergeland, *Skrifter Norske Videnskaps-Akad. Oslo*, No. 1, (1941); H. Wergeland, *Fysik. Verden* **3**, 223 (1945); see also H. A. Bethe, *Revs. Modern Phys.* **9**, 86 (1937).

excitations not so high that the collective model fails. No breakdown of the total level density according to angular momentum has yet been carried out, nor—therefore—any comparison with the experimental data summarized by Blatt and Weisskopf.<sup>22</sup>

### Crossover and “Slippage”

The connectivity of the many-sheeted potential energy surface is a matter of interest and importance for the collective model. There are two contradictory tendencies at work: (a) Potential surfaces never cross nor even touch provided that the wall configurations under consideration are devoid of all symmetry, whether of rotation or reflection or inversion. Let the representative point of the system be required to stay away from those lower dimensional regions in  $\alpha$ -space which describe shapes with symmetry properties. Also let jumps from one surface to another be ruled out. Then the connectivity of the sheets is such that no path in  $\alpha$ -space, however tortuous, can ever carry the representative point from one sheet to another. The surfaces therefore admit a unique serial numbering according to energy, this *canonical classification*  $V_1(\alpha)$ ,  $V_2(\alpha)$ ,  $\dots$ , being the same for whatever  $\alpha$  it is carried out, provided  $\alpha$  does not lie in the forbidden set of “symmetry points.” (b) For deformations which *do* possess one or more symmetry properties, crossovers from one energy surface to another *do* take place as one or another deformation parameter is varied. Consequently there exist shapes,  $\alpha$ , for which two successive surfaces,  $V_k(\alpha)$  and  $V_{k+1}(\alpha)$ , touch each other. For shapes of appropriate symmetry it is possible for more than two surfaces to meet, the contact point then being of higher order.

When the representative point is allowed freedom to take on all values of  $\alpha$ , it can then by appropriate choice of path work its way up mine-shaft-like from surface to surface, sliding smoothly from  $V_k$  to  $V_{k+1}$  at one point in  $\alpha$ -space, and from  $V_{k+1}$  to  $V_{k+2}$  at another point. We shall use the word “slippage” to describe this fundamental process, which in the theory of polyatomic molecules is known under the name of “radiationless transition,”<sup>24</sup> and the word “funnel” to speak of the potential energy surface near the crossover point.

Qualitative description of the character of the many sheeted potential energy surface requires (a) ascription of a suitable set of index numbers to each crossover point, telling the number of surfaces that meet there and the lowest order in deviations  $\delta\alpha$  from the crossover point in which the degeneracy is removed, (b) giving of the lowest nonzero coefficients in the power series development of the energy values about this point, (c) evaluation of the frequency distribution of transition points in  $\alpha$ -space for a typical potential surface, (d) order of magnitude estimate of the height or depth—energywise—of funnel vertices relative to the immedi-

ately surrounding potential energy surface, (e) order of magnitude estimate of the curvature of a given surface in the large (looking apart from funnels), this quality being described by coefficients of curvature with respect to the several axes in  $\alpha$ -space. To discuss these points in detail would require more study than has been given to the subject so far. However, some glances at the matter from various sides (Figs. 10–25) may give an impression of the situation. In most of the idealized cases to be mentioned, attention has been given to the behavior, not of the surface for total oscillational potential energy,  $V_k(\alpha)$  [Eq. (6)], but of the individual particle energy,  $E_n(\alpha)$ . Of course every crossover in  $E_n(\alpha)$  implies a crossover in  $V_k(\alpha)$ , so that the connection between the two kinds of surface is not remote.

### Survey of Level Behavior

Figure 10 deals with two energy levels of a particle in a rectangular potential well, a configuration of high symmetry, except that this symmetry is destroyed by a slight irregularity in the wall. This irregularity is sufficient to prevent the two energies from crossing, as they would for the symmetric surface. In that case a given function would have a well-defined number of nodal planes normal to each coordinate surface, a number which does not change during the course of the deformation. The energy of the state decreases or increases according as the principal part of the wave propagation is parallel or perpendicular to the direction of stretch—as is to be expected from the corresponding classical problem. Interesting is the contrast with the one-dimensional case. There an expansion in the one direction lowers *all* energies; two levels never cross. A similar character is given to the three dimensional problem by removal of symmetry.

Figures 11 and 12 connect the discussion of the single-nucleon curves  $E_n(\alpha)$  with the total potential curves  $V_k(\alpha)$ . The curves of Fig. 12 give the closest over-all analogy at this moment available to the potential surfaces for the collective nuclear model. However, it should be noted that Fig. 12 represents a cross section through the energy surfaces along an abnormal line in deformation space; namely, a slice which cuts all surfaces in such a way as to reveal their crossovers. Were an irregular deformation superposed on the distortion shown, then every crossover would be replaced by a curve such as shown in Fig. 10. Noteworthy is the qualitative connection of the irregularly scalloped potential energy curves with the smooth curve predicted by the statistical concept of kinetic surface tension. Zero potential energy contribution to surface tension has been assumed in this simple example, and also zero electrostatic energy. One sees that the statistical concept of a constant surface tension is limited in accuracy.

Frequency of crossing of individual particle energy levels is easily estimated. Stretch of the system in one direction by a fractional amount  $\alpha$  raises or depresses levels of energy  $F$  by an amount of the order  $F\alpha$ ,

<sup>24</sup> E. Teller, J. Phys. Chem. **41**, 109 (1937); see also J. von Neumann and E. P. Wigner, Physik. Z. **30**, 467 (1929).

according as the propagation vector is primarily perpendicular or parallel to the stretch axis. The average spacing of levels of a particle without spin at the  $(A/4)$ th level—this level having energy  $F$ —is of the order  $8F/3A$  (Fig. 11). Consequently an increase in  $\alpha$  of the order  $1/A$  will on the average suffice to make a given level cross one more of the levels originally below or above it—provided that the symmetry of the surface allows crossings.

Considerable can be said about single particle energy levels within an ellipsoidal wall. Inequality of the three axes (Fig. 13) removes rotational symmetry and leaves the configuration invariant with respect only to inversion and reflection. Figures 14–18 illustrate the level splitting brought about by small ellipsoidal deviations from sphericity. Larger deviations, leading all the way from sphere to fission, are considered in Figs. 19–22—at the price of having to make the wall axially symmetric, and therefore having to deal with the atypical case of many crossovers.

The relation between individual particle levels and system levels is further illuminated by Fig. 23. This diagram shows how the quadrupole-producing force for nearly spherical nuclei rises to a maximum when the number of nucleons is about right to give a half-filled shell. This diagram will not be valid for substantial deviations from symmetry, for then levels change their character, as seen in Fig. 10 and Figs. 19–22. More about splitting of single particle levels and behavior in the large of system levels is seen in Figs. 24–25. The irregularities in the totalized potential energy curve for a system of many particles will not be expected to be greater in order of magnitude than the bumps in the potential energy curve for the highest individual particle state. The rise of a lower one of the filled states to an inverted funnel and the fall of a next higher surface to a mating upright funnel represent perturbations which when added together largely cancel out.

#### IV. QUADRUPOLE MOMENTS IN THE GROUND STATE

Figure 26 discusses the qualitative dependence to be expected for quadrupole moment as a function of degree of shell-filling so long as the deformations in question are not large enough to carry the system past a funnel. Still sticking to this restrictive condition on the size of distortions, Fig. 27 discusses possible consequences of the existence of two well separated minima in the potential energy surface for the ground state of the system. While passage of a heavy nucleus through a high barrier of this kind might conceivably require a time exceedingly long in comparison with characteristic nuclear times, passage around the barrier can take place with greater facility in the  $\alpha$ - $\gamma$  plane (Fig. 28) through a sequence of ellipsoids with three unequal axes. Knowledge of nuclear deformation potential energy surfaces is far too scanty as yet to allow any well-founded

discussion of energies or lifetimes of such deformation-isomeric states.

Figure 29 recalls the empirical evidence on periodicity in nuclear quadrupole moments. Here too it would be inappropriate to carry out any detailed discussion of the correlation between the observational data and the model without a more detailed knowledge of the deformation potential energy surface than is now available (see forthcoming paper by K. W. Ford on this point).

Quadrupole moments of the sizes now already well-attested experimentally will have very substantial consequences for alpha-decay phenomena, as indicated in Figs. 30 and 31. Likewise they must wash out the minima in nuclear diffraction scattering (Fig. 32), an effect which it would appear possible to observe granted a primary beam of sufficiently short wavelength, sufficiently well defined in energy and in direction of incidence. Asymmetries in nuclear shape, far from being isolated phenomena, are seen to connect closely with important questions of principle in nuclear physics. It is evidently important for the development of nuclear physics to learn the quadrupole moments of many more nuclei, particularly among the heavy elements and alpha-emitters. In this connection diffraction scattering, anomalies in alpha-decay half-lives (Fig. 31), in isotope shift,<sup>25</sup> and level splittings in the muresonic Chang<sup>26</sup>  $K$ -radiation offer additional means to increase the experimental evidence.

#### V. RATE OF EXCHANGE OF ENERGY BETWEEN OSCILLATION AND NUCLEONIC EXCITATION

##### Cross Section for Slippage

The distinction is not sharp between deformations with complete lack of symmetry and complete ordering of energy levels on the one hand, and on the other hand deformations of high symmetry with energy levels crossing each other. The most relevant illustration is the probability for a jump from the lower potential energy surface to the upper one when the system executes an axially symmetric elongation upon which is superimposed a small amount of an ellipsoidal deformation of each cross section of the figure away from its otherwise circular form. The two energy levels in question would cross were the elliptical deformation absent. The actual coupling splits the levels as shown in Fig. 33. It follows that if the elongation were carried out very slowly the system would remain on the lower potential curve as previously discussed. However, if the time of passage through the critical region is comparable with, or shorter than, the minimum time  $\hbar/(E_{\text{up}} - E_{\text{low}})_{\text{minimum}}$  associated by quantum mechanics with the splitting, then the jump from the lower state

<sup>25</sup> L. Wilets, Phys. Rev. **87**, 1018 (1952).

<sup>26</sup> W. Y. Chang, Revs. Modern Phys. **21**, 166 (1949).

to the upper state can occur with appreciable probability (Fig. 34).<sup>27</sup>

The possibilities for a nonradiative transition are seen in more detail in Fig. 35, which is a representation of the two potential surfaces near their conical point of contact. Figure 36 describes one of the limiting cases of leakage from the upper funnel down to the lower one, or the reverse process. The considerations<sup>24</sup> of Fig. 35 lead to a formula,

$$\sigma = (\hbar\dot{\alpha}/s)^{\frac{1}{2}},$$

for the cross section for a collision with the cone with transition from lower to upper surface ("slippage"). Here  $\dot{\alpha}$  is the speed of motion of the representative point, regarded classically, while  $s$  represents the slope of the cone (energy per unit of deformation), the cone itself being here taken for simplicity to be right circular. The system point continues its motion in the  $(\alpha, \gamma)$  deformation space after this switchover as before. However, a part of the energy which was previously available in the form of vibration has now gone into nucleonic excitation as the system moves on the higher potential surface. Such radiationless switches near points of contact between two potential surfaces give the means for pure nucleonic excitation to go into vibration; for oscillations in turn to be damped and thereby to raise the nucleonic energy; and for all these exchanges of energy to take place in a relatively smooth manner, without discontinuous changes in velocity or deformational potential energy.

We evidently can view the collective model as being internally self-consistent for those energies and states of excitation—if any—for which the probability of slippage out of the given potential surface is substantially less than one during the time of one oscillation. Even if the contrary is true and the characteristic time to make one slippage is *short* compared to the vibration period, the model will still be consistent provided that the *fractional* change during one period in the energy available for oscillation is small compared to this energy itself. In other words the general requirement for consistency is that the coefficient of fractional "damping" per period must be small compared to unity.

"Slippage" evidently constitutes the elementary act in a viscous phenomenon. This primary mechanism is of course reversible, as in the case of all frictional processes. Any irreversibility comes from asymmetry in time of the initial conditions. Consider for example the case where the representative point oscillates rapidly and with large amplitude on the lowest potential energy surface. The partition between nucleonic excitation and oscillational energy is as one sided as it can possibly be. Then the statistical result of slippages sometimes up, sometimes down, will on the average be a degradation of much of the vibration into nucleonic excitation. If the collective model is self-consistent, then this damping must be small enough to be susceptible to a statistical

description, with an appropriate kind of macroscopic friction coefficient. In contrast to most familiar physical systems, the present one has a quite restricted number of degrees of freedom. Consequently degradation of the energy cannot continue indefinitely. Statistical fluctuations in the distribution of energy over the degrees of freedom will go on until a given one of these modes of excitation will have accumulated all or a large part of the maximum available amount. When the nucleus has sufficient energy, the accumulation may take place on the lowest mode of capillary oscillation and lead to fission; or the energy may pile up in excitation of one nucleon, followed by neutron emission. In either case, the energy concentration process will have a history which is the reversal in time of the corresponding dissipation process. If there are circumstances when the dissipation is describable by an appropriate friction coefficient, then the reverse concentration of energy will be describable by a coefficient of the same magnitude and opposite sign.

#### Estimates of Damping

It is too soon to say anything definitive about the magnitude of the dissipation per oscillation cycle, and therefore premature to decide whether the collective model is self-consistent. A first crude estimate may not be amiss, as indicating a few of the many factors that must be taken into account in an ultimate assessment. We shall limit the discussion to collective oscillations in the  $\alpha$ - $\gamma$  plane, i.e., to deformations of order  $n=2$  (Fig. 1). In actuality the representative point of the system moves in a multidimensional space. Its chance of slippage from one potential surface to another might therefore seem to depend upon the number of dimensions taken into account. However, consider the effect of some high order deformation coordinate,  $\alpha_n$ . The characteristic quantum of energy associated with this mode will be large. Therefore it will be reasonable to assume this part of the system to be always in its lowest quantum state. The amplitude of zero-point oscillation will be small. Moreover, per unit of amplitude of the coordinate  $\alpha_n$  the displacement of individual particle levels will be small, because the relevant wave functions do not well feel surface deformations of small wavelength. Consequently the effects of the given high order displacement can be disregarded in a reasonable approximation. In this sense the theory of the slippage rate shows a satisfying invariance with respect to cut-off of the number of dimensions taken into account, provided that this number is large enough. However, it is doubtful that it is sufficient to consider only deformations of order 2, as we shall do. In this case the deformation space is two-dimensional in the dimensionless parameter,  $\alpha$ ; the probability of slippage on near encounter with a funnel is measured by a cross section,  $\sigma$ , one dimensional in the parameter  $\alpha$ ; and the damping

<sup>27</sup> C. Zener, Proc. Roy. Soc. (London) **A137**, 696 (1932).

coefficient is of the form

$$\left(\frac{\text{Damping}}{\text{coefficient}}\right) = \frac{\left(\frac{\text{probability per}}{\text{second of slippage}}\right) \left(\frac{\text{energy change}}{\text{on slippage}}\right)}{\left(\frac{\text{circular frequency}}{\text{oscillational energy}}\right)} \sim \frac{\dot{\alpha}\sigma \left(\frac{\text{number of funnels}}{\text{accessible to oscillator}}\right)}{\omega \left(\frac{\text{area in } \alpha\text{-space}}{\text{accessible to oscillator}}\right)}$$

To evaluate this expression, we shall assume that the potential surface in question has roughly the same overall curvature that is predicted by the simple liquid drop model. Then we have for the order of magnitude of the excursion in  $\alpha$  (Fig. 1) roughly  $\delta\alpha \sim (v + \frac{1}{2})^{1/2} / A^{7/12}$ , where  $v$  is the vibrational quantum number and  $A$  is the mass number; and for the circular frequency,  $\omega \sim 24 \text{ Mev}/\hbar A^{1/2}$ . The slope of a funnel (energy per unit of  $\alpha$ ) we shall assume to be of the order of the Fermi energy,  $F \sim 25 \text{ Mev}$ . The number of funnels accessible to the oscillator is of the order  $A\delta\alpha$ , provided that we limit attention to a low-lying potential surface. About the size of the accessible area in  $\alpha$ -space we have the least information. The simplest assumption is that this area is of the order  $(\delta\alpha)^2$ , though it is easy to imagine shapes for the potential surface which make this number either much larger or much smaller (see Fig. 28). We obtain as an exceedingly uncertain estimate of the damping coefficient:

$$\begin{aligned} &< \sim (\omega\delta\alpha\sigma/\omega)(A\delta\alpha/(\delta\alpha)^2) = A\sigma \\ &= A(\hbar\omega\alpha/\text{funnel slope})^{1/2} \sim A(\alpha/A^{1/2})^{1/2} \sim (v + \frac{1}{2})^{1/2} A^{11/24}. \end{aligned}$$

If we assume instead that the accessible area is of the order constant  $\cdot \delta\alpha$  (normal quadrupole moment; ring shaped region accessible in  $\alpha$ -space), then we find as order of magnitude for the damping coefficient  $\sim (v + \frac{1}{2})^{1/2} A^{-1/4}$ . Without knowing the numerical coefficients, we cannot say whether these numbers are less than one or greater.

"Damping" is one way to speak of the exchange of energy between vibration and nucleonic excitation; another is to ask for the eigenvalues of the energy of the combined system after this coupling is taken into account. This manner of speaking can hardly be expected to be very fruitful in the nuclear case. The number of parts of the system is so great, and the number of ways of dividing up energy between them is so enormous, that it seems beyond reason to trace out all the couplings and their consequences. Figure 37 presents a one-dimensional example of the influence of small and large slippage effect upon energy level pattern. When many degrees of freedom are involved, the treatment of the case of strong slippage would be utterly complicated. That of weaker slippage is obviously much simpler. It corresponds to the notions of the idealized collective nuclear model. The partition between nucleonic and vibrational energy is well defined in first approximation. We limit ourselves to the study of the collective model because there is in sight no other mathematically analyzable picture that makes the

necessary combination of elementary particle model and liquid drop picture. If it should turn out that the slippage rate is too great to make the collective model a self-consistent scheme, then it would seem necessary to content ourselves with a much vaguer conception of the nucleus, but still one that inescapably unites the individual and droplet characteristics.

### Franck-Condon Principle

The molecule-like partition that we envisage between vibrational and nucleonic energy recalls the Franck-Condon principle (Fig. 38) and its many important applications to the field of molecular physics. Analogous consequences for the nucleus will be expected to include vibrational excitation following either nuclear photo-absorption or mu-meson charge exchange reactions or impact of a fast particle that disturbs directly only a single nucleon. Likewise, anomalies in the apparent spacing of nuclear levels will be anticipated from the action of the Franck-Condon principle.

### Wall Coupling as Doppler Effect

The collective model makes the wall the coupling between individual particle energies and oscillatory motion. For this reason it is interesting to examine the coupling in its time-dependent aspects. The shift,  $\delta E_n$ , of a particle level due to a wall displacement,  $\delta\alpha$ , has so far been visualized without reference to the rate at which it occurs:  $\delta E_n = (\partial E_n / \partial \alpha) \delta\alpha$ . Alternatively, the level change can be considered as due to Doppler effect at a moving wall: a change in energy in one reflection at the wall of the order  $\delta_1 E_n \sim (\text{wall velocity/nucleon velocity}) E_n \sim R_0 \dot{\alpha} E_n / v_n$ ; a number of reflections per unit time of the order  $v_n / R_0$ ; and a time equal to  $\alpha / \dot{\alpha}$ ; or a total change  $\delta E_n \sim E_n \alpha$ . Left out of account in this order of magnitude estimate is a numerical coefficient of the order of unity, which will of course be negative if the wave propagation takes place primarily towards a retreating part of the wall, otherwise positive. We are speaking here of a neutron already inside the nucleus being reflected at the wall; but similar considerations apply to a neutron which comes from outside and undergoes a change of wavelength on entry (Fig. 39): then the particle will have less energy than would be expected for a static wall, provided that the wave comes in at a region of expansion of the nuclear surface; conversely at a region of contraction. When the energy of the incident neutron is smaller than the depth of the average potential at the nuclear interior, then the energy change due to the wall motion will

still be of the order  $\delta_1 E_n \sim R_0 \alpha E_n / v_n$ , where  $E_n$  and  $v_n$  are energy and velocity inside the barrier. The mechanism to take energy away from an incident particle and give it to collective oscillation—for later redistribution to other nucleons—is obviously of interest in connection with the neutron capture process (Fig. 40).

### Nucleus as Quantum Fluid

We have encountered in this discussion some of the properties of an unusual idealized quantum fluid. It is considered to be completely transparent internally with respect to motion of the constituent particles, and to receive disturbances solely by way of surface deformations. Its near incompressibility comes about, not by particle to particle push, as in an ordinary liquid, but by more subtle means. It is capable of collective oscillations, but it is the wall which organizes these disturbances, not nucleon to nucleon interactions. Oscillations experience a damping, but the mechanism of the damping is unlike that encountered in ordinary liquids. The liquid can evaporate a particle, but in a way quite different from evaporation from ordinary liquids. The wave function of the particle to come out is spread over the whole nucleus and has energy pumped into it by Doppler effect; it is not concentrated near a part of the surface before emission. The rotational properties of the quantum fluid are quite different from those of ordinary fluids. Altogether one is dealing with a most interesting new form of matter.

## VI. FISSION PROCESSES

### Barriers and Thresholds

In the account of fission given earlier,<sup>5</sup> it was noted that energy imparted to the nucleus by radiation or impact of a material particle becomes redistributed over the whole system and later by a chance fluctuation may be concentrated either on a neutron (evaporation process) or on the mode of deformation which leads to fission. For fission then to take place with appreciable probability it is necessary that the available energy exceed the fission threshold (Fig. 3)—the energy required to produce a critical deformation (Fig. 2). This energy was estimated then, and calculated more accurately later by Frankel and Metropolis<sup>28</sup> by way of the simple liquid drop model. According to this model, the same mode of deformation, when endowed with less energy, will oscillate quasi-periodically, with a characteristic quantum energy shown in Fig. 41, but fission will still be able to occur with a very low probability by way of penetration through the barrier. These predictions about barrier height, oscillation frequency, and tunnel probability will be expected to be qualitatively correct in the liquid drop model, but there will be characteristic differences in detail. The same kind of

TABLE I. Fission thresholds obtained from neutron impact and photofission experiments, compared with thresholds calculated from simple liquid drop treatment, neglecting corrections for polarizability and compressibility. The irregular deviations between observation and calculation are of the order of magnitude to be expected from the size of typical quadrupole moments (Fig. 29).

Target nucleus	Compound nucleus	Neutron fission thresholds		Observed barrier $E_n + B_n = F_n$ (obs)	Calculated <sup>d</sup> barrier $F_n$ (calc)
		Neutron threshold <sup>a</sup> $E_n$	Neutron binding <sup>b</sup> $B_n$		
<sup>90</sup> Th <sup>232</sup>	<sup>90</sup> Th <sup>233</sup>	1.05 Mev	4.9±0.2	6.0±0.2	6.5
<sup>91</sup> Pa <sup>231</sup>	<sup>91</sup> Pa <sup>232</sup>	0.45 Mev	4.9±0.4	5.4±0.4	5.0
<sup>92</sup> U <sup>238</sup>	<sup>92</sup> U <sup>239</sup>	0.92 Mev	4.6±0.2	5.5±0.2	5.5
<sup>92</sup> U <sup>234</sup>	<sup>92</sup> U <sup>235</sup>	0.28 Mev	4.9±0.4	5.2±0.4	4.5
<sup>93</sup> Np <sup>237</sup>	<sup>93</sup> Np <sup>238</sup>	0.25 Mev	5.0±0.4	5.3±0.4	4.2

Target nucleus (=compound nucleus)	Photofission thresholds	
	Observed photofission threshold <sup>b</sup>	Calculated threshold
<sup>90</sup> Th <sup>232</sup>	5.40±0.22	6.21
<sup>92</sup> U <sup>238</sup>	5.18±0.27	4.19
<sup>92</sup> U <sup>235</sup>	5.31±0.27	4.53
<sup>92</sup> U <sup>238</sup>	5.08±0.15	5.24
<sup>94</sup> Pu <sup>239</sup>	5.31±0.25	3.40

<sup>a</sup> See reference 29.

<sup>b</sup> See reference 30.

<sup>c</sup> The tabulated neutron binding energies are obtained by interpolation and extrapolation among the binding energies derived from  $(\gamma, n)$  and  $(d, p)$  reactions, as listed by J. A. Harvey [Phys. Rev. **81**, 353 (1950)], and assuming the systematic deviation due to the 126 neutron shell which these values indicate for the actual binding energies from those predicted by the Weizsacker-Fermi semi-empirical mass formula [E. Fermi, *Nuclear Physics* (University of Chicago Press, Chicago, 1949), notes by Orear, Rosenfeld, and Schluter; E. Feenberg, *Revs. Modern Phys.* **19**, 239 (1947)]. The calculated fission barriers are taken from the formula of Fig. 3.

<sup>d</sup> The fission barrier formula of Fig. 3 yields the listed values of  $F_n$  when the values of  $\gamma = 1 - x$  are inserted. Here the "fissionability parameter"  $x$  is defined as in Fig. 2 to be  $\frac{1}{2}$  the ratio of Coulomb energy to surface energy of the spherical nucleus,

$$x = \frac{1}{2} \frac{E_c}{E_s} = \frac{1}{2} \frac{\frac{3}{4} (e^2/r_0) Z^2}{4\pi r_0^2 O A} = (Z^2/A)/(Z^2/A)_{\text{limiting}}$$

If we set  $r_0 = \frac{1}{2} e^2/mc^2 = e^2/1.022$  Mev, and  $4\pi r_0^2 O = 14$  Mev [E. Feenberg-Phys. Rev. **55**, 504 (1939); *Revs. Modern Phys.* **19**, 239 (1947)] we get  $(Z^2/A)_{\text{limiting}} = 45.7$ . Because of the uncertainty in these constants, however, we compute  $(Z^2/A)_{\text{limiting}}$  by another method:

With  $\xi_{\text{max}}$  as given in Fig. 3,

$$F_n = (4\pi r_0^2 O) A^{\frac{1}{3}} \xi_{\text{max}};$$

we choose  $x$  to reproduce the experimental value of 5.5 Mev for the fission barrier of <sup>92</sup>U<sup>238</sup>, carrying through the work both for  $(4\pi r_0^2 O) = 13.0$  Mev, as given by the Weizsacker-Fermi formula, and for  $(4\pi r_0^2 O) = 14.0$  Mev, as given by Feenberg's estimate. The resulting values of  $(Z^2/A)_{\text{limiting}}$  are, respectively, 46.78 and 46.45. We do not here make the small correction ( $-0.38$ ) following from the fact that the zero-point excitation of the fission mode diminishes from 0.45 Mev for the spherical form to zero for the form at the peak of the barrier curves of Fig. 3. Noting the insensitivity of these results to the choice of surface energy, we arbitrarily fix the value of  $(4\pi r_0^2 O)$  at 13.0 Mev to compute the barriers listed in the table.

We see that the calculated and the observed barriers differ by more than the experimental uncertainties, the calculated values showing a steeper change with  $Z^2/A$  than the experimental values.

individualities in the potential energy surfaces that cause quadrupole deformations of the order  $\alpha \sim 0.03$  in nuclear ground states will cause fluctuations of fission thresholds of the order of  $\sim 1$  Mev with respect to a uniform dependence on  $Z^2/A$  (Fig. 42). The experimental results<sup>29,30</sup> summarized in Table I show a similar fluctuation about the liquid drop predictions.

<sup>28</sup> S. Frankel and N. Metropolis, *Phys. Rev.* **72**, 914 (1947); see also R. D. Present and J. K. Knipp, *Phys. Rev.* **57**, 751, 1188 (1940); and Present, Reines, and Knipp, *Phys. Rev.* **70**, 557 (1946).

<sup>29</sup> U. S. Atomic Energy Commission Unclassified Document AECU-2040, 1952 (unpublished), compilation of the Atomic Energy Commission Neutron Cross Section Advisory Group.

<sup>30</sup> Koch, McElhinney, and Gasteiger, *Phys. Rev.* **77**, 329 (1950).

### Cross Sections

The dependence upon energy of the cross section for neutron induced fission (Fig. 43) is characterized first of all by a threshold, below which the cross section begins to fall off in a general way exponentially with energy. Above, it rises to an approximate plateau. Writing the fission cross section in the form

$$\sigma_f = \sigma_{\text{geom}} \Gamma_f / (\Gamma_f + \Gamma_n),$$

where  $\Gamma_f$  and  $\Gamma_n$  represent the probabilities per second for the compound nucleus to dispose of its excitation by fission or by neutron evaporation, we have to conclude from the existence of the plateaus that the ratio of  $\Gamma_f$  to  $\Gamma_n$  does not change much, though both rate constants individually are of course rapidly increasing functions of energy. Still another feature of fission cross sections at neutron energies of the order of 8 Mev is a rise towards a new plateau—a rise associated with the possibility for the nucleus to make a "second try at fission, if in the first try it has instead evaporated away one neutron."<sup>31</sup> Aside from these general features, the results collected in Fig. 43 show most interesting irregularities in the lower energy regions in the dependence of fission cross section upon neutron energy. While the shape and density distribution of potential energy curves are irregular, and while these irregularities must react upon the fission cross section, it seems premature to try to trace out the connection any more specifically.

Also the individualities of the potential energy surfaces must have their influence upon the life time for spontaneous fission (Figs. 44 and 45): most important of all in causing fluctuations from nucleus to nucleus in the heights of the fission barrier, upon which the tunneling probability is most dependent; but also important in changing the shape of the barrier as between two nuclei with about the same barrier height. From this point of view one can understand how it is possible for the lifetime<sup>31a</sup> with respect to spontaneous fission of  $U^{235}$  to exceed that of  $U^{238}$  whereas the smooth dependence upon  $Z^2/A$  given by the liquid drop model would attribute to  $U^{235}$  the shorter life.

### Fission Asymmetry

#### *Energy Release not an Explanation*

An outstanding feature of the fission process is the disparity in size of the two fragments (Fig. 46).  $U^{235}$  split by thermal neutrons has 600 times less chance to divide into equal parts than to break up into the most frequent 2:3 mass ratio. The energy release is not markedly different between the different pairs of fission fragments, a point upon which beautiful observations have been made by Brunton and Hanna.<sup>32</sup> Moreover, at the critical moment of passage over the fission barrier, the critical form for uranium (Fig. 2) is calcu-

lated to have still a diameter,  $11 \times 10^{-13}$  cm, as great as that of the copper nucleus. It is difficult to see how a system so far from the actual act of scission can have any feel for, or be influenced by, the energy or nature of the fragments to which it can potentially give rise.

#### *Shell Effects not an Explanation*

Magic number and shell binding effects have been considered as possible causes of fission asymmetry.<sup>33</sup> While we have much to learn about shell structure, the considerations of Sec. II show how greatly the order of levels in a deformed nucleus differs from that familiar from the study of spherical potential wells. Again it is difficult to see how the nucleus in the transition state can feel any potential shell structure in the not yet formed products. And of systematic differences in abundance between fission chains of even charge numbers and odd charge numbers there is yet no trace, much as the energies of even-even and even-odd nuclei differ from each other. There is some suggestion of shell structure in recent more detailed studies of the fission yield curve (Fig. 47), but just this circumstance makes it seem all the more unlikely that the division into two broad mass peaks come from the same cause. Attempts have been made to show<sup>33a</sup> statistically that shell structure determines the most probable division of mass. But any account of fragment abundances would seem unreasonable which overlooks the nature of the transition state, however thoroughly it analyzes the *statistical* weight of the various *final* configurations. A simple counting of statistical factors, with or without an examination of the relative size of the energy release, would for instance suggest that ternary fission should be far more probable than binary division, quite contrary to observation (Table III).

#### *Barrier Penetration not an Explanation*

Passage, not over the fission barrier, but through it, is the process considered in quite another explanation of fission asymmetry put forward by Frenkel.<sup>34</sup> Recalling the expression for probability of barrier penetration<sup>5</sup> in spontaneous fission,

$$\begin{aligned} & \exp \left[ (-2/\hbar) \int \{ 2[V(\alpha) - E] \sum_i M_i (d\mathbf{r}_i/d\alpha)^2 \}^{\frac{1}{2}} d\alpha \right] \\ & = \exp \left[ (-2^{\frac{1}{2}}/\hbar) \int \left\{ \left( \begin{array}{l} \text{potential minus} \\ \text{available energy} \end{array} \right) \right. \right. \\ & \quad \left. \left. \times \left( \begin{array}{l} \text{effective} \\ \text{mass} \end{array} \right)^{\frac{1}{2}} d(\text{distance}) \right\} \right], \end{aligned}$$

<sup>33</sup> M. G. Mayer, Phys. Rev. **74**, 235 (1948); G. C. Wick, Phys. Rev. **76**, 181 (1949); K. H. Kingdon, Phys. Rev. **76**, 136 (1949).

<sup>33a</sup> T. D. Newton, Phys. Rev. **87**, 187 (1952); Peter Fong, Phys. Rev. **89**, 332 (1953).

<sup>34</sup> S. Frenkel, J. Phys. (U.S.S.R.) **10**, 533 (1946); also E. Bagge, Z. Naturforsch. **2a**, 565 (1947).

<sup>31</sup> N. Bohr, Phys. Rev. **58**, 864 (1940).

<sup>31a</sup> E. Segré, Phys. Rev. **86**, 21 (1952).

<sup>32</sup> D. C. Brunton and G. C. Hanna, Phys. Rev. **75**, 990 (1949).

he ascribes the greater probability of unequal masses to the smaller value in this case of the reduced mass of the system. However, such a picture does not seem to be relevant in the case of induced fission. There, the nuclear excitation exceeds the critical energy, and passage over the barrier is far more probable than penetration through it. Were the excitation so low that barrier leakage became critical, then the cross section for fission would have a dependence upon energy quite different from that observed. Also the absolute probability of division would be impossibly low. Specifically, we have between 140–94 division and 117–117 splitting a difference in reduced mass of fragments, 56.2 vs 58.5, of one part in 25, or—on the hypothesis in question—a difference in penetration exponent of one part in 50. This difference in exponent is called upon to explain a factor of  $10^{-2}$  in relative probability of symmetrical and unsymmetrical partition. Then the absolute probability of penetration would have to be  $(10^{-2})^{50}$ , and fission could not occur, contrary to observation.

#### *Indications that Saddle Point Configuration is Symmetric*

It has also been proposed as a mechanism giving preference for asymmetric fission<sup>35</sup> that the critical form of unstable equilibrium is itself asymmetric. The potential barrier over which the nucleus must pass is defined, as already illustrated in Fig. 4, by giving the deformation energy in terms of the quantities  $\alpha_2, \alpha_3, \dots$ , which specify the shape of the nucleus. For a nucleus which has just barely enough energy to pass over the fission barrier, one would on a classical picture expect the unrolling of the motion to proceed in a unique way, leading to fragments of well-defined mass. If there are several minima in the potential energy ridge which must be surmounted for fission, one would therefore expect several different possibilities for the course of fission, each leading to a specific and distinct mass division. This deterministic classical picture of what happens after passage over the fission barrier is, of course, quite untenable. At most it can be taken to suggest that there might be some correlation between the mass division and the shape of the one or more critical forms of unstable equilibrium, which correspond to the one or more conceivable passes over the potential energy ridge. Passage over various passes would occur with relative probabilities depending on the various critical energies,  $E_f$ , and upon the effective temperature,  $T$ , as expected from the usual Boltzmann formula. One might in this way, for example, try to understand why symmetric fission is so improbable at low excitation and why the relative probability for equal division increases with energy of bombardment.

No theoretical argument yet shows that the fission barrier should have this suggested asymmetry. Frankel and Metropolis<sup>28</sup> have explored by ENIAC calculations the shape of the fission barrier and find that a well-

defined saddle point occurs for a symmetric division. The energy of the potential ridge increases, they find, with asymmetric departures from this symmetric critical form. There is no evidence for any other saddle point, symmetric or unsymmetric. Swiatecki<sup>18</sup> has noted that nuclear polarizability and compressibility will change slightly the simple liquid drop dependence of energy on deformation, and has suggested that this effect will work in such a direction to split the symmetric saddle-point into two asymmetric ones. Even in the absence of this Wigner-Feenberg-Swiatecki phenomenon of slight redistribution of electric charge over the nuclear volume, such a splitting of the saddle point will be expected to occur for sufficiently small fissionability parameter  $x$  (proportional to  $Z^2/A$ ) as indicated in Fig. 48. The redistribution effect will move to higher  $x$  the point of first occurrence of asymmetric saddle-point forms. However, the amount of the redistribution effect does not off-hand seem great enough to lead to asymmetric critical forms for uranium; and for still heavier nuclei the calculated critical form approaches closer and closer to a sphere (Fig. 49).

#### *Asymmetry Favored by Shape-Dependent Viscosity*

It is conceivable that a certain symmetry phenomenon in the collective model of the nucleus may also act to favor an asymmetric deformation of the nucleus. For a completely symmetric deformation, individual particle states can be divided into two classes according as the wave function does not change sign on reflection (“gerade”) or does change sign (“ungerade”). For small departures from sphericity both sets of states will be filled approximately to a common energy,  $F$ . As the deformation increases, the gerade states will rise more in energy than the ungerade ones because the one kind of wave function feels the pinch of the necking-off process more than the other. Consequently the energy of the deformed system could be lowered, and fission made easier, if the particles were allowed to move from the higher gerade states into ungerade ones. Such slippages cannot occur for a completely symmetrical deformation, but will readily take place if a sizeable asymmetry is present. Consequently a quite appreciable effect is at work to favor an asymmetric configuration for the critical form.

Whatever the shape of the nucleus at the moment it goes over the barrier, there is room for variations in the division ratio between one fission act and another, granted the same nuclear species and the same excitation energy, just a little above the barrier. There will be a quantum-mechanical spread in the possible paths which can be taken in configuration space, from the moment of surmounting the saddle-point, to the moment of actual scission. A simple way to visualize this effect qualitatively is to imagine the trajectory of the representative point in configuration space to be completely definable classically but the direction of this point at the moment of transmigration to have an

<sup>35</sup> R. D. Present and J. K. Knipp, Phys. Rev. **57**, 751 (1940).

uncertainty of the order of that to be expected from the unavoidable zero-point amplitudes of the simplest modes of capillary oscillation.

*Asymmetry Favored by Inviscid Hydrodynamic Instability*

These unavoidable asymmetries at the moment of passage over the barrier can also lead to large asymmetries if there is any intrinsic hydrodynamical instability at work to magnify the amplitude of the disturbances. Qualitative arguments for the existence of such an instability phenomenon are easily visualized (Fig. 50) and seem to receive some preliminary support from the initial calculations on the subject which have so far been carried out (Figs. 51 and 52). Consequently it seems appropriate to say that there appears nothing paradoxical about the phenomenon of asymmetric fission. On the contrary, the problem that remains is to decide which of the two effects that work in the same direction is the more important quantitatively: gerade-ungerade differences in individual particle wave functions, or hydrodynamic instability.

The more disturbed the nucleus is at the moment of passage over the fission barrier, by reason of more than adequate energy, the more will be the tendency to override the more delicate factors that favor asymmetric fission, and the greater will be the yield of fission fragments of equal mass. Consistent with this view is the experimental evidence on variation of fission yield with excitation of the initially formed compound nucleus (Fig. 53). The ratio of symmetric to asymmetric fission varies qualitatively as one might expect<sup>5</sup> from the usual statistical-mechanical formula  $\exp[-(\text{difference in activation energy})/(\text{temperature})]$  for the ratio of rates of competing processes, where in the nuclear case the temperature goes roughly as the square root of the excitation. The activation energy difference is reasonably interpreted as the extra cost energy-wise of a disturbance of the nuclear surface which pinches in the critical form of unstable equilibrium around its equatorial symmetry plane. Any attempt to evaluate this critical energy difference from the observational material is of course complicated because at high energies one is dealing with a superposition of fission of newly formed compound nuclei, and fission of residual nuclei subsequently formed by evaporation of one or more neutrons. A preliminary estimate for the activation difference, neglecting these complications of identification, gives a value of the order of a few Mev<sup>36,37</sup> which seems not unreasonable.

In spontaneous fission the distribution of fragment sizes will have as little directly to do with considerations of energy release as in induced fission. Energy factors can be expected to apply only to passage through the critical state. The sequence of events which follow will be expected to go as in induced fission. The final result

will therefore depend upon the same kind of mirror symmetry and hydrodynamic instability effects. We should therefore not expect any great differences between the fragment distribution and neutron release in case of spontaneous fission and of induced fission with moderate excitation, in conformity with the observations<sup>38</sup> (see Fig. 46 and caption).

*Angular Distribution of Fragments*

From the moment of input of energy into the nucleus by radiation or impact of a material particle to the time when that energy is concentrated on the mode of deformation that leads to fission, the simple liquid drop picture envisages a complicated many-stage process of redistribution of energy to go on in the nucleus. Consequently it would be expected on that impenetrable-fluid idealization that correlation should be practically absent between direction of incidence of the energy and direction of emergence of the fission fragments. On the contrary, Halpern and Winhold<sup>39,40</sup> find a correlation in the photofission of thorium between the two directions, separated by an angle  $\theta$ , of the form  $1+b \sin^2\theta$ , where in preliminary measurements  $b$  is  $0.3 \pm 0.1$  for 16-Mev radiation and about four times that value at 8 Mev. What does the collective model predict? According to the Franck-Condon principle (Fig. 38), starting with the nucleus in its ground state, the act of absorption will lead to an excited potential energy surface, with nuclear wall still in its original configuration—which is ordinarily not at all a shape of equilibrium for the new potential energy surface. Consequently a very sizeable oscillatory motion will ordinarily be set up, making excursions on both sides of the new shape of equilibrium. If the departures from sphericity are great enough in the course of this motion, then the restoring force will weaken, the potential curve will bend over, and one will be dealing, not with a periodic phenomenon, but with passage over a potential barrier leading to fission. On this view the correlation between the act of absorption and the act of fission is much more direct than in the picture of a nearly impenetrable liquid drop. Of course we are discussing an idealized version of the collective model, in which the viscous forces due to slippage phenomena are neglected. How much these frictional effects complicate the picture is not yet clear theoretically; from the experiments themselves one can hope to learn more about this point.

The qualitative nature of the directional correlation in photofission suggests the following very schematic and tentative picture: (1) The gamma-ray is absorbed

<sup>38</sup> Hanna, Harvey, Moss, and Tunnicliffe, *Phys. Rev.* **81**, 466 (1951).

<sup>39</sup> Winhold, Demos, and Halpern, *Phys. Rev.* **87**, 1139 (1952).

<sup>40</sup> I. Halpern and E. J. Winhold, Progress Report of the Laboratory of Nuclear Science and Engineering, Massachusetts Institute of Technology (1952) (unpublished). We are indebted to Professor Halpern and Mr. Winhold for interesting discussions of their results.

<sup>36</sup> Jones, Fowler, and Paehler, *Phys. Rev.* **87**, 174 (1952).

<sup>37</sup> J. L. Fowler *et al.*, *Phys. Rev.* **88**, 71 (1952).

by photoeffect on a single proton. (2) Among all proton orbits those will absorb radiation the most strongly whose angular momenta are greatest, and whose planes are normal to the direction of the incident beam. (3) The most probable type of absorption is that in which the angular momentum increases by one unit, the direction of the plane of the orbit remaining unchanged. Points (1), (2), (3) are simple consequences of the theory of absorption of light by a single charged particle. (4) The greater centrifugal force exerted by the now faster moving excited particle pushes out parts of the nuclear wall normal to the direction of the photons. (5) The deformational oscillation generated as a consequence of the Franck-Condon principle therefore leads preferentially to fission in the observed direction.

If this description of directional asymmetry in photofission is correct, then a similar effect should be observed in fission induced by neutrons of 1 Mev or more. However, here the fragments should go preferentially parallel to the direction of incidence. The pressure exerted by the neutron against the nuclear wall in the act of capture (Figs. 39 and 40) will be predominantly such as to produce an elongation of the nucleus parallel to the beam. The application of the Franck-Condon principle to this process goes through otherwise as in the case of photofission.†

How probabilities for the compound nucleus to undergo neutron evaporation or fission depend upon excitation energy and angular momentum, and how fission widths will be expected to vary with passage from the region of tunnel effect to the region of free passage over the fission barrier, and what explanation can be given for irregularities in the dependence of fission cross section upon energy, are interesting questions on which nothing will be said here now from the standpoint of the collective model.

### Charge Division

Another feature of the act of division is a certain variation from fission act to fission act in the number of protons which come off in a fragment of given mass number. In connection with these charge fluctuations,

† *Note added in proof*:—The angular distribution of fragments from neutron-induced fission has been studied, since this paper was written, by W. C. Dickinson and J. E. Brolley, Jr., of the Los Alamos Scientific Laboratory [reported January 24, 1953, at Cambridge Meeting of the American Physical Society]. They have measured the ratio of fission fragments moving parallel to those moving perpendicular to the beam of incident neutrons, both for thermal and for 14-Mev neutrons, with results in agreement with the above expectations:

Target nucleus	$I(0^\circ)/I(90^\circ)$	
	thermal	14 Mev
$^{92}\text{U}^{238}$	$1.00 \pm 0.08^a$	$1.32 \pm 0.11^a$
$^{92}\text{U}^{235}$	$0.99 \pm 0.09$	$1.27 \pm 0.17$
$^{90}\text{Th}^{232}$		$1.53 \pm 0.21$
$^{92}\text{U}^{238}$		$1.53 \pm 0.17$
$^{93}\text{Np}^{237}$		$1.20 \pm 0.13$

<sup>a</sup> Statistical errors defined to give 0.95 chance of bracketing true values.

it is evidently quite inappropriate to consider the dividing nucleus as a fluid continuum of precisely defined charge to mass ratio. But it would be even more misleading to view the two kinds of nucleons as behaving like gas molecules, with quite independent motions, susceptible to simple statistical considerations. On the contrary, the energy of correlation of the neutrons and protons is quite high; and a separation of the two sorts of entities can be considered to come about at the moment of splitting only as a result of their specific quantum-mechanical zero-point relative motions.

To give a treatment of the zero-point motions sufficient for an accurate analysis of the charge fluctuations would of course be most difficult. However, an approximate estimate may be obtained by considering only that mode of motion which Teller and Goldhaber<sup>21</sup> call the "dipole vibration" of the nucleus, a movement of all of the protons of the nucleus relative to the neutrons. They give reasons for assigning to this vibration the marked maximum in the photofission cross section—and presumably also of the photoneutron cross section—observed for U and Th at about 17 Mev. The frequency and the restoring force associated with this motion are high, but not so high as to exclude some variability in the number of protons which go into a given one of the two fragments. Thus, comparing the actually rather complicated scission form with a sphere, and denoting the displacement of neutrons relative to protons by  $x$ , we have for the excess of protons on the left-hand fragment the number

$$\delta Z = [Z/(4\pi R^3/3)]\pi R^2 x,$$

and for the relative probability of a displacement  $x$  the usual quantum mechanical expression

$$\exp[-M_N M_Z (M_N + M_Z)^{-1} \omega x^2 / 2\hbar].$$

Thus, the charge variation at half-maximum probability in the present approximation has the form

$$\begin{aligned} \delta Z_{\frac{1}{2}} &= (3Z/4)(0.693\hbar^2/M_{\text{red}}R^2\hbar\omega)^{\frac{1}{2}} \\ &\sim 69(0.693 \times 0.010 \text{ Mev}/17 \text{ Mev})^{\frac{1}{2}} \\ &\sim 1.38. \end{aligned}$$

Two corrections have to be applied to this result, in opposite directions. First, higher modes of vibration up to an order  $n \sim A^{\frac{1}{3}} = 6$  have to be considered, on which account there should be introduced inside the square root above a further factor qualitatively of the form

$$1 + \frac{1}{2} + \frac{1}{3} + \dots + \frac{1}{6}.$$

Second, the quantum energy 17 Mev in the denominator should be substantially increased because a given movement of charge will be more expensive of energy for the deformed nucleus than for the approximately spherical system. That this second correction will outweigh the first, and reduce the expected charge fluctuation to one unit or less in  $\delta Z$ , is the conclusion suggested by examination of the elongated shape of the  $U$  nucleus as

TABLE II. The known delayed neutron half-lives, energies, and yields.<sup>a</sup>

Half-life	Energy kev	Yield (percent relative to total neutron emission)	Reference
0.05 sec		0.025	42
0.43	420	0.085	42
1.52	620	0.241	42
4.51	430	0.213	42
22.0	560	0.166	42
55.6	250	0.025	42
3 min		$8 \times 10^{-7}$	43
12		$3 \times 10^{-9}$	43
120		$1.3 \times 10^{-10}$	43
		Total: 0.755 percent	

<sup>a</sup> Delayed neutrons associated with fission to the extent of roughly one per hundred events were interpreted in an earlier discussion (reference 5) as follows: (1) fission occurs; (2) fission fragment is deexcited by radiation; (3) the fragment undergoes beta-decay; (4) in the case of certain fission products the energy release in the beta-decay is greater than the binding of the neutron in the product nucleus; (5) in these cases the product nucleus is occasionally left excited and promptly emits a neutron. The average kinetic energies of some of the delayed neutron groups have in the meantime been measured and found to be consistent with this explanation. Some of the beta-active sources have been identified radiochemically. In these cases the odd-even changes are such as to permit beta-decay processes with more energy release than the neutron binding.

it approaches the point of scission (Fig. 2). A final source of fluctuations has to be considered, due to release of secondary neutrons. Fission chains of mass number  $A$  originate partly from fragments of mass  $A+n$  which have given off  $n$  neutrons, and partly from products of mass  $A+n+1$  which have lost  $n+1$  secondaries. A difference of mass of  $\pm 0.5$  in the relevant part of the nuclear table corresponds to a change in charge of about  $\pm 0.2$ . Recalling that one has first to square the magnitudes of independent fluctuations before combining them, we conclude that we can neglect the influence of variability in secondary neutron release in an account of charge fluctuations. Then it appears that we have a reasonable order of magnitude account of the fluctuations in length of given fission chains,

$$\delta Z_{\frac{1}{2}} = 1.0,$$

observed by Glendenin, Coryell, and Edwards.<sup>41</sup> It is therefore reasonable to conclude that these variations in charge distribution are indeed directly attributable to the unavoidable quantum zero-point uncertainties in the positions of the nucleons.

### Fission Neutrons

Emission of a neutron associated with fission requires an amount of energy for which three sources are available: hydrodynamic disturbances at the moment of scission; excitation of the fragments after division; and re-excitation of stopped fragments following beta-decay. The last effect is well known to give a reasonable account of the phenomenon of delayed emission (Table

<sup>41</sup> Glendenin, Coryell, and Edwards, *Radiochemical Studies, The Fission Products* (McGraw-Hill Book Company, Inc., New York, 1951), Paper No. 52, National Nuclear Energy Series, Plutonium Project Record, Vol. 9, Div. IV.

II)<sup>42,43</sup> responsible for somewhat less than a percent of all the secondary neutrons from the fission of uranium. The other 99+ percent of neutrons are observed to come off within less than  $10^{-12}$  sec of the moment of fission and must be attributed to the first two processes of excitation.

Between hydrodynamic disturbances just before scission, and just afterwards, it is difficult to make any simple comparison of importance in exciting a neutron to a level sufficient for escape. The rapid change of wall shape throughout the whole scission process via Doppler effect will raise the energy of neutrons with suitably oriented propagation vector. However, it may well be that the final stages of raising of energy to the emission threshold occur only as the newly formed and quite distorted fission fragments relapse towards a spherical form. On this basis it will be expected that most of the prompt neutrons will be given out after that particular stage of the fission process which we name scission. Moreover, the walls of both fragments being at that time in rapid contraction along the axis of fission, the Doppler effect in internal nucleonic reflections will be in such a direction as to give maximum energy to neutrons with propagation vector parallel to this axis. It thus seems reasonable to expect maximum neutron emission parallel to the axis of fission.

The observed distribution in energy of fission neutrons (Fig. 54) is qualitatively consistent with the picture of isotropic emission from moving fission fragments, with a distribution in energy in the moving frame of reference of the general character to be expected on the evaporation picture,  $dN/dE \sim E \times \exp(-E/T)$ . It is primarily simplicity that has suggested this form of representation in the past, and there is little doubt that a substantial preference for emission parallel and antiparallel to the line of fragment motion is also compatible with the observed distribution in energy.

The observations on angular distribution fall into two classes. De Benedetti and collaborators<sup>44</sup> have measured the angular correlation of prompt neutrons from the neutron-induced fission of  $U^{235}$ . They find that the number of coincidences is fairly constant from  $30^\circ$  to  $90^\circ$ , and increases by a factor about 2 from  $90^\circ$  to  $180^\circ$ . Assuming that neutrons go mainly in the direction of the fragment from which they are emitted, they conclude that fission neutrons are emitted preferentially by opposite fragments, and that there are at least twice as many pairs of neutrons emitted from opposite fragments as from the same fragment.

Fraser<sup>45</sup> has measured the correlation of fast neutrons with collimated fission fragments, finding  $4.35 \pm 0.15$  times as many neutrons parallel to the line of fission as

<sup>42</sup> Hughes, Dabbs, Cahn, and Hall, *Phys. Rev.* **73**, 111 (1948).

<sup>43</sup> Kunstadter, Floyd, Borst, and Weremchuk, *Phys. Rev.* **83**, 235 (1951).

<sup>44</sup> de Benedetti, Francis, Preston, and Bonner, *Phys. Rev.* **74**, 1645 (1948).

<sup>45</sup> J. S. Fraser, *Phys. Rev.* **85**, 726 (1952).

perpendicular to that direction; and finding indication that the light fragment emits about 30 percent more neutrons on the average than does the heavy one. It is premature to try to say from the observations whether there is an indication of preference *in the moving frame of reference* for emission parallel to the line of fission.

### Tripartition

Another interesting phenomenon is the occasional observation of alpha-particles (Fig. 55) and other light nuclei in fission (Table III).<sup>46-54</sup> For this effect, a simple explanation offers itself in terms of the liquid drop model of nuclear division. From classical hydrodynamics it is well known that the disintegration of a liquid jet into drops leads to the formation between these fragments of tiny droplets. Likewise in the case of nuclear fission it is not surprising to find some portion of the nuclear substance set free between the fission fragments in the act of scission. It is necessary to distinguish between alpha-particles, protons and neutrons. Of these only the alpha-particles represent nearly saturated nuclear matter, and only they are energetically capable of emerging from the original nucleus already in its unexcited state. But an alpha-particle at the surface of the original nucleus is far below the level of the Coulomb potential, on account of the coupling to its surroundings. In contrast, an alpha-particle in the region of scission lies at the point of maximum Coulomb potential, and yet has less than the normal amount of nuclear matter immediately around it with which to form bonds. This particular alpha-particle has in effect been raised to a point but little lower than the top of the barrier, by means of the changes of nuclear form which took place up to the moment of scission. An alpha-particle in such a position will have a significant probability to pass through the barrier. Thus it is reasonable to connect up the energy of the observed alpha-particles with the value of the electrostatic potential in the small interval between the newly formed fission fragments. On this view the alpha-particle will be expelled in a direction roughly perpendicular to the line of separation with an energy of about 20 Mev. The unequal repulsion by the lighter and heavier fission fragments will be responsible for some deviation from perpendicular emission, as observed.

Similar effects will be expected for other light nuclear fragments, except that here the relevant potential barriers will be higher, and emission probabilities lower.

TABLE III. Modes of ternary fission.<sup>a,b</sup>

Compound nucleus	Mass of third particle in atomic mass units	Range in c.a.e.	Energy in Mev	Binary fissions per event	Reference	
U <sup>235</sup>	+slow neutron	40 to 90	>40	7×10 <sup>6</sup>	46	
U <sup>233</sup> U <sup>235</sup>	+slow neutron	13±3 13±3	0 to 0.8 0 to 0.8	75 75	47 47	
Th <sup>232</sup>	+2.5-Mev neutron	8	20	10 <sup>3</sup> to	48	
U <sup>235</sup>	+23-Mev photon	8	20	10 <sup>4</sup>	49	
U <sup>233</sup> U <sup>235</sup> Pu <sup>239</sup>	+slow neutron	4 4 4	10 to 50 10 to 50 10 to 50	5 to 25 maximum frequency at 15	400 500 450	50 50 50
Th <sup>232</sup> U <sup>238</sup>	+2.5-Mev neutron	4 4	5 to 23 5 to 21	~400 ~400	51 51	
Th <sup>232</sup> U <sup>238</sup>	+23-Mev photon	4 4	17	~400	52 53	
U <sup>235</sup>	+slow neutron	1	up to 2.1	5000	54	

<sup>a</sup> The range is given in c.a.e. (cm of air equivalent). One c.a.e. is an absorptive unit equivalent, for range diminution of an alpha-particle or proton, to one cm of air at 15°C and 760 mm Hg pressure.

<sup>b</sup> Following the original work by Alvarez (see reference 54) many modes of fission into more than two charged fragments have been identified. The earliest published measurements [L. L. Green and D. L. Livesey, *Conference on Physics of Fundamental Particles* (Cambridge University Press, 1946); Tsien, Chastel, Ho, and Vigneron, *Compt. rend.* **223**, 986, 1119 (1946); **224**, 272 (1947); Farwell, Segrè, and Wiegand, *Phys. Rev.* **71**, 327 (1947)] identified  $\alpha$ -particles emitted in coincidence with fission. This work was refined and extended [Tsien, Ho, Chastel, and Vigneron, *J. phys. et radium* **8**, 165 (1947); **8**, 200 (1947); L. L. Green, and D. L. Livesey, *Phil. Trans.* **A241**, 323 (1948)] as indicated by the present extensive literature, from which some of the more recent and complete papers are cited for each of the fission modes listed in the table. For the fission alpha-particles it has also proved possible to measure the angular distribution [Wollan, Moak, and Sawyer, *Phys. Rev.* **72**, 447 (1947); L. Marshall, *Phys. Rev.* **75**, 1339 (1949)] which turns out to be near-Gaussian about 82° (relative to the light fragment) with a half-width of 25° (Titterton, reference 52). The infrequency of symmetric tripartition serves to emphasize the principle (which is already apparent in binary fission) that the mass division is primarily determined by the dynamics of passage through the transition forms (Fig. 50) rather than by the total energy content of the final nuclei, which is much lower for the fragments of symmetric ternary fission than for the fragments of binary fission.

When C<sup>12</sup> or He<sup>4</sup> are emitted, the mass division between the heavy fragments is comparable to that observed in binary fission [Allen, reference 50, and L. Marshall, *Phys. Rev.* **75**, 1339 (1949)].

Lines 4 and 5 of the table refer to Be<sup>8</sup> nuclei, which are actually observed as two He<sup>4</sup> particles in small angular separation. Thus from the description of ternary fission follows a process which might be classified as quaternary fission, occasionally reported elsewhere (Tsien *et al.*) as occurring with similar intensity but with all four fragments of mass number greater than 20. However, in this connection see E. W. Titterton [Nature **170**, 794 (1952)], where strong reasons are given to doubt any evidence so far presented in favor of quadripartition.

Emission of protons will be practically forbidden in comparison with alpha-particle emission, because the binding of the particle to nuclear matter—even near the scission neck—places its energy far below the top of the Coulomb barrier. Those protons which are observed (Fig. 56) have rather to be interpreted as due to processes of impact between fission fragments and the stopping material through which they pass. Their energy distribution is consistent with this view, and quite contrary to what would be expected if they came directly from either the dividing system or the fission fragments.

<sup>46</sup> L. Rosen and A. M. Hudson, *Phys. Rev.* **78**, 533 (1950).

<sup>47</sup> K. W. Allen and J. T. Dewan, *Phys. Rev.* **82**, 527 (1951).

<sup>48</sup> E. W. Titterton, *Phys. Rev.* **83**, 1076 (1951).

<sup>49</sup> Goward, Titterton, and Wilkins, *Nature* **164**, 661 (1949).

<sup>50</sup> K. W. Allen and J. T. Dewan, *Phys. Rev.* **80**, 181 (1950).

<sup>51</sup> E. W. Titterton, *Phys. Rev.* **83**, 673 (1951).

<sup>52</sup> E. W. Titterton, (private communication, March, 1950).

<sup>53</sup> E. W. Titterton and F. K. Goward, *Phys. Rev.* **76**, 142 (1949).

<sup>54</sup> D. L. Hill, *Phys. Rev.* **87**, 1049 (1952).

## VII. CONCLUSION

This summary of the collective model of the nucleus and some of its connections with fission phenomena, while not comprehensive, may indicate how liquid drop and individual particle models come naturally together in a larger unity, consistent with experiment; and indicate also how important is the nuclear wall in the exchange of energy within the nucleus.

## VIII. ACKNOWLEDGMENT

To Professor Niels Bohr we are indebted for many fruitful discussions over the past few years of topics

treated in this paper, especially on the unification of the individual particle picture and the liquid drop model, the asymmetry of nuclear fission, and other fission phenomena. Many of these considerations were embodied in an earlier manuscript prepared jointly with Professor Bohr. For Professor Bohr's permission to include these specific parts of the early discussion in the present article, as well as for the hospitality of his Institute on many past occasions, we wish to express our deep appreciation. We also wish to thank the many collaborators we have had in the preparation of figures, performance of calculations, discussion of experimental results, and completion of the manuscript.

## APPENDIX. FIGURES AND DISCUSSION

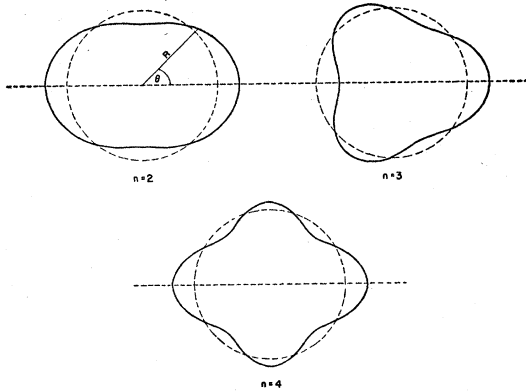


FIG. 1. Independent modes of small oscillation of a liquid droplet.

Illustrated are the first three orthogonal modes of small oscillation for a liquid moving under the constraint of surface tension. Addition of uniform volume electrification, as in the liquid drop model of the atomic nucleus, does not affect the form but does affect the frequency of the orthogonal oscillations, for the decrease in Coulomb energy somewhat offsets the increase in surface energy when the shape deviates from the spherical form of equilibrium.

To evaluate these frequencies of oscillation for, say, the uranium nucleus according to this model, note that a component of orthogonal oscillation is represented by each term (except the term for  $i=1$ , which gives no oscillation, but only a shift for the center of mass) in the expression

$$R(\mu) = a_0 \left[ 1 + \sum_{i=1}^N \alpha_i P_i(\mu) \right]$$

for the distance from the center of mass to the surface of a cylindrically symmetric nucleus as a function of  $\mu = \cos\theta$ , argument of the Legendre polynomials  $P_i(\mu)$ . ( $a_0$  is chosen for volume normalization.) Evaluating the coefficients in the quadratic forms for kinetic and potential energies of small oscillations, one finds for the frequency of general order  $n$ :

$$\nu_n = A^{-1/2} \left[ \frac{O}{3M_p \pi} n(n-1) \frac{(2n+1)(n+2) - 20x}{2n+1} \right]^{1/2},$$

where  $M_p$  is the proton mass, and the other notation as in Fig. 2. Quantization of the surface oscillations gives, for the zero-point energy,  $\langle E_n \rangle_{z.p.} = \frac{1}{2} h \nu_n$ , and for the zero-point value of the mean square relative amplitude:

$$\langle \alpha_n^2 \rangle_{z.p.} = A^{-7/6} \left\{ \frac{\hbar^2}{12M_p \pi^2 (4\pi r_0^2 O)} \frac{n(2n+1)^3}{(n-1)[(2n+1)(n+2) - 20x]} \right\}^{1/2}.$$

Evaluating these quantities for the first three modes of oscillation gives:

$n$	$\nu_n$	$\langle E_n \rangle_{z.p.}$	$\langle \alpha_n^2 \rangle_{z.p.}^{1/2}$
2	$2.15 \times 10^{20}/\text{sec}$	0.45 Mev	0.064
3	$6.21 \times 10^{20}/\text{sec}$	1.29 Mev	0.054
4	$10.78 \times 10^{20}/\text{sec}$	2.23 Mev	0.053

It should be noted that the rms values of  $\alpha_n$  here predicted are smaller by a factor 5 or 6 from the values used in illustrating the orthogonal oscillations, each drawing having been computed from the expression for  $R(\mu)$  by assuming  $\alpha_n = 0.3$  and all other  $\alpha_i$  zero.

The infinite sequence of possible oscillations for an ideal liquid drop must be terminated at some value of  $n$  between 6 and 10 when applied to the atomic nucleus because of the finite number of constituent nucleons present. If we then estimate the diffuseness of the nuclear surface for the collective model in its ground state, with the help of the quantity

$$\alpha_{\text{effective}} = \left[ \sum_{i=2}^N \langle \alpha_n^2 \rangle \right]^{1/2},$$

we find the aggregate indetermination of the surface position to be about 15 percent of the nuclear radius.

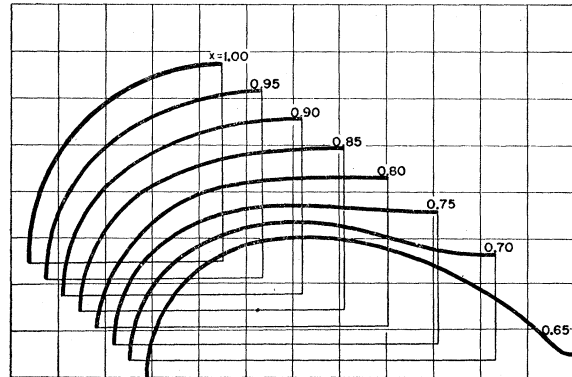


FIG. 2. Critical form of unstable equilibrium.

This critical form depends, in the approximation of the simplest liquid drop model, only upon the ratio of the square of the charge number to the first power of the mass number; or more conveniently, upon the dimensionless parameter:

$$x = \frac{(\text{charge})^2}{10 \times \text{volume} \times \text{surface tension}} = \frac{Z^2 e^2}{10A(4\pi/3)r_0^2 O} = \frac{(Z^2/A)}{(Z^2/A)_{\text{limiting}}},$$

where  $(Z^2/A)_{\text{limiting}} = 2(4\pi r_0^2 O)/(3e^2/5r_0) \cong 47.8$ . For an imaginary nucleus, "cosmium," sufficiently far beyond the known limits of stability,  $x$  will be 1, and the nucleus will already be unstable against fission in its spherical form. For values of  $x$  very close to 1 the critical form has been found (reference 5) to be  $R = R_0 \sum a_n P_n(\cos\theta)$ , where  $R_0$  is the original radius,  $a_0 = 1$ ,  $a_2 = 7(1-x)/3$ , and all other

coefficients  $a$  are negligible. For four values of  $x$  the critical form has been calculated by S. Frankel and N. Metropolis [Phys. Rev. **72**, 914 (1947)]. Interpolating between their results and extrapolating beyond them, we find the continuous sequence of shapes illustrated in the diagram. Each form is an equilibrium shape for a different nucleus. It is also possible to view the set of curves as describing the changes in a given nucleus—a nucleus with a fixed  $x$ —as it undergoes a conceivable deformation. The curves when used in this sense need not be considered to have anything to do with the question of equilibrium forms. For this reason it is appropriate to distinguish each individual shape by the value of a parameter  $y$ , equal to 1 minus the value of  $x$  shown on the curve. Thus  $y$  describes the *shape*, and  $x$  describes the (charge)<sup>2</sup>-to-mass ratio of that particular droplet which is calculated to have this critical form; but we can speak of a deformation  $y$  for a system with a different  $x$ . The curves are calculated from the interpolation and extrapolation formulas:

$$\begin{aligned}
 a_0 &= 1 - y^2 \left[ 1.06 + \frac{9.76 \times 10^{-4}}{(0.49 - y)^4} \right], \\
 a_2 &= y \left[ 2.3 + \frac{5.42 \times 10^{-4}}{(0.49 - y)^4} \right], \\
 a_4 &= y^2 \left\{ 1.6 + y \left[ 3.0 + \frac{2.84 \times 10^{-3}}{(0.49 - y)^4} \right] \right\}, \\
 a_6 &= \frac{-2.36 \times 10^{-5}}{(0.49 - y)^4}, \\
 a_8 &= \frac{-4.72 \times 10^{-5}}{(0.49 - y)^4}.
 \end{aligned}$$

Other  $a$ 's zero.

It is possible that for values of the [(charge)<sup>2</sup>/mass] parameter  $x$  near 0.65, the symmetric equilibrium form may not represent the lowest saddle point configuration in a multidimensional plot of deformation energy as a function of shape. It may be that two asymmetric forms, mirror images of each other, may lie lower. It is also conceivable that nuclear compressibility and redistribution of neutrons and protons between surface and interior may appreciably modify both the shapes themselves and the value of  $x$ , if any, for which the asymmetric saddle point is preferred. These effects have less and less influence the closer  $x$  is to unity, provided that  $y$  is rewritten as  $1 - x^*$ . Here  $x^* = x + z$ , where the quantity  $x$  is as previously defined, and  $z$  is a measure of the compressibility and redistribution effects first considered in this connection by E. Feenberg [Revs. Modern Phys. **19**, 239 (1947)] and W. J. Swiatecki [Proc. Phys. Soc. (London) **A63**, 1208 (1950)] having a value of the rough order of magnitude of 0.04 for nuclei near uranium, and uncertain by a factor of perhaps two. Assumption

of a nonzero value for  $z$  will require a readjustment in the number which now has the value 47.8, in order to leave the height of the fission barrier unchanged.

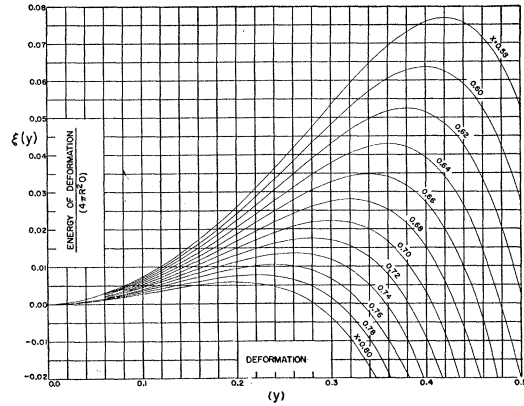


FIG. 3. Energy as a function of deformation en route to fission.

A given curve of the family here drawn describes the deformation energy, relative to the total surface energy of the spherical shape, for the forms described as a function of the shape parameter  $y$  of Fig. 2. Different curves represent different nuclei, as described by the parameter  $x$  of Fig. 2.

In the general formula,

$$\xi(x, y) = 2.178(1-x)y^2 - 4.09(1-0.645x)y^3 + 18.64(1-0.894x)y^4 - 13.33y^5,$$

we note that the value of  $y$  corresponding to the maximum value of  $\xi$  for a given  $x$  represents the critical shape of unstable equilibrium for the nucleus so specified. Hence upon setting  $y = 1 - x$ , we obtain the expression for the fission threshold energies for any  $x$  value,

$$\xi_{\max} = 0.728(1-x)^3 - 0.661(1-x)^4 + 3.330(1-x)^5.$$

An examination of the deformation potential energy surface (see projection in Fig. 4) indicates that for the sequence of shapes as here defined by  $y$  the curve  $\xi(x, y)$  is a fair approximation to the minimal path following the valley stream in the potential surface of a given  $x$ , and traversing the pass to scission.

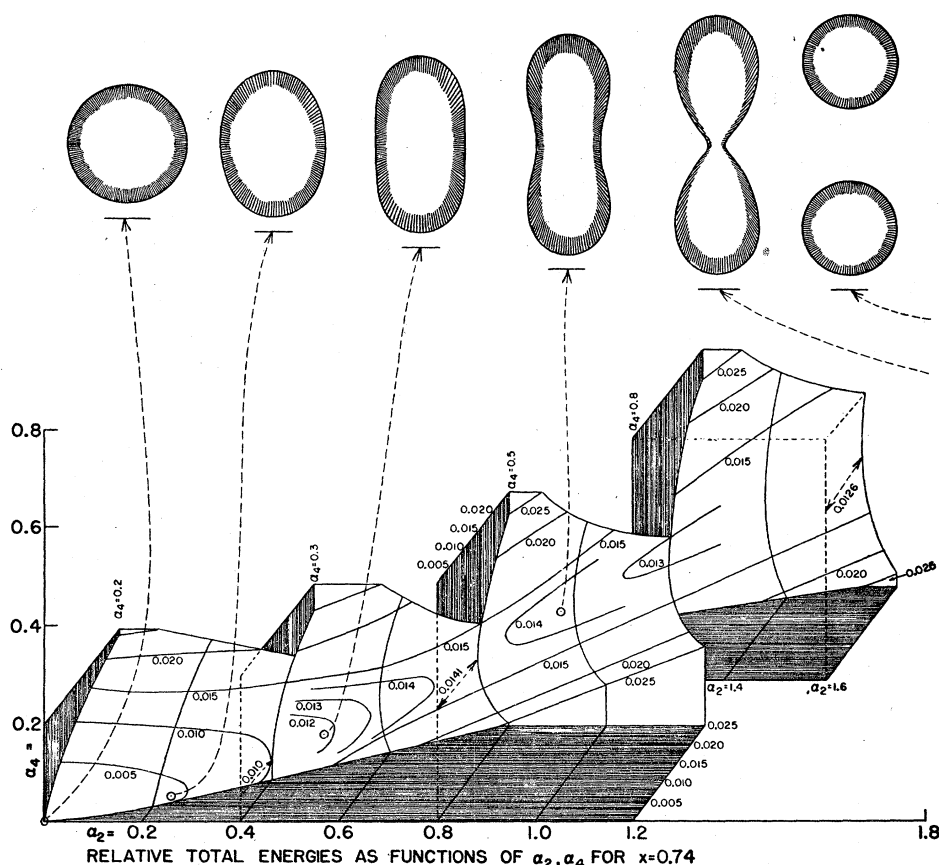


FIG. 4. Sequence of acts in fission.

The sequence of shapes leading from the initial uranium nucleus to the separated fragments is here shown, in correlation with the potential energy surface [taken from S. Frankel and N. Metropolis, *Phys. Rev.* **72**, 914 (1947)] of deformations described by points in the  $\alpha_2$ - $\alpha_4$  plane (see Fig. 1). The events leading to fission may be imagined as follows. The capture of a neutron by a uranium nucleus converts it into an excited compound nucleus, in which the energy of excitation is partly in the internal motion of individual nucleons, and partly in the collective motion of the entire nucleus for which typical components are illustrated in Fig. 1. The collective motion may be represented by the path of a "system point" on an energy hypersurface of which the surface shown is the projection in the  $\alpha_2$ - $\alpha_4$  plane. This representative point will describe a Lissajous pattern with amplitude changing as the energy content of the nucleus passes back and forth between internal and collective modes of excitation.

Consider a case in which the total excitation is only slightly greater than the height of the saddle point in the energy surface, corresponding to the threshold for fission. Such a case results from the capture of thermal neutrons in uranium. Then it must follow that fission cannot occur until (1) essentially all of the excitation is in the collective motion, and (2) the phases and amplitudes of the different modes of collective motion are such as to lead the system point nicely along the valley stream toward the pass in the surface. Clearly the many degrees of freedom in the internal and collective motion of the system will permit many nuclear eons to elapse before the capture of a slow neutron will, on the average, bring about fission. A similar comment applies to the competing processes of neutron and photon emission.

Once the system point passes the saddle, however, the increase in surface energy with further elongation is more than offset by the decrease in Coulomb energy, and the motion is self-accelerating until division occurs. The resulting fragments will contain high excitation, both internal and collective, giving rise to prompt photon and neutron emission.

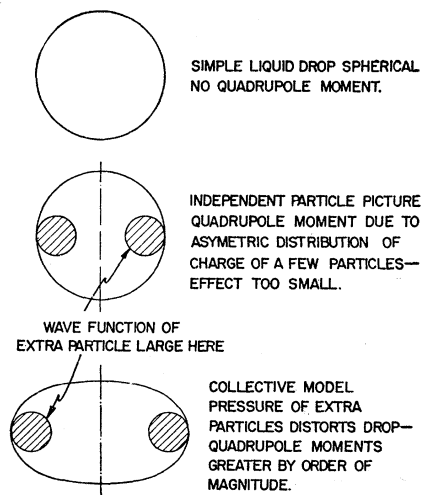


FIG. 5. Quadrupole moments and nuclear models.

Neither the simple liquid drop model nor the independent particle picture individually are capable of accounting for the order of magnitude of the quadrupole moment, or the asymmetry in the distribution of electric charge, of typical nuclei.

A negative quadrupole moment does follow in the liquid drop model if we assume that the entire nucleus with uniform volume electrification is rotating with  $l$  units of angular momentum. For a nucleus the size of uranium we find, upon minimizing the sum of deformation energy (see Fig. 3) and rotational energy, that the

reduced quadrupole moment is [K. Way, Phys. Rev. 55, 964 (1939)]

$$Q/eR^2 = 6\alpha Z/5 = -I^2 \times 2.8ZA^{-7/3}/(1-x).$$

As nuclear spins seldom exceed 4, the size of this moment is sharply at variance with the moments of 1 to 10 units commonly observed. Moreover, no mechanism is apparent by which the liquid drop could assume the prolate form required to produce a positive quadrupole moment.

More instructive is the inability of the independent particle model to predict moments of the proper size. The shaded ring-shaped region is the region of large probability amplitude for the wave function of a single proton in excess of a closed-shell (spherically symmetric) configuration. The quadrupole moment due to it in typical cases is 5 to 15 times too small to agree with observation. From the wave function  $\Psi_{lm}(\mathbf{r})$  of a particle in a spherical well, the quadrupole moment may be computed on the assumption that the charge density controlled by the nucleon in question is proportional to  $|\Psi_{lm}(\mathbf{r})|^2$ . Taking the total charge so described to be one electronic unit, we discover that, even for very large angular momenta, and for any value of the total quantum number  $n$ , the largest value of the reduced quadrupole moment attainable is 0.5, and that the values to be commonly expected are less than 0.2 in magnitude. Thus, even the assumption that the effects of four or five nucleons could be simply additive does not allow us to account for observed moments.

However, Rainwater (reference 12) pointed out that the pressure of the nucleon against the surface works against surface tension to produce a sizeable deformation. The resulting bulk displacement of charge gives rise to a quadrupole moment an order of magnitude greater than that directly due to the extra particle. Thus the study of quadrupole moments provided the first convincing proof of the importance of the interaction of nucleons with the wall, a central point in the collective model of the nucleus.

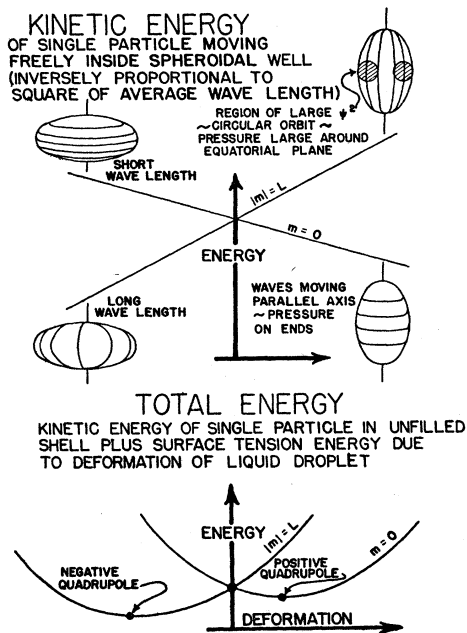


FIG. 6. More detailed picture how a single extra nucleon causes a deformation.

The upper diagram shows the energy of the particle itself as a function of the static deformation. When the angular momentum is parallel to the axis, the waves run around azimuthally, and the wavelength is increased by an oblate, pancake-like deformation. The lower diagram shows the sum of energy of the extra particle, plus the energy of the residual closed shell nucleus, this latter parabola being calculated from the simple surface tension idealization,  $\text{energy} = (2/5)(\text{radius})^2(\text{surface tension})(\text{deformation}, \alpha)^2$ . The sign of the resultant quadrupole moment differs according as the projection of the angular momentum along the symmetry axis is small or nearly equal to the total angular momentum.

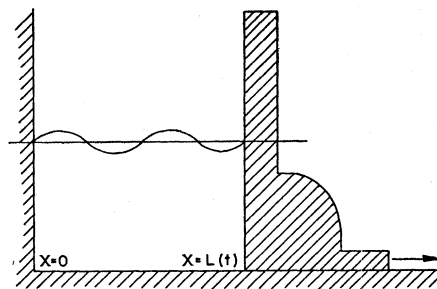


FIG. 7. Effect of wall motion on state of particle in simple one-dimensional case.

For the case of a stationary wall, the wave function  $(2/L)^{1/2} \times \sin(n\pi x/L) \exp(-i \int^t E dt/\hbar)$ , where  $E = n^2 \pi^2 \hbar^2 / 2ML^2 = \text{constant}$ . For the case of a slowly moving wall, an approximate wave function  $\psi(x, t)$  is obtained by inserting in this expression the assumedly known functional dependence of  $L$  on  $t$ , and multiplying the resulting preliminary wave function by  $\exp(-iM\phi(x, t)/\hbar)$ . Here  $\phi(x, t)$  is the classical velocity potential; its derivative,  $v(x, t) = -\partial\phi/\partial x$ , gives the velocity with which a classical gas of infinite sound velocity would respond to the motion of the wall. The term in the velocity potential ensures that the wave function satisfies the equation of continuity,

$$\frac{\partial}{\partial x} \left\{ \frac{\hbar}{2Mi} \left( \psi^* \frac{\partial \psi}{\partial x} - \psi \frac{\partial \psi^*}{\partial x} \right) \right\} + \frac{\partial}{\partial t} (\psi^* \psi) = 0.$$

It describes a motion of matter to the right as the restraining wall goes in that direction. The resulting wave function satisfies exactly the potential-free wave equation between the walls when the distance  $L$  increases linearly with time. For a more general dependence of  $L$  upon time the wave function satisfies the equation,

$$i\hbar \partial \psi / \partial t = -(\hbar^2 / 2M) (\partial^2 \psi / \partial x^2) - (M \dot{x}^2 L / 2L) \psi.$$

Here the extra term on the right will be negligible for the case of a slowly accelerating wall. In this approximation the effect of the wall motion on the state of the particle is adequately described by the factor in the classical velocity potential.

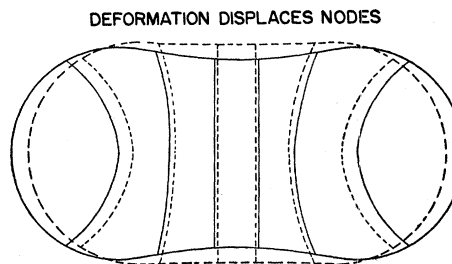


FIG. 8. Effect of wall motion on particle state—three-dimensional.

We shall derive here the result that the expectation value of the energy of a set of identical particles held within a slowly changing boundary of constant volume content is given at any instant approximately by the energy the particles would have were the wall stationary, augmented by a term which represents the classically calculated kinetic energy of an incompressible fluid of the same mass,  $M$ , urged into irrotational motion by the same walls. Let the symbol  $x$  typify the three space coordinates of one particle, the symbol  $\alpha$  specify the configuration of the wall,  $f(x, \alpha)$  and  $E(\alpha)$  stand for wave function and energy for the case of the static wall, and  $\phi(x, \alpha, \dot{\alpha})$  represent the velocity potential of the classical fluid motion:  $\partial\phi/\partial t - \frac{1}{2}(\nabla\phi)^2 - p/\rho = 0$ ;  $\nabla^2\phi = 0$ ;  $-\partial\phi/\partial n = \text{normal velocity of wall}$ . We represent the wave function of the particle in the approximate form

$$\psi(x, t) = f(x, \alpha(t)) \exp \left[ -i \int^t E(\alpha(t)) dt / \hbar - iM\phi / \hbar \right].$$

To test this function in the Schrödinger equation, we calculate

$$i\hbar \partial \psi / \partial t = \exp \left[ \dots \right] [i\hbar \dot{\alpha} \partial / \partial \alpha + E + M \partial \phi / \partial t] f.$$

We now argue that in first approximation the nodes and values of  $f$  are carried along with the classical fluid velocity, so that

$$\dot{\alpha} \partial f / \partial \alpha \doteq (-1)^2 (\nabla \phi) \cdot (\nabla f).$$

Thus

$$i \hbar \partial \psi / \partial t \doteq \exp \left[ \int [i \hbar (\nabla \phi) \cdot (\nabla f) - (\hbar^2 / 2M) \nabla^2 f + (Mf/2) (\nabla \phi)^2 + (M \dot{\phi} / \rho) f] dt \right] \left[ -(\hbar^2 / 2M) \nabla^2 \psi + (M \dot{\phi} / \rho) \psi \right].$$

We conclude that the wave function in question satisfies approximately Schrödinger's equation, through velocity dependent terms, and neglects essentially only the accelerative terms of the form (pressure/density). For the kinetic energy of the state we now find

$$\begin{aligned} (\hbar^2 / 2M) \int (\nabla \psi^*) (\nabla \psi) d(\text{vol}) &= (\hbar^2 / 2M) \int (\nabla f^*) (\nabla f) d(\text{vol}) \\ &+ (i \hbar / 2) \int (f^* \nabla f - f \nabla f^*) \nabla \phi d(\text{vol}) + (M/2) \int (\nabla \phi)^2 f^* f d(\text{vol}), \end{aligned}$$

a result in which the last term—summed over the occupied states—goes over into the kinetic energy of the classical fluid in the limit of large quantum numbers, as was to be shown. The first term gives energy of the particles in a static potential. The second is important for the interaction between unpaired particles and wall rotation.

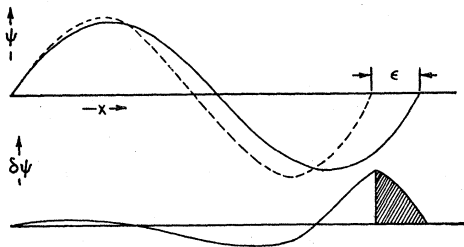


FIG. 9. Approximate orthogonality of the nucleonic wave functions of Eq. (3) for two slightly different values of the deformation parameter,  $\alpha$ .

The general principles involved here are illustrated by the example of a one-dimensional potential well, extending from  $x=0$  to  $x=a=R_0(1+\alpha)$  or to  $x=b=R_0(1+\alpha)(1+\epsilon)$ , according as we deal with the one or the other value of  $\alpha$ . The determinantal wave functions,  $\Phi$ , of the  $N$  particle system are constructed out of individual particle wave functions of the form  $u(n, x) = (2/a)^{1/2} \times \sin(n\pi x/a)$ . The desired matrix element between the wave functions for the same nucleonic state but slightly different values of  $\alpha$  is

$$\sum_{\substack{\text{permutations} \\ 1 \ 2 \ \dots \ N \\ \alpha \ \beta \ \dots \ \nu}} (-1)^P \int u(n_1, x, a) u(n_\alpha, x, b) dx \dots \times \int u(n_N, x, a) u(n_\nu, x, b) dx,$$

where the sum goes over all permutations,  $P$ , of the labels,  $n_1, \dots, n_N$ , of the occupied states. When the state labels are the same in one of the individual integrals, the integral has the approximate value

$$1 - \epsilon^2 [(1/8) + (n^2 \pi^2 / 6)],$$

and, when the labels are different, the approximate value

$$\epsilon (-1)^{n+m} 2mn / (m^2 - n^2).$$

Combining factors of the form  $(1 - \epsilon_1)(1 - \epsilon_2) \dots (1 - \epsilon_N)$  into exponentials of the type  $\exp(-\epsilon_1 - \epsilon_2 - \dots - \epsilon_N)$ , we have for the value of the scalar product  $\int \dots \int \Psi_\alpha \Psi_\beta d(\text{volume})$  the approximate formula

$$\exp[-\epsilon^2 \{ (N/4) + (41/288) + (12)^{-1} (6N^2 + 6N + 1) \ln 3.562N \}]$$

from which there follows the result quoted in the text. Thus wave functions of the one-dimensional system are nearly orthogonal for a fractional extension  $\epsilon \sim N^{-1} (\ln 3.562N)^{-1}$  or for a volume change equal to a fraction  $(\ln 3.562N)^{-1}$  of the cell occupied by the typical particle. Generalizing to three dimensions, we conjecture that the nucleonic system wave functions are practically orthogonal as soon as the volume not common to the two configurations exceeds some small fraction of one cell.

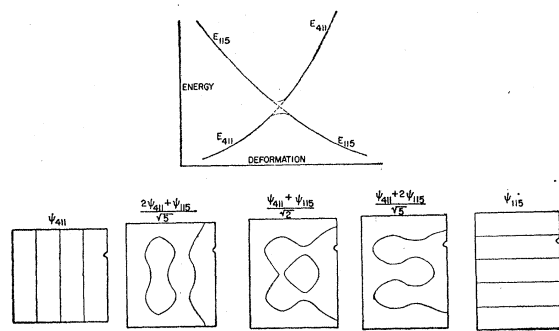


FIG. 10. Effect of a small asymmetry in mixing two otherwise orthogonal states.

We examine here the mixing of two states of a particle in a rectangular box, possessing a small irregularity, as two of the box dimensions are altered in a volume-preserving deformation. Shown are the nodes of the total wave function at successive stages of the deformation. In the absence of the irregularity in the surface, the two levels cross without interaction as the deformation proceeds. The irregularity mixes the two wave functions in comparable proportions only near the point of cross-over. The nodes were found by solving the equation  $R \sin 4x \sin z + \sin x \sin 5z = 0$ , where  $x$  and  $z$  represent the distances from the lower left hand corners of the rectangles expressed in such units that  $x = \pi, z = \pi$  at the diagonally opposite corners.

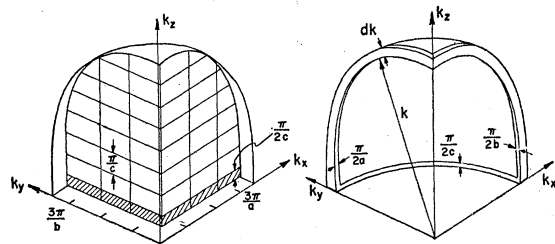


FIG. 11. Asymptotic frequency of proper values.

We shall "derive" here the asymptotic formula for the number of solutions of the equations  $\nabla^2 \psi + k^2 \psi = 0, \psi_{\text{surface}} = 0$ , with wave numbers in the interval  $k$  to  $k + dk$ :

$$dN = V k^2 dk / 2\pi^2 - S k dk / 8\pi + \left[ \int \kappa dS \right] dk / 8\pi^2.$$

Here  $V$  is the volume of the region under consideration,  $S$  its surface, and  $\kappa$  the local total curvature of the surface. The case actually considered is that of a rectangular parallelepiped, of dimensions  $a, b, c$ . Each proper solution,  $\sin k_x x \sin k_y y \sin k_z z$ , corresponds to a lattice point in  $k$  space,  $k_x = l\pi/a, k_y = m\pi/b, k_z = n\pi/c$ , with which is associated a characteristic "box" of volume  $(\pi/a)(\pi/b)(\pi/c)$ . When the states are filled out to a given wave number  $k_{\text{max}}$ , the boxes occupy an octant of a sphere (left-hand diagram) except for slab-like regions near the coordinate planes. The region thus to be excluded from the volume count is shown in more detail in the right-hand diagram, for the case when the number of states between  $k$  and  $k + dk$  is desired: relevant volume = shell - correction for ring like strips + correction for corners subtracted twice in counting volume of rings

$$= (4\pi/8) k^2 dk - (\pi/2) (k dk) \left[ (\pi/2a) + (\pi/2b) + (\pi/2c) \right] + dk \left[ (\pi/2a)(\pi/2b) + \text{two similar terms} \right].$$

Division by the volume of one box gives for the number of states:  $dN \doteq abc k^2 dk / 2\pi^2 - (2ab + 2bc + 2ca) k dk / 8\pi + (4a + 4b + 4c) dk / 16\pi$ .

Generalization of this expression to an enclosure whose shape is not too irregular gives the cited formula. Then the number of states with wave number less than  $k$  is

$$N \doteq V k^3 / 6\pi^2 - S k^2 / 16\pi + L k / 8\pi^2,$$

and their totalized kinetic energy,  $E$ , is given by

$$2ME/\hbar^2 = V\hbar^5/10\pi^2 - Sk^4/32\pi + Lk^3/24\pi^2 \\ = (V/10\pi^2)(6\pi^2 N/V)^{5/3} + (S/32\pi)(6\pi^2 N/V)^{4/3} \\ + (6\pi^2 N/V)(S^2/128V - L/12\pi^2).$$

The proportionality of a part of this energy with the surface implies the existence of a contribution to the surface tension of kinetic origin [C. F. Weiszäcker, *Die Atomkerne* (Akademische Verlagsgesellschaft, Leipzig, 1937); E. Feenberg, *Revs. Modern Phys.* **19**, 239 (1947)]. For nuclei with approximately equal numbers of neutrons and protons, and a volume per particle of  $4\pi r_0^3/3$  the appropriate term in the surface tension is

$$O_{kin} = 4(\hbar^2/64\pi M)(9\pi/8r_0^3)^{4/3},$$

with

$$4\pi r_0^2 O_{kin} = 28 \text{ Mev.}$$

This calculated value is twice as great as the empirical figure, 14 Mev, for the *sum* of kinetic and potential surface tension coefficients. However, the calculated value is reduced to a more nearly reasonable magnitude when the height of the potential wall is diminished from infinity to a finite value, according to a kind private communication of Professor Feenberg.

After having completed this manuscript we were kindly shown by Professor Eugene Feenberg the June, 1951 Washington University thesis of K. C. Hammack, "Topics in Nuclear Structure," which discusses the asymptotic density of independent particle levels for potential wells both of infinite and of finite depth, and proposes also the three-term asymptotic formula which appears in this caption.

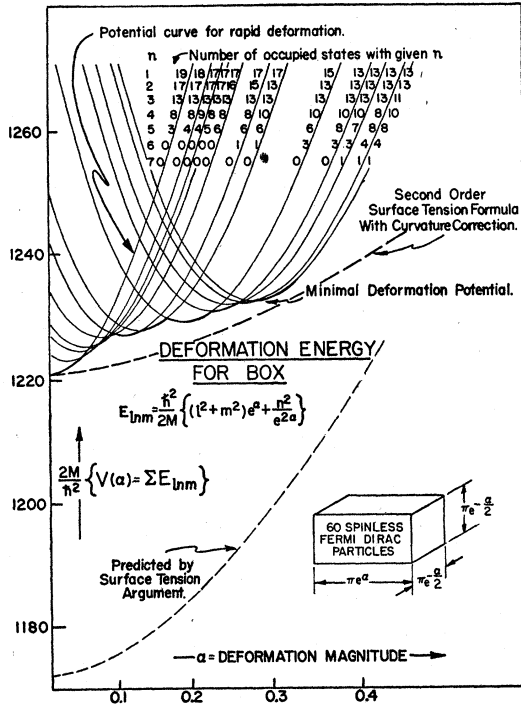


FIG. 12. Potential curves for a deformable rectangular box.

The energy of deformation depends upon the nucleonic state of the system as well as upon the magnitude of the deformation itself. Each potential curve in the diagram is obtained by considering the 60 particles in question to be placed in 60 specified distinct individual particle states, and summing their energies. For the energy of the system to keep to a minimum value, it is necessary that the distribution of particles among states should change during the course of the deformation. The scalloped curve therefore gives a qualitative representation of the type of potential energy curve to

be expected for actual nuclei. If the deformation changes so fast that switches from one potential curve to another do not have time to occur with appreciable probability, or if such switches are altogether forbidden because of the high symmetry of the system—as in the case of a box with smooth rectangular walls—then the distribution of particles among states will not change during the course of the deformation. Then the energy required to produce the distortion will be much greater than one would estimate from the notion of surface tension. The dashed curve is predicted by applying the statistical arguments and formula of Fig. 11 to the present idealized problem, putting  $N=60$ , volume  $=\pi^3$ , surface  $=2\pi^2 e^{-\alpha} + 4\pi^2 e^{\alpha/2}$ , integrated curvature  $=2\pi^2 e^{\alpha} + 4\pi^2 e^{-\alpha/2}$ ,

$$\Sigma 2ME/\hbar^2 = (\pi/10)(360/\pi)^{5/3} + (\pi/16)(360/\pi)^{4/3}(e^{-\alpha} + 2e^{\alpha/2}) \\ + (45/4)e^{-2\alpha} + (45-120/\pi)e^{-\alpha/2} + (45-60/\pi)e^{\alpha}.$$

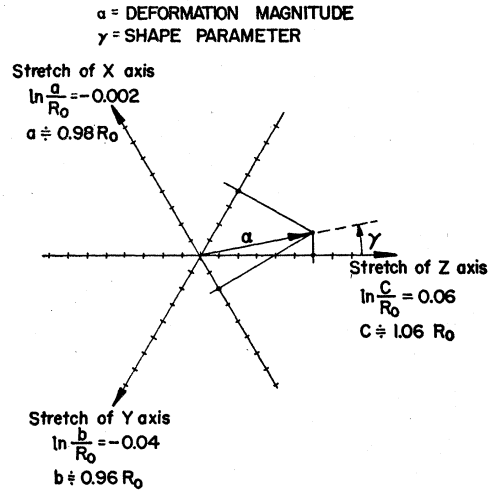


FIG. 13. Coordinates  $(\alpha, \gamma)$  for volume-preserving ellipsoidal deformations.

Volume-preserving ellipsoidal deformations may be described by two polar coordinates in a plane:  $\alpha$  = deformation magnitude,  $\gamma$  = shape parameter. These coordinates are defined in terms of the semi-major axes of the ellipsoid,

$$\frac{x^2}{a^2} + \frac{y^2}{b^2} + \frac{z^2}{c^2} = 1,$$

by the equations

$$a = R_0 \exp[\alpha \cos(\gamma - 2\pi/3)], \\ b = R_0 \exp[\alpha \cos(\gamma + 2\pi/3)], \\ c = R_0 \exp[\alpha \cos \gamma],$$

which are required to satisfy the condition of volume constancy,

$$abc = R_0^3.$$

For example, a deformation in which the changes of length of the  $x$ ,  $y$ , and  $z$  axes are  $-1$  percent,  $-2$  percent, and  $+3$  percent, or any small positive common multiple of these fractions, is described by one or another positive value of the positive "deformation magnitude"  $\alpha$  and a value of the "shape parameter,"  $\gamma$ , equal to  $10.895^\circ$ .

As another example, let  $\alpha$  be given a positive value, say  $0.02$ , and let  $\gamma$  be increased, starting with  $\gamma=0$ . Then the ellipsoid takes on the following shapes:

$\gamma$	$a/R_0$	$b/R_0$	$c/R_0$	Shape	Symmetry axis
$0^\circ$	0.990	0.990	1.020	prolate spheroid	$z$
$30^\circ$	1.000	0.983	1.017	ellipsoid	none
$60^\circ$	1.010	0.980	1.010	oblate spheroid	$y$
$90^\circ$	1.017	0.983	1.000	ellipsoid	none
$120^\circ$	1.020	0.990	0.990	prolate spheroid	$x$

With further increase of  $\gamma$  the cycle repeats, except for cyclic interchange of the labels  $x, y, z; a, b, c$ .

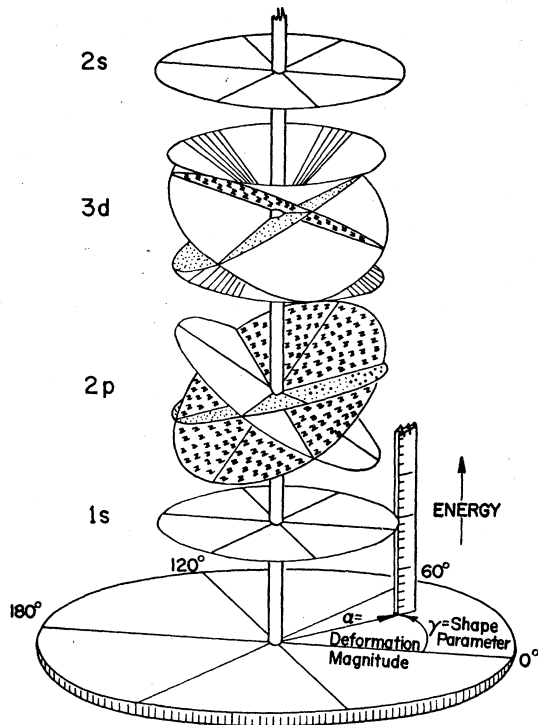


FIG. 14. Qualitative effect of small ellipsoidal deviations from sphericity upon the first few energy levels of a single nucleon.

Spin-orbit coupling is neglected. Consequently this diagram and those in following few figures are to be considered as primarily illustrative. The deformation of the ellipsoid is expressed in terms of the polar variables,  $\alpha$  and  $\gamma$ , as indicated in Fig. 13. The simplest case to consider is distortion into a prolate spheroid, rotation-symmetric about the  $z$  axis ( $\gamma=0$ ). Then the quantum number  $m$  is well defined. The level of orbital angular momentum  $l\hbar$  breaks up into components, of which the one with quantum number  $m$  is raised by an amount

$$\delta E = 2\alpha E \frac{3m^2 - l(l+1)}{(2l-1)(2l+3)}$$

with respect to the original energy,  $E$ . Levels with  $m = +|m|$  and  $m = -|m|$  coincide. Points not shown in this diagram: (1) Effect on the energy surfaces of displacements so large that  $\delta E$  is no longer proportional to  $\alpha$ . Then terms of order higher than the first have also to be taken into account. The resulting curvature of the energy surfaces is most easily visualized by saying that energy surfaces repel each other except in the neighborhood of exceptional points. At such a point the two surfaces ordinarily meet in a double funnel, as shown in Fig. 35. Many such funnels would be seen in a more extended version of the present diagram. (2) Dependence of energy upon surface deformations of order higher than the second is not shown here, for want of dimensions. In treating the asymmetry of nuclear fission it is important to consider deformations of order  $n=3$  as well as the ellipsoidal distortions ( $n=2$ ) envisaged here.

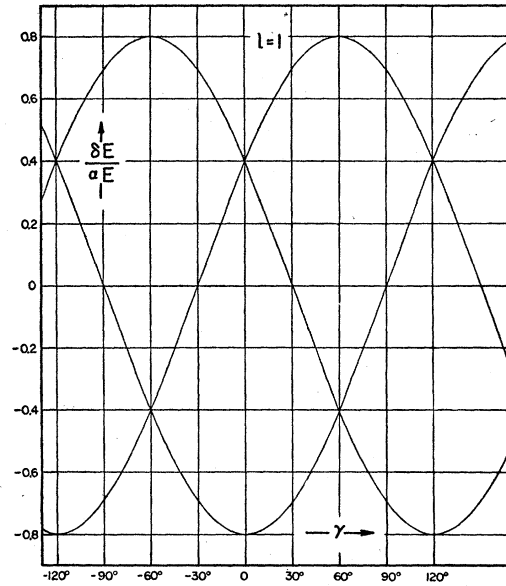


FIG. 15. Splitting of levels of a  $p$  particle (orbital angular momentum  $l=1$ ) in a potential well of constant depth, the boundaries of which have received a slight volume-preserving ellipsoidal deformation away from the spherical form.

In the diagram  $E$  represents the kinetic energy of the nucleon in the original spherical well, and  $\delta E$  the displacement of the level for a small distortion of magnitude  $\alpha$ . This quantity, and the shape parameter  $\gamma$  which is plotted horizontally, are as defined in Fig. 13. Note that a  $p$  particle will have the lowest possible energy when it goes into a nucleus shaped like a prolate spheroid.

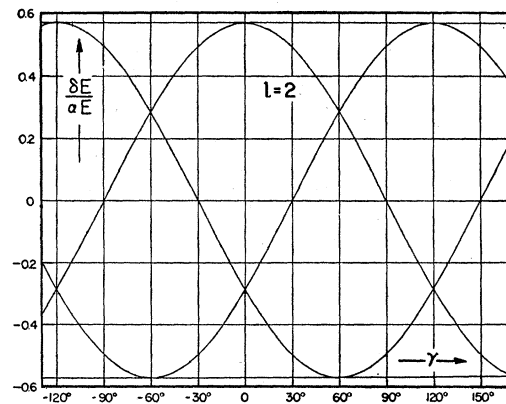


FIG. 16. Splitting of levels of a  $d$  particle (orbital angular momentum  $l=2$ ), shown as a function of the shape parameter  $\gamma$  of the ellipsoidal deformation.

The five levels group as three for an axially symmetric deformation ( $\gamma=0^\circ, \pm 60^\circ, \pm 120^\circ$ , etc). The energy of a single  $d$  nucleon

which goes into the lowest accessible level in first approximation is independent of the shape parameter  $\gamma$ . The present case,  $l=2$ , is the neutral point. For  $l=1$  a prolate deformation gives the greatest energy lowering, and for  $l=3$  or more a prolate deformation is energetically preferred in the case of a single nucleon.

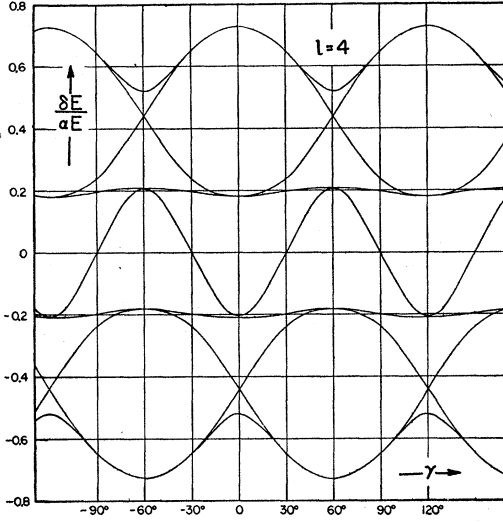


FIG. 17. Removal of the ninefold degeneracy of a  $g$  nucleon ( $l=4$ ) by small ellipsoidal deformation.

A single  $g$  particle achieves the lowest possible energy when it goes into an oblate ellipsoid ( $\gamma = \pm 60^\circ; 180^\circ$ ). The calculation of first-order energy displacement is made as follows: Let  $u_1$  be the wave function which vanishes at the surface of the sphere and which satisfies  $\nabla^2 u_1 + k_1^2 u_1 = 0$  inside; let the very slightly different function  $u_2$  vanish on the surface of the ellipsoid and satisfy  $\nabla^2 u_2 + k_2^2 u_2 = 0$  within that surface. Then, by Green's method,

$$k_2^2 - k_1^2 = \frac{\int (u_2^* \partial u_1 / \partial n - u_1 \partial u_2^* / \partial n) dS}{\int u_1 u_2^* d(\text{vol})},$$

where the integral in the denominator is taken over the volume common to the two solids, and the integral in the numerator over the surface which encloses that common volume. Let  $S_1$  be innermost at a certain point of  $S$ . Then on  $S_1$ ,  $u_1 = 0$  and in terms of the normal displacement,  $\delta n$ , of  $S_2$  with respect to  $S_1$ ,

$$u_2 \doteq -(\delta n)(\partial u_2 / \partial n) \doteq -(\delta n)(\partial u_1 / \partial n).$$

A similar result is found when  $S_1$  lies outermost. Consistent with the neglect of terms of order higher than the first, we thus have

$$\delta(k^2) = - \int |\partial u_1 / \partial n|^2 \delta n dS / \int |u_1|^2 d(\text{vol}),$$

provided that the difference between  $u_2$  and  $u_1$  is indeed small; i.e., provided that we have chosen, or will choose for  $u_1$ —as below—the proper linear combination of the wave functions of the originally degenerate levels. Let the corresponding proper linear combination of spherical harmonics be denoted by

$$Y(\theta, \varphi) = \sum c_m Y_L^{(m)}.$$

Also let  $F_l(\rho)$  denote the regular solution of the radial equation

$$d^2 F_l / d\rho^2 + [1 - l(l+1)/\rho^2] F_l = 0,$$

so that

$$\int_0^\rho F_l^2 d\rho = \frac{1}{2} \rho [(F_l)^2 + (F_l')^2] - \frac{1}{2} F_l F_l' - l(l+1)(F_l)^2 / 2\rho = \frac{1}{2} \rho (F_l')^2 \text{ when } \rho \text{ is a node.}$$

Then the unperturbed wave function is

$$u_1 = r^{-1} F_l(kr) Y(\theta, \varphi),$$

and the first-order perturbation in energy is given by

$$\frac{\delta E}{\alpha E} = \frac{\delta(k^2)}{\alpha k^2} = - \frac{2}{\alpha R_0} \int Y^*(\delta R) Y d\Omega / \int Y^* Y d\Omega.$$

Let  $I$  be that idempotent operator which, when applied to any general surface harmonic,

$$U = \sum_{l,m} b_{l,m} Y_{l,m}(\theta, \varphi),$$

annuls all terms except those which belong to the value of  $l$  of present interest to us, and leaves these terms unaltered. Then

$$\int Y^* \Lambda Y d\Omega = \int Y^* I \Lambda Y d\Omega,$$

where  $\Lambda$  is an abbreviation for the perturbation

$$\Lambda = -2\delta R(\theta, \varphi) / \alpha R_0.$$

A proper linear combination  $Y$  will satisfy the eigenvalue equation

$$I \Lambda(\theta, \varphi) Y(\theta, \varphi) = \lambda Y(\theta, \varphi),$$

where  $\lambda$  is a numerical constant. This is a secular equation for the determination of the coefficients  $c_m$  and the energy shift,

$$\delta E = \lambda \alpha E.$$

In the standard equation for the ellipsoid (caption of Fig. 13), we write

$$\begin{aligned} x &= (R_0 + \delta R) \sin \theta \cos \varphi, \\ y &= (R_0 + \delta R) \sin \theta \sin \varphi, \\ z &= (R_0 + \delta R) \cos \theta, \end{aligned}$$

and insert the expressions for the semi-major axes,  $a, b, c$ , in terms of  $R_0$  and the deformation parameters  $\alpha$  and  $\gamma$ . To terms of the first order it is found that the alteration,  $\delta R$ , in the length of the radius vector from the origin to the surface is given by the equation

$$\Lambda(\theta, \varphi) = -2\delta R(\theta, \varphi) / \alpha R_0 = 3^{\frac{1}{2}} \sin^2 \theta \cos 2\varphi \sin \gamma - 2P_2(\cos \theta) \cos \gamma.$$

Of this quantity the matrix element vanishes between spherical harmonics  $Y^{(m)}$  of the same  $l$  value (the one of interest) but of different  $m$  values, except in the following cases:

(1) Same  $m$  values (diagonal elements of matrix).

$$\Lambda_{mm} = \frac{2 \cos \gamma [3m^2 - l(l+1)]}{(2l-1)(2l+3)}.$$

(2) Values of  $m$  which differ by two units:

$$\Lambda_{m\pm 1, m\mp 1} = \frac{+3^{\frac{1}{2}} \sin \gamma [l^2 - m^2]^{\frac{1}{2}} [(l+1)^2 - m^2]^{\frac{1}{2}}}{(2l-1)(2l+3)}.$$

The solution of the secular equation,

$$\text{determinant } |\Lambda_{jk} - \lambda| = 0,$$

gave the values for the energy shifts of the present and preceding figures.

The effects of deformations upon energy levels, as calculated here for the case of an infinite well, will be decreased in the case of a finite well by a factor analyzed by Feenberg and Hammack (reference 9).

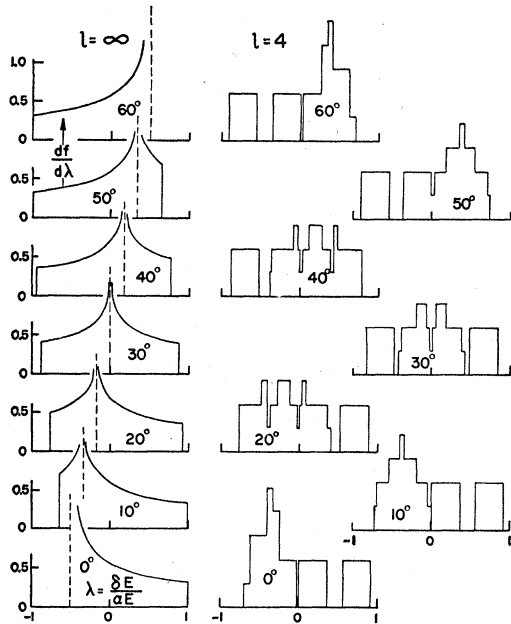


FIG. 18. Splitting of levels for case of small ellipsoidal deformations but very large orbital angular momentum.

The secular equation (preceding figure) has in this case so many roots that it is appropriate to describe their distribution statistically. Plotted horizontally is the value of the root of the secular equation,  $\lambda = \delta E/\alpha E$ . Plotted vertically is the fraction of the number of such roots, per unit range of  $\lambda$ :

$$\int (df/d\lambda)d\lambda = 1.$$

Whatever be the value of the "shape parameter,"  $\gamma$ , the distribution function has a singularity at one value of  $\lambda$ , the dimensionless measure of level shift. In other words, there are many levels for which  $\lambda$  lies in the neighborhood of this singular value,  $\lambda_{\text{sing}} = \cos(\gamma - 2\pi/3)$  (when  $\gamma$  lies between  $0^\circ$  and  $60^\circ$ ). The extremal values of the level shift in the present limit of large  $l$  are  $\lambda_{\text{min}} = \cos(\gamma + 2\pi/3)$ ;  $\lambda_{\text{max}} = \cos\gamma$ . Plotted at the right for comparison is the distribution of levels found from the secular determinant for the case  $l=4$ , except that each level has been spread out to give an approach to a continuous distribution. There is a qualitative but of course not a quantitative correspondence between the cases  $l=4$  and  $l=\infty$ . As the predictions of quantum mechanics approach those of classical mechanics in the limit of large quantum numbers, the method of calculation was to write

$$\lambda = \delta E/\alpha E = (\text{average of the perturbation, } \Lambda(\theta, \phi) = -2\delta R(\theta, \phi)/\alpha R_0, \text{ over the unperturbed classical motion}).$$

In the unperturbed classical motion the particle moves in a plane which passes through the center of the sphere. The motion is a series of straight line segments, with abrupt changes of direction each time the particle hits the surface. In all orbits except a set of measure zero, the angular period of the motion will be incommensurable with  $2\pi$ , and the particle will come arbitrarily close in the course of time to every point on a certain great circle. Let the normal to this great circle have the polar angles  $\theta^*$  and  $\phi^*$ . Then the average of  $\Lambda$  over this great circle gives

$$\Lambda_{\text{av}} = \lambda = \cos\gamma P_2(\cos\theta^*) + 2^{-1}3^{1/2} \sin\gamma \sin^2\theta^* \cos 2\phi^*.$$

To ask that this quantity should lie in an interval  $\lambda$  to  $\lambda+d\lambda$  is to pick out upon the surface of the sphere a band of points, any one of which specifies the direction of the axis of angular momentum of an acceptable orbit. The solid angle,  $d\Omega$ , subtended by this band tells the fraction of eigenvalues which lie between  $\lambda$  and  $\lambda+d\lambda$ :

$$\frac{df}{d\lambda} = \frac{1}{4\pi} \frac{d\Omega}{d\lambda} = \pi^{-1}3^{-1/2} (\sin\gamma)^{-1} (\cos\gamma - \lambda)^{-1/2} K(\kappa),$$

where  $K$  is the complete elliptic integral and

$$\kappa = \left\{ \frac{(\lambda - \cos 120^\circ + \gamma) \sin 120^\circ + \gamma}{(\cos\gamma - \lambda) \sin\gamma} \right\}^{1/2},$$

this expression applying when  $\gamma$  lies between  $0^\circ$  and  $60^\circ$  and when in addition  $\lambda$  lies between  $\lambda_{\text{min}}$  and  $\lambda_{\text{sing}}$ . When  $\lambda$  lies between  $\lambda_{\text{sing}}$  and  $\lambda_{\text{max}}$ , the corresponding formula is

$$\pi^{-1}3^{-1/2} (\lambda - \cos 120^\circ + \gamma)^{-1/2} (\sin 120^\circ + \gamma)^{-1/2} K(\kappa^{-1}).$$

These formulas were used in the plotting of the distribution curves  $df/d\lambda$ .

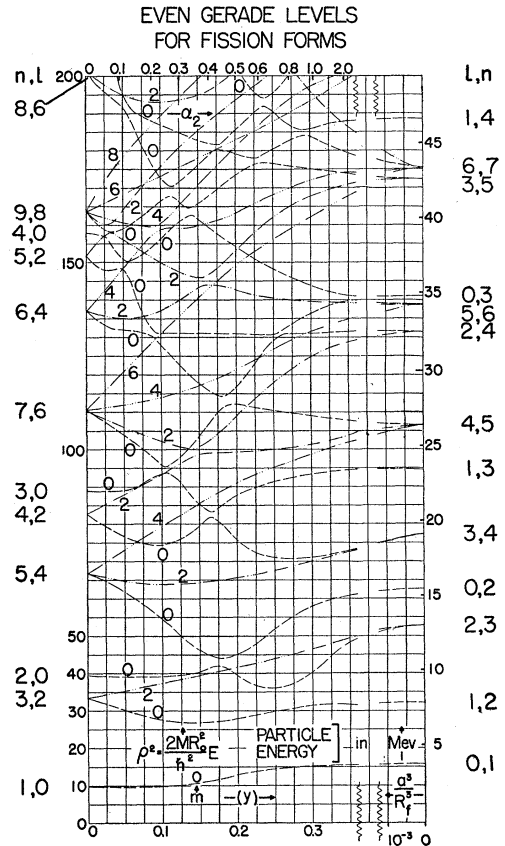


FIG. 19. Effect of deformation leading to fission upon single-particle energy levels of even-gerade symmetry.

The Frankel-Metropolis sequence of forms (Fig. 2) is considered for definiteness. Plotted vertically are the values of the dimensionless measure of energy,  $\rho^2 = 2MR_0^3E/h^2$ , where  $R_0$  is the radius of the original sphere. The magnitude of the deformation is measured by the parameter  $\alpha_2 = (7/3)y = (7/3)(1-x)$ , where  $x$  and  $y$  have the meanings described in Fig. 2. This definition of  $\alpha_2$  agrees with the definitions in Fig. 1 and in Fig. 13 to the first order for small distortions, but all three definitions differ for large disturbances. The right-hand edge of the diagram gives the energy levels when the boundary is deformed into two spheres of half the original volume, connected with each other by a small orifice. Whatever the magnitude of the single deformation parameter here considered, the boundary is invariant with respect to inversion ( $x, y, z \rightarrow -x, -y, -z$ ) and with respect to reflection at a plane through the origin normal to the axis,  $z$ , of rotational symmetry ( $x, y, z \rightarrow x, y, -z$ ). Consequently, the levels fall into four classes:

		Ratio of values of wave function at two points which differ by a reflection = $(-1)^{l+m}$	
		+(gerade)	-(ungerade)
Ratio of values of wave function at two points which differ by an inversion = $(-1)^l$	+	$l$ even	$l$ even
	(even)	$m$ even	$m$ odd
-	$l$ odd	$l$ odd	$l$ odd
	(odd)	$m$ odd	$m$ even

Among these only even-gerade levels are shown in the present diagram. Of the levels which are plotted in this and the following three figures, only those are shown in full detail which have a quantum number of angular momentum about the symmetry axis equal to  $m=0$  or  $m=3$ . The full line curves in these four figures were calculated in detail as described in the caption of Fig. 21; the dotted curves are only schematic and have no *quantitative basis* other than the initial and final ordinates and slopes, and the use of inflection points here and there to permit level jumps as needed to preserve the proper relation between the number  $n$  of nodal surfaces in the initial and final wave functions.

$n-l$	1	2	3	4
0	9.870	39.479	88.827	157.914
1	20.191	59.679	118.899	197.858
2	33.218	82.719	151.854	
3	48.831	108.516	187.635	
4	66.955	137.005		
5	87.531	168.130		
6	110.519	201.850		
7	135.886			
8	163.605			
9	193.649			

The number  $n$  represents—in the case of spherical and nearly spherical configurations—the total number of nodal surfaces in the wave function, counted as follows:  $m$  in the  $\phi$  direction,  $l-m$  in the  $\theta$  coordinate,  $n-l$  in the radial direction (counting the boundary itself as a nodal surface). As the magnitude of the deformation is increased,  $l$  ceases to be a good quantum number and even the total number,  $n$ , of nodal surfaces ceases to remain constant as such surfaces migrate to the outer boundary or coalesce inside. The only firm ordering principle is the requirement that levels of the same  $m$  do not cross.

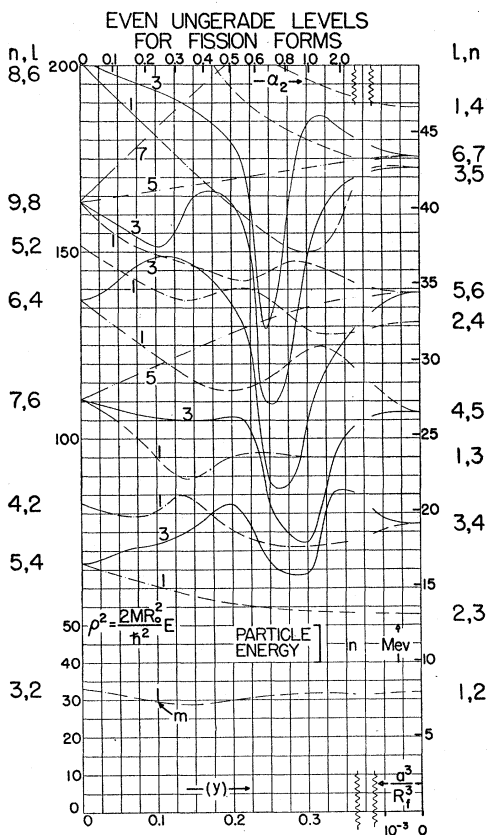


FIG. 20. Energy levels of even-ungerade symmetry inside a boundary of Frankel-Metropolis form.

The energy level diagram is consistent with the usual well known correlation principle: two levels are then and only then incapable of crossing—granted arbitrary deformation magnitude—when they belong at the same time to the same one of the four symmetry classes (here the even-ungerade class) and to the same value of  $m$ . This principle applies only so long as the system has axial symmetry. If instead the boundary were an ellipsoid with three unequal axes, then  $m$  would not be a good quantum number and *none* of the levels would cross which belong to a particular one of the four symmetry classes. For configurations near the original sphere, the energy levels  $E = (\hbar^2/2MR_0^2)\rho^2$  are obtained from the perturbation formula (Fig. 17),

$$\rho^2 = \rho_{nl}^2 \left[ 1 + 2\alpha_2 \frac{3m^2 - l(l+1)}{(2l-1)(2l+3)} \right].$$

Here the quantity  $\rho_{nl}$  is the  $(n-l)$ th root of the regular solution  $F(\rho)$  of the differential equation,

$$d^2F/d\rho^2 + [1 - l(l+1)/\rho^2]F = 0,$$

for the radial part of the wave function,

$$\psi(r, \theta, \phi) = r^{-1}F(kr)P_l^{(m)}(\cos\theta) \exp(im\phi).$$

All values of  $\rho_{nl}^2$  less than 200 [Tables of Spherical Bessel Functions, Vol. I (Columbia University Press, New York, New York, 1947)] follow:

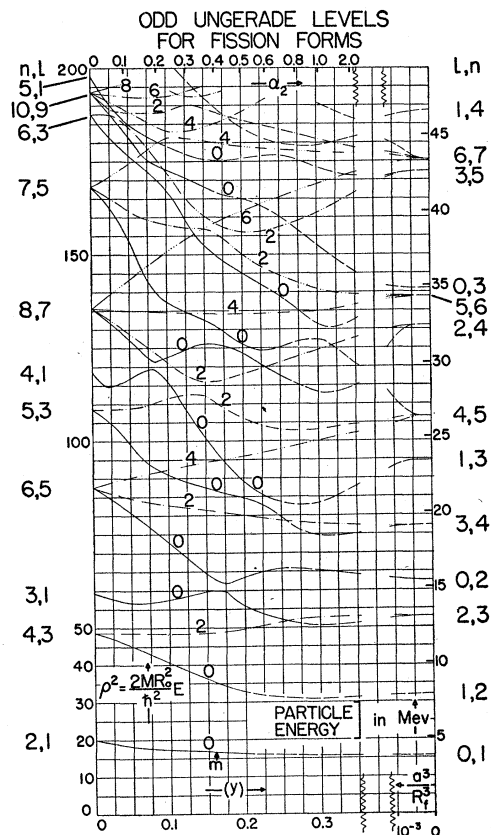


FIG. 21. Odd-ungerade levels in the Frankel-Metropolis sequence of forms.

Only the levels with  $m=0$  are here shown in full detail. The wave functions are taken to satisfy the equation  $\nabla^2\psi + k^2\psi = 0$  in the interior, and on the surface  $\psi = 0$  (infinite potential wall). W. Elsasser [J. phys. et radium 5, 625 (1934)] and H. Margenau [Phys. Rev. 46, 613 (1934)] have in this approximation obtained the level spacings for nucleons in spherical nuclei. This neglect of penetration of the wave function into the region of negative kinetic energy outside the boundary (finite potential wall) can be considered to be compensated approximately by appropriate small readjustment of the dimensions of the figure: normal displacement by the distance  $\hbar/[2M(W-E)]^{1/2}$ , where  $W$  is the height of the potential wall and  $E$  is the kinetic energy of the state in question. In detailed calculations (smooth curves) the wave function for odd-gerade levels with angular momentum  $m$  about the symmetry axis were written as the product of the factor  $\exp(im\phi)$  by

the sum

$$\sum C_l j_l(\rho r/R_0) P_l^{(m)}(\cos\theta),$$

where  $R_0$  is the original radius of the sphere and  $\rho^2 = 2MR_0^2 E/\hbar^2$  is the dimensionless measure of energy plotted in the figure. The sum goes over even values of  $l$  for the case of a level of even parity, and over odd  $l$  for odd parity. This function automatically satisfies the differential equation. Vanishing of the solution over the boundary,  $r/R_0 = f(\cos\theta)$ , as specified in Fig. 2, gives a continuous infinity of conditions on the infinitely many coefficients  $C_l$ . The approximation was made to use only five terms in the sum, and to require the vanishing of the sum only at the five points on the surface for which  $\mu = \cos\theta = \mu_s$ , with  $\mu_s = 0.19, 0.38, 0.57, 0.76, 0.95$  for ungerade levels, and  $\mu_s = 0.105, 0.315, 0.525, 0.735, 0.945$  for gerade levels. The resulting five equations for the five unknown coefficients  $C_l$  possess a solution when and only when  $\rho$  is such as to annul the determinant,

$$|j_l(\rho f_s) P_l^{(m)}(\mu_s)|,$$

where  $s = 1, 2, \dots, 5$  is the column index and  $l = 0, 2, 4, 6, 8$  is the row index, for example, for the case of  $m = 0$  and even parity, and for  $m = 0$  and odd parity  $l = 1, 3, 5, 7, 9$ . The functions  $j$  and  $P$  were generated in an IBM-CPC electronic calculator—the associated Legendre functions [divided by  $(1 - \mu^2)^{m/2}$ ] from their terminating power series expressions, the spherical Bessel functions  $j(x)$ , which satisfy the equation

$$\frac{1}{x^2} \frac{d}{dx} \left( x^2 \frac{dj}{dx} \right) + \left[ 1 - \frac{l(l+1)}{x^2} \right] j = 0,$$

from their standard power series expansions when the ratio  $x/(l + \frac{3}{2})^{\frac{1}{2}}$  was less than 5, and for larger values of the argument from the well known expressions  $j(x) = (\text{terminating polynomial in } 1/x) \sin x + (\text{terminating polynomial in } 1/x) \cos x$ . The roots,  $\rho$ , of the determinant were found by a refined scheme of trial and error. We are indebted for help in these calculations to Stewart Schlesinger, Seymour Parter, Max Goldstein, and others in Group T-1 of the Los Alamos Scientific Laboratory.

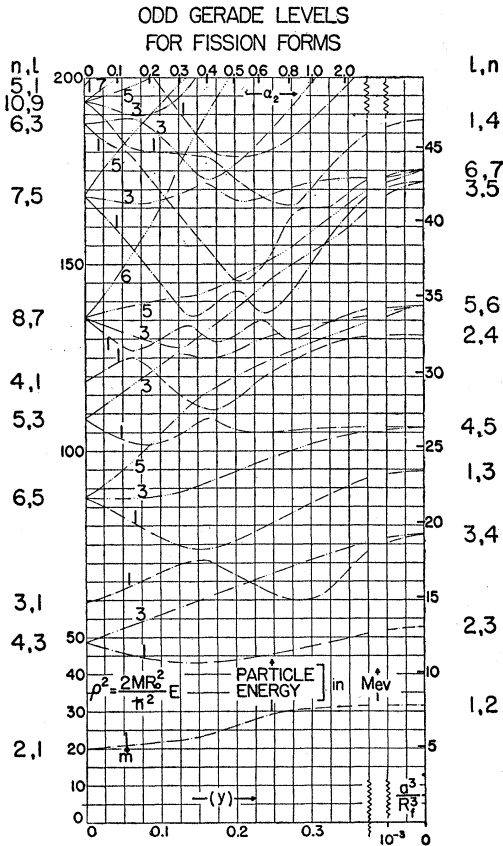


FIG. 22. Odd-gerade levels in the Frankel-Metropolis sequence of forms leading to fission.

Shown at the right in this and the three preceding figures are the levels for two spheres of radius  $R_f = R_0/2^{\frac{1}{2}}$ , connected by a circular orifice of radius,  $a$ , small compared with  $R_0$ . When  $a = 0$ , the levels are those of a sphere, and consequently the appropriate values of the dimensionless energy parameter  $\rho^2$  are  $2^{\frac{1}{2}}$  times those listed in the caption of Fig. 20. When the orifice is opened slightly, the wave functions in the two spheres join together, and two cases have to be recognized: gerade case—the wave functions in the two spheres join up so as to have no node at the point of join (mirror symmetry with respect to the plane of the orifice); ungerade case—node in the over-all wave function at the point of join (wave function antisymmetric with respect to mirroring in the orifice plane). A half-volume sphere contains up to a given energy (top of Fermi distribution) only approximately a half as many levels as the full volume sphere, so the doubling of number of states by reason of the two ways of joining at the window gives the right number of individual particle states for the system. The energies of the ungerade states are in first approximation independent of the size of the orifice opening (wave function vanishes at point of perturbation). On the other hand, the energies of the corresponding gerade states fall as the orifice is opened, the fractional magnitude of the drop being

$$(1/\rho^2) \delta(\rho^2) \approx -(2/3\pi)(2l+1)(a^2/R_f^2)$$

for states with  $m = 0$ , and much smaller (higher power of  $a/R_0$ ) for higher values of  $m$ . To derive this result, compare the gerade wave function  $\psi_0$  for the case of completely closed orifice and  $\psi_1$  for the case of small orifice opening. The two functions look alike except within distances of the order  $a$  from the center of the orifice.

There  $\psi_0 = r^{-1} F_1(kr) P_l^{(m)}(\cos\theta) \exp(im\phi)$  (in the left-hand sphere; the mirror image of this in the right-hand sphere) behaves for positive  $m$  approximately as  $\psi_0 = Qz^m \exp(im\phi)$ , where  $z$  is distance measured normally from the orifice towards the center of the left-hand sphere,  $\rho$  is the appropriate cylindrical polar coordinate, and the constant has the value  $Q = -R_f^{-1-m} k F_1'(kR_f) \times (l+m)!/2^m m!(l-m)!$ . In the case  $m = 0$  our approximation for  $\psi_0$  increases linearly with distance from the surface. We have to deal with the wave mechanical analog of a constant electric field. In electrical terms, opening the orifice now allows lines of force to leak out. Superposed on the linearly varying electric potential is another term—a local disturbance—which also satisfies Laplace's equation approximately: the bucklings of this term normal to the orifice and parallel to the plane of the orifice are opposite in sign and both very large compared to the net buckling,  $k_1^2$ . This net buckling we therefore neglect in considering the correction,  $\delta\psi = \psi_1 - \psi_0$ , in the wave function. Hence, we compute this difference by solving Laplace's equation subject to the boundary conditions: (1)  $\delta\psi$  falls off relative to  $\psi_0$  for large distances from the orifice; (2)  $\partial(\delta\psi)/\partial z$  vanishes over portions of the surface (here treated as flat) not pierced by the orifice; (3) over the orifice the correction term has such a normal derivative as to make  $\psi_1$  itself have zero derivative (condition of mirror symmetry):  $\partial(\delta\psi)/\partial z = -Q\rho^m \exp(im\phi)$ . General positive  $m$  is used in the last equation because nothing about the basic argument is peculiar to  $m = 0$ . The use of new coordinates, such that  $z = auv$ ,  $\rho = a[(1-u^2)(1+v^2)]^{\frac{1}{2}}$ , translates Laplace's equation to a form with separable solutions of the type  $P_n^{(m)}(u)f(v) \exp(im\phi)$ . Here the function  $f$  is such as to be annulled by the operator

$$\frac{d}{dv} (1+v^2) \frac{d}{dv} + \frac{m^2}{1+v^2} - n(n+1).$$

The original wave function  $\psi_0$ , not too far from the median plane, is of exactly this form, with  $n = m + 1$ , and with  $f(v)$  a multiple of  $P_{m+1}^{(m)}(iv)$ :

$$\psi_0 = Q a^{m+1} u (1-u^2)^{m/2} v (1+v^2)^{m/2} \exp(im\phi).$$

In the corresponding product expression for  $\delta\psi$ , everything must be the same except the function  $f_{m+1}^{(m)}(v)$ , which is now to fall off at large positive  $v$ :

$$\delta\psi \approx Q a^{m+1} u (1-u^2)^{m/2} \exp(im\phi) v (1+v^2)^{m/2} \times \int_0^\infty v^{-2} (1+v^2)^{-m-1} dv / \int_0^\infty v^{-2} [1 - (1+v^2)^{-m-1}] dv.$$

Here the definite integral in the denominator normalizes  $\delta\psi$  so as to satisfy the required boundary conditions. The change in wave number produced by the perturbation is found to first order by inserting in Green's accurate relation,

$$k_1^2 - k_0^2 = \int \psi_1^* (\partial\psi_0/\partial n) dS / \int \psi_1^* \psi_0 d(\text{vol}),$$

the expression for  $\psi_1 = \psi_0 + \delta\psi$  in terms of ellipsoidal coordinates

in the numerator,

$$\partial\psi_0/\partial n = -Qa^m(1-u^2)^{m/2} \exp(im\phi)$$

$$\psi_1^* = \delta\psi^* = Qa^{m+1}u(1-u^2)^{m/2} \exp(-im\phi) \frac{2 \cdot 2 \cdot 4 \cdot 6 \cdots (2m)}{\pi \cdot 3 \cdot 5 \cdot 7 \cdots (2m+1)},$$

and in the denominator replacing  $\psi_1^*$  by  $\psi_0^*$ ,

$$\int \psi_1^* \psi_0 d(\text{vol}) = (R_f/2) [F_1'(kR_f)]^2 [4\pi/(2l+1)] (l+m)!/(l-m)!$$

Thus we find for the shift in gerade levels due to a small orifice:

$$\frac{k_1^2 - k_0^2}{k_0^2} = -\frac{2(2l+1)(l+m)!}{\pi(l-m)!}$$

$$\times \frac{1}{1^2 \cdot 3^2 \cdot 5^2 \cdots (2m+1)^2 \cdot (2m+3)!} \left(\frac{a}{R_f}\right)^{2m+3}$$

This formula was used in constructing the right-hand portion of the diagrams for gerade levels.

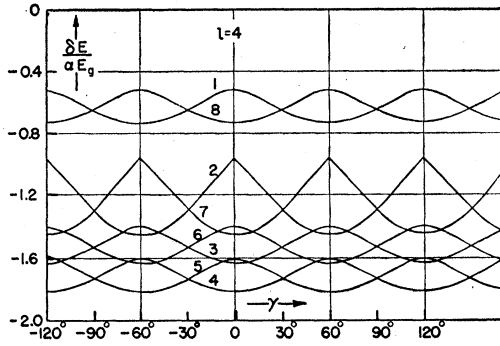


FIG. 23. Total nucleonic energy as a function of  $\gamma$ , for one to nine nucleons in states with  $l=4$ .

The total nucleonic energy of a many-particle closed shell configuration plus an incompletely filled  $g$  shell containing the indicated number of particles, for ellipsoidal deformations of small magnitude,  $\alpha$ , in the approximation of the idealized collective model, is  $E = E_0 + \alpha E_g f(\gamma) + c\alpha^2$ , where  $f(\gamma)$  is plotted here as a function of the shape parameter,  $\gamma$ , of Fig. 13, and  $E_0$ ,  $E_g$ , and  $c$  are constants,  $E_g$  being the kinetic energy of one nucleon with four units of angular momentum. The diagram has been drawn for simplicity as if nucleons had no spin and only 9 particles were required to fill the shell. The appropriate correction by a factor two is easily made. The quantity  $f(\gamma)$  is obtained by summing over the appropriate number of nucleons the corresponding individual particle coefficients already plotted in Fig. 17, taking in each case the lowest energy—or most negative coefficient—allowed by the Pauli principle. It is seen from the diagram how the quadrupole-producing force, as measured by the coefficient  $f(\gamma)$ , increases to a maximum for a half-filled shell and then decreases. Oblate deformations are favored at the beginning of the shell and cigar-like ones at the end. Of course, this discussion refers to intrinsic quadrupole moment, not the moment after averaging with respect to precession about the nuclear spin axis.

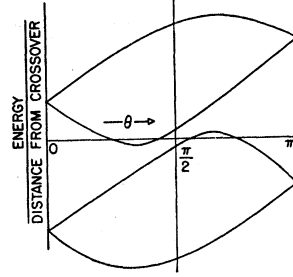
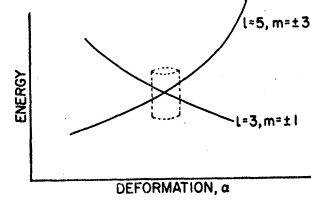


FIG. 24. Splitting of two double levels near a point of crossover.

Levels which cross without interaction for deformations of high symmetry experience a mutual repulsion for deformations of lower symmetry. For axially symmetric deformations the crossing levels are themselves ordinarily doubly degenerate except in the case  $m=0$ , so that four levels result from introduction of a slight ellipticity in the cross section of the otherwise axially symmetric form. The appropriate deformation coordinate  $\eta = \alpha \sin \gamma$  (Fig. 13) is perpendicular to the plane of the upper diagram. The cylinder sketched in perspective there cuts the four sheeted energy level surface in the four lines which are shown as functions of angle in the lower diagram. An example in point would be the crossing of the doubly degenerate level  $l=3, m=1$  by the level  $l=5, m=3$ . Details: Let  $\xi = \alpha \cos \gamma - \alpha_0$  denote the component of departure from the crossing point which is visible in the upper diagram. Then, near the crossing point, the energy matrix of the four level system, omitting unessential complications, has the form

$$H = \begin{vmatrix} s\xi + t\eta & 0 & f\eta & -g\eta \\ 0 & s\xi - t\eta & g\eta & -f\eta \\ f\eta & g\eta & -s\xi + u\eta & 0 \\ -g\eta & -f\eta & 0 & -s\xi - u\eta \end{vmatrix},$$

where  $s, t, u, f,$  and  $g$  are constants, and the diagonal elements represent the level locations in the absence of coupling between the one pair of levels and the other. We write  $\xi = r \cos \theta$ ,  $\eta = r \sin \theta$ , and  $(\text{energy})/r = y$ , and find the secular equation for the four plotted roots:

$$y^4 - [2s^2 \cos^2 \theta + (2f^2 + 2g^2 + t^2 + u^2) \sin^2 \theta] y^2 + 2s(u^2 - t^2) \times \cos \theta \sin^2 \theta y + s^4 \cos^4 \theta + s^2(2f^2 + 2g^2 - t^2 - u^2) \sin^2 \theta \cos^2 \theta + (g^2 - f^2 + ut)^2 \sin^4 \theta = 0.$$

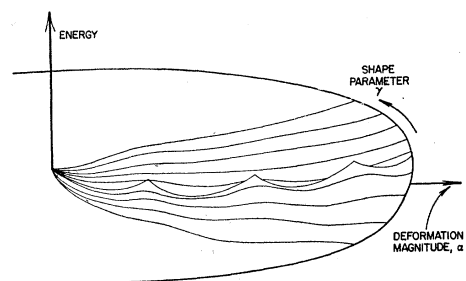


FIG. 25. Qualitative picture of inverted cones in lowest potential energy surface.

Here the lowest sheet of the multi-sheeted system potential energy surface is sketched qualitatively in its dependence on the ellipsoidal deformation parameters of Fig. 13. Only at the inverted funnels, i.e., only for prolate and oblate spheroidal deformations, which have  $\gamma = 0^\circ, 60^\circ, 120^\circ$ , etc., does this surface touch the one above it. That surface in turn (not shown) possesses both upright and inverted funnels. Important in affecting the probability of slippage from one surface to the one above or below it is the general curvature of the surface and particularly the size of the region upon this surface which is accessible to the representative point of the system when it has any given amount of total (potential plus oscillational kinetic) energy.

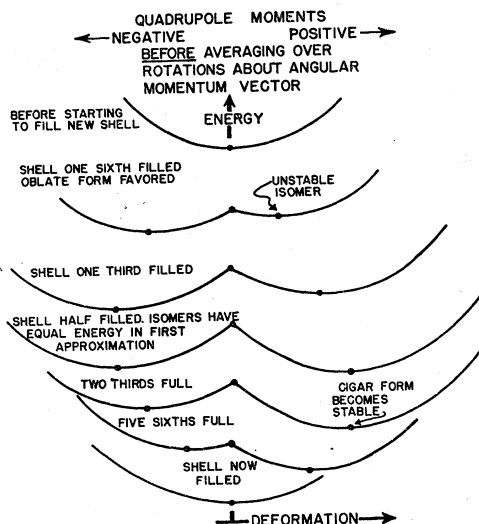


FIG. 26. Deformation potentials and quadrupole moments expected as a function of filling of shells.

This is a qualitative picture of the effect of shell building on the intrinsic quadrupole moments, i.e., on the shape of the nucleus as it affects the motion of particles inside, not as it appears to an atomic electron after averaging over nuclear precession—an averaging which cuts to zero the quadrupole moment observed in atomic spectra when the nuclear spin is  $\frac{1}{2}$  or 0 (even-even nuclei). Several particles in a partly filled shell bring about a deformation in the same way that one does (Fig. 6), with these amendments: (a) The particles cooperate. Coupling with the wall makes it energetically preferable for the second particle's orbit to line up in the plane of the first's. In first approximation the deformation thereby produced is twice as great, and the energy lowering (with respect to the spherical configuration) four times as large, as for one particle. (b) With increasing number of particles the quadrupole-producing force (see, for example, Fig. 23) goes through a maximum, showing a certain symmetry between the start of filling (oblate forms energetically preferred) and the near completion of the shell (prolate form lower in energy). (c) In the region extending roughly from  $\frac{1}{3}$  filling to  $\frac{2}{3}$  completion, both pancake- and cigar-like forms lie at relative minima of the energy curves, suggesting

the possibility of configurationally-isomeric forms of the same nucleus. (d) All these considerations assume that the contribution to the deformation potential from all the residual, closed shell, nucleons is a quadratic function of the deformation parameter,  $\alpha$ . In actuality a sufficiently large distortion will rearrange the order of levels and even the term "closed shell" will no longer have any simple meaning. On this account the suggested regular variation of quadrupole moment with progress of the filling will no longer necessarily be a reasonable expectation.

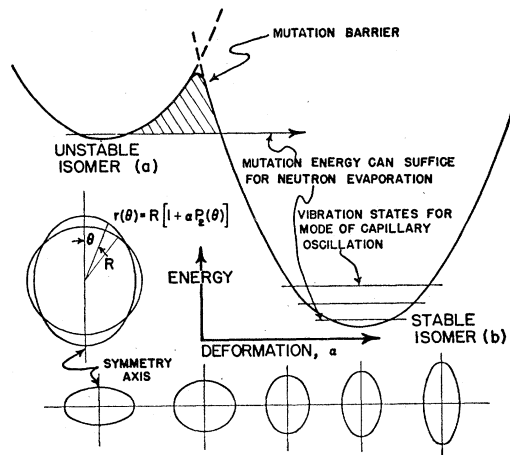


FIG. 27. Nuclear mutation forms.

The phenomenon of nuclear mutation from oblate to prolate form, or conversely, according to direction of energy release, is suggested by the considerations of Fig. 26 as conceivable for nuclei about  $\frac{1}{3}$  or  $\frac{2}{3}$  the way through the process of filling up a long shell. For deformations as great as those required to give the effect in question, it seems unreasonable to believe that the deformation energy of the closed shells is still proportional to  $\alpha^2$ . Consequently this diagram has to be viewed as only an idealized schematization of the actual potential energy surface, and this only for walls of spheroidal character (axial symmetry). The spherical configuration represents a peak in the potential barrier against mutation from the stable to the unstable isomeric form.

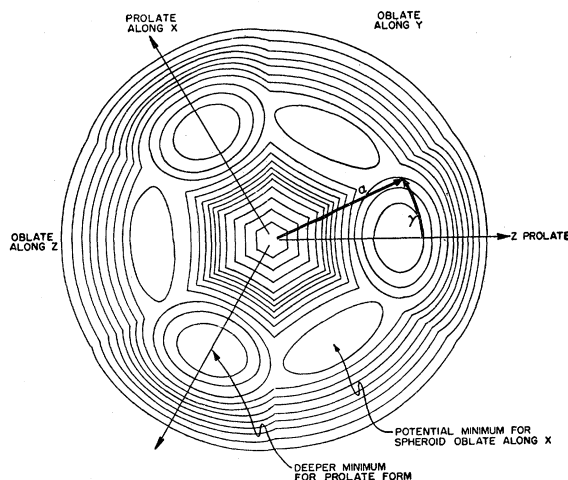


FIG. 28. Contour plot of energy as a function of the deformation variables  $\alpha$  and  $\gamma$  of Fig. 13 for the ground state of a heavy nucleus with a shell which is little more than half full.

This energy is idealized as the sum of surface energy and the energies of the single particle states which lie lowest in a potential well of the given shape. The minima of the total energy occur

when the angular momenta of the nucleons lie as nearly parallel-antiparallel to the symmetry axis as possible (oblate form) and when the angular momenta lie as nearly perpendicular as possible to the symmetry axis (prolate form). To pass from prolate to oblate form via the spherical form is very expensive of energy. The easiest route, as pointed out to us by Professor Edward Teller, is passage over the potential ridge in the diagram. On this ridge the system has the form of an ellipsoid with three unequal principal axes.

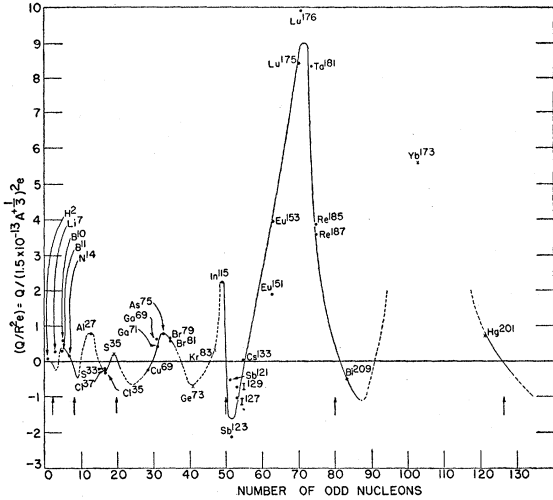


FIG. 29. Effective nuclear quadrupole moments for hyperfine structure divided by the square of the nuclear radius  $(1.5 \times 10^{-13} A^{1/2})^2$ .

The known moments of odd-proton nuclei and odd-neutron nuclei (excepting  $Li^6$  and  $Cl^{35}$ ) are plotted as circles against the number of protons, and the moments of odd-neutron nuclei as crosses against the number of neutrons. The arrows indicate closing of major nucleon shells. The solid curve represents regions where quadrupole moment behavior seems established, the dashed curve more doubtful regions. This figure and caption are taken from the report of Townes *et al.* (reference 11). See Fig. 5 for relation between  $Q$  and  $\alpha$ .

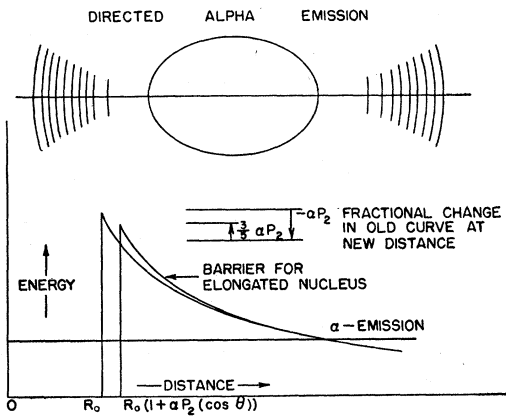


FIG. 30. Directed alpha-decay.

An alpha-active nucleus will ordinarily have a quadrupole moment and will therefore emit preferentially from the outermost parts of its surface, where the peak of the potential energy barrier has been lowered. The reduced wavelength,  $\lambda = \lambda/2\pi$ , of a 5-Mev alpha-particle is  $1 \times 10^{-13}$  cm, a quantity small compared to a typical nuclear diameter of  $18 \times 10^{-13}$  cm. Consequently the directionality of emission will have a definition relative to the nuclear axes which is ordinarily better specified than the correlation of the

nuclear axes themselves relative to a direction fixed in space. In particular a nuclear state of angular momentum zero will be characterized by alpha-emission isotropic in the laboratory frame of reference, however anisotropic the surface emissivity is in the nuclear frame of reference. The maximum observable directionality will be found when at the same time the nuclear spin,  $I$ , is large, when the projection,  $I_z$ , of  $I$  upon a chosen space axis (strong magnetic field, low temperature) is  $\pm I$ , and when the nucleus in question is on a time average prolate with respect to the nuclear spin axis  $I$ . Then emission will take place preferentially parallel and antiparallel to the magnetic field. Under the same conditions observations of maximum probability for directions perpendicular to the magnetic field will indicate an oblate ellipsoid.

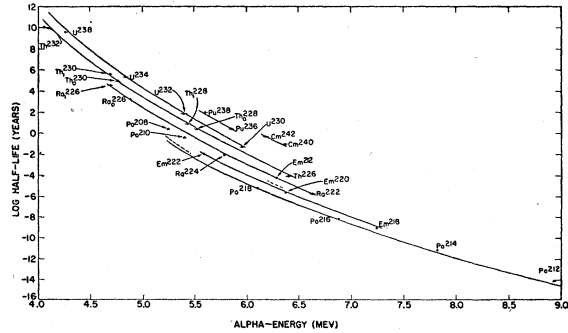


FIG. 31. Alpha-particle half-lives versus alpha-energy.

The Geiger-Nuttall relationship between alpha-particle energy and life time with respect to alpha-particle decay is not a one-to-one correspondence, as shown in this recent compilation of results for even-even nuclides taken from Perlman, Ghiorso, and Seaborg [Phys. Rev. 77, 26 (1950)]. For other compilations and analyses of alpha-decay data, see the references cited in this paper, including A. Berthelot, J. phys. et radium 3, 17 (1942); also I. Kaplan, Phys. Rev. 81, 962 (1951) and J. M. Blatt and V. F. Weisskopf, *Theoretical Nuclear Physics* (John Wiley and Sons, Inc., New York, 1952), Chapter XI.] Perlman *et al.* give similar curves for the other classes of nuclei. Nor should it be. The Gamow treatment of barrier penetration gives a formula [see also Rasmussen, Thompson, and Ghiorso, Phys. Rev. 89, 33 (1953)]:

$$\left( \begin{array}{c} \text{probability} \\ \text{per second of} \\ \text{alpha-decay} \end{array} \right) = \left( \begin{array}{c} \text{intrinsic alpha} \\ \text{emission prob-} \\ \text{ability} \end{array} \right) \times \exp\{-2(2Z/137)(2M_{\alpha}c^2/E_{\alpha})^{1/2}f(u)\},$$

in which there enters not only the alpha-particle energy (we look apart from the well-known small corrections for the finite mass and recoil energy of the residual nucleus), but also the charge and radius of the nucleus:

$$u = \frac{E_{\alpha}}{\text{barrier height}} = \frac{E_{\alpha}R_0}{2Ze^2} = \frac{E_{\alpha}A^{1/2}}{4mc^2Z};$$

$$f(u) = \arccos u^2 - u^2(1-u)^{1/2}.$$

Nevertheless, the fluctuations of the points of such diagrams away from the curve for the appropriate  $Z$  appear too great and also too irregular to be laid solely to the Gamowian dependence upon  $Z$  and  $A$ . Binding anomalies for nuclei near shell limits give irregular variations of  $E_{\alpha}$  from element to element, but such variations in energy cannot by themselves account for deviations from the barrier penetration formula. However, the existence of quadrupole moments necessarily implies a deviation from the Gamow formula which will be very sensitive to departures from closed-shell structure—or more directly, sensitive to the nuclear deformations called forth by asymmetric pressure against the surface by nucleons in unfilled shells. For a distortion  $R = R_0[1 + \alpha P_2(\cos\theta)]$  the potential energy of an alpha-particle outside the nucleus is altered in first order to

$$V = (2Ze^2/r)[1 + (3R_0^2/5r^2)\alpha P_2(\cos\theta)].$$

Re-evaluating the integral

$$(2/\hbar) \int_{R(\theta)}^{\text{turning point}} [2M_{\alpha}(V - E_{\alpha})] dr,$$

in the exponent of the penetration factor, we find that the factor  $f(u)$  is changed by the amount

$$\delta f(u) = -(2/5)\alpha P_2 (\cos\theta)u^3(1-u)^3(2-u).$$

This consideration neglects the fact that the area of the surface from which significant emission takes place has been cut down from  $4\pi R_0^2$  to some smaller amount. This reduction we neglect compared to the improvement in penetration through the thinner barrier. Accordingly we insert for the angle  $\theta$  the value at the point of maximum emission:

$$\begin{aligned} -\alpha P_2 (\cos\theta) &= -\alpha \text{ for prolate ellipsoids;} \\ -\alpha P_2 (\cos\theta) &= \alpha/2 \text{ for oblate ellipsoids;} \\ \delta f(u) &= \text{a negative number in both cases.} \end{aligned}$$

The factor of improvement in decay rate made by the ellipsoidal deformation is

$$\exp -2\left(\frac{2Z}{137}\right)\left(\frac{2M\alpha c^2}{E}\right)^{1/2} \delta f(u),$$

or, for  $Z=90$ ,  $A=234$ , barrier height of 30 Mev before deformation, decay energy  $E=5$  Mev, rest energy of alpha-particle  $Mc^2=3700$  Mev, with the dimensionless ratio  $u=5$  Mev/30 Mev,

$$\exp -101\delta f = \exp -101 \times \begin{cases} \exp 28\alpha \text{ (prolate)} \\ \exp -14\alpha \text{ (oblate)} \end{cases}.$$

Thus a deformation which stretches the axis by the fractional amount  $\alpha=0.1$ —a value well within the range indicated by observed quadrupole moments—will be expected to increase the decay rate by a factor of roughly  $e^{2.8}=16$ . Of course, from the observed decay rate associated with a given alpha-emission process one cannot determine *both* the nuclear radius and the quadrupole moment. One gets only some combination of the two, which we have to identify—in the absence of other effects—with the quantity generally known as the effective radius. Between it, the radius  $R_0$  of a sphere of the same volume, and the quadrupole moment exists the relation

$$R_{\text{eff}} = (2Ze^2/E_\alpha)u_{\text{eff}} = (2Ze^2/E_\alpha)[u + \delta f/(df/du)] \\ = R_0[1 + (2/5)(2-u)\alpha P_2],$$

or with sufficient accuracy for most nuclei

$$(R_{\text{eff}} - R_0)/R_0 = \begin{cases} 0.533\alpha \text{ (prolate)} \\ -0.267\alpha \text{ (oblate)} \end{cases}.$$

These considerations have an interesting application to the alpha-activity of samarium. The alpha-energy has been measured as 2.18 Mev by W. P. Jesse and J. Sadauskis [Phys. Rev. **78**, 1 (1950)] and the activity has been assigned to  $\text{Sm}^{147}$ . [A. J. Dempster, tentative result given in Argonne National Laboratory Report ANL-4355, 1949 (unpublished); Rasmussen, Reynolds, Thompson, and Ghiorso, Phys. Rev. **80**, 475 (1950)]. We are indebted for discussion of this case to Professor I. Perlman, who with a nuclear radius of  $7.81 \times 10^{-13}$  cm, such as would normally be expected, calculates [I. Perlman and T. J. Ypsilantis, Phys. Rev. **79**, 30 (1950)] a half-life  $2.9 \times 10^{12}$  years (private communication) compared to a measured half life 10–20 times shorter. Perlman also concludes that a 80-kev increase in the value of the decay energy, or a roughly 10 percent increase in nuclear radius, would resolve the discrepancy. Alternatively we can say that a prolate distortion of 10 percent/0.533 = 19 percent or an oblate deformation of 10 percent/0.267 = 37 percent would account for the situation, assuming that  $7.81 \times 10^{-13}$  cm is indeed an appropriate figure for the radius of a sphere of the same volume. Quadrupole deformations of these general magnitudes are found experimentally for nuclei in the general neighborhood of samarium. P. Brix and H. Kopfermann [Z. Physik **126**, 344 (1949)] mention their reasonable bearing on the alpha-lifetime of this substance. Of course the shortening of life that occurs for  $\text{Sm}^{147}$  in extreme measure must also occur for most other nuclei in greater or lesser degree. Consequently the nuclear radii which have been found from analysis of alpha-decay must on this account at least be larger on the average than the appropriate volume-equivalent spherical radii. For this reason the nuclear radii reported [Phys. Rev. **77**, 26 (1950)] for polonium isotopes, previously thought of as abnormally low, are perhaps now to be considered as the more nearly normal figures. Obviously direct measurements of the quadrupole moments of alpha-active nuclei—where possible—are most relevant to the further discussion of this topic. Mention should also be made of anomalies in the isotope shifts in atomic spectra, (reference 25), which may be in good measure explained by increase in electron-

effective nuclear radius *via* ellipsoidal deformations, according to recent interesting discussions with Dr. Lawrence Willets of Princeton. From the characteristic or “Chang” radiation given out when mu-mesons drop from  $2p$  to  $1s$  Bohr orbits it is not impossible that one may be able to develop another experimental tool to study nuclear quadrupole moments—closely related to the study of atomic spectra, but with energy shifts and splittings percentage-wise enormously greater than in the atomic case because of the larger fraction of time spent within the nucleus by the meson. Alpha-lifetimes are affected not only by the Gamow-Gurney-Condon penetration factor, but also by the Franck-Condon principle; not only by the equilibrium deformation in the original nucleus, but also by the *difference* in normal shapes between initial and final nucleonic states. If this difference is large, the residual nucleus will have little chance to be formed in the state of zero-point oscillation. On this account there will be a reduction in alpha-decay rate not taken into account in the above discussion. Transitions to the lowest vibration state will be inhibited relative to transitions to those vibration states favored by the Franck-Condon principle. This circumstance must evidently be taken into account in interpreting the fine structure of typical alpha-spectra.

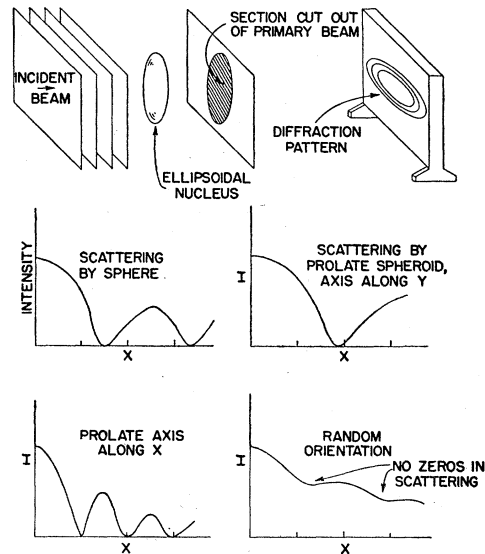


FIG. 32. Diffraction by ellipsoidal nucleus.

Will not diffraction or “shadow” scattering by an ellipsoidal nucleus be sufficiently different from that by a spherical nucleus to allow observation of the difference? This interesting question was raised in discussion with us by Dr. J. B. Cladis of Los Alamos. The qualitative analysis in the figure shows that the ratio of minima to maxima in the diffraction by randomly oriented nuclei of the given species is indeed a sensitive measure of nuclear deformation, being zero (in the diffraction-idealization of scattering) only for spherical scattering centers. A quantitative analysis can be made along the following lines. Let  $f$  and  $g$  be the principal axes of the ellipsoid as projected in imagination onto the plane of the receptor, and let the  $X$  and  $Y$  axes be oriented parallel to the  $f$  and  $g$  axes. The absence of the ellipsoidal piece from the transmitted beam produces the same scattered wave as if this piece alone were present. A portion  $dS = d\xi d\eta$  of its area makes a contribution to the scattering amplitude at a distance  $r_{12}$  and at not too great an angle  $\theta$  to the primary beam equal to  $(-ik/2\pi r_{12}) \times \exp(ikr_{12})dS$ , where  $k$  is the wave number. The differential scattering cross section is the square of  $r$  times the absolute value of the integrated scattering amplitude:

$$d\sigma/d\Omega = \left| (k/2\pi) \int \exp[-ik(x\xi + y\eta)/r] d\xi d\eta \right|^2.$$

Here the direction of the scattering is indicated by the ratios  $x/r$  and  $y/r$ . We write  $\xi = fu \cos\theta$ ,  $\eta = gu \sin\theta$ , and integrate first over

$\theta$ , then over  $u$  from 0 to 1, finding

$$d\sigma/d\Omega = \left\{ \frac{kfgJ_1 \left[ \frac{(k^2 f^2 x^2/r^2 + k^2 g^2 y^2/r^2)^{1/2}}{(k^2 f^2 x^2/r^2 + k^2 g^2 y^2/r^2)^{1/2}} \right]}{(k^2 f^2 x^2/r^2 + k^2 g^2 y^2/r^2)^{1/2}} \right\}^2$$

for the scattering for one orientation of the ellipsoid. A superposition of such curves gives the distribution which is to be compared with observation. Richardson, Ball, Leith, and Moyer [Phys. Rev. 86, 29 (1952)] first mentioned the existence of this effect which with present experimental accuracy remains undetected.

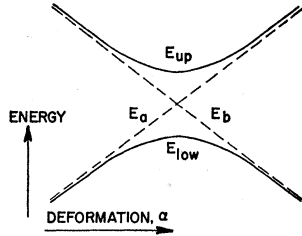


FIG. 33. Behavior of two levels at a point of near cross-over,  $\alpha = \alpha_0$ .

The levels, as they would be in the vicinity of cross-over in absence of interaction, are

$$E_a = E_0 + a(\alpha - \alpha_0); \quad E_b = E_0 + b(\alpha - \alpha_0).$$

The coupling which brings about the interaction is  $H_{ab} = H_{ba}$ ; its dependence upon  $\alpha$  is neglected in immediate neighborhood of  $\alpha_0$ . The actual wave function for a stationary state of the system is

$$\psi = A\psi_a + B\psi_b.$$

The equation for determination of coefficients  $A$  and  $B$  and energy value  $E$  in case of any fixed value of the deformation parameter,  $\alpha$ , is

$$\begin{aligned} i\hbar\dot{\psi} &= E\psi = H\psi, \\ EA &= E_a A + H_{ab}B, \\ EB &= H_{ba}A + E_b B. \end{aligned}$$

The two eigenvalues of the energy are shown in the diagram:

$$\begin{aligned} E_{up} &= \left( \frac{1}{2}E_a + \frac{1}{2}E_b \right) + \left\{ \left( \frac{1}{2}E_a - \frac{1}{2}E_b \right)^2 + |H_{ab}|^2 \right\}^{1/2}, \\ E_{low} &= \left( \frac{1}{2}E_a + \frac{1}{2}E_b \right) - \left\{ \left( \frac{1}{2}E_a - \frac{1}{2}E_b \right)^2 + |H_{ab}|^2 \right\}^{1/2}. \end{aligned}$$

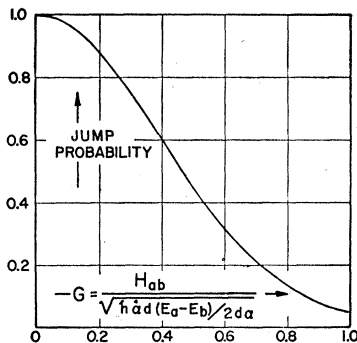


FIG. 34 Probability of transition from state  $\psi_a$  to state  $\psi_b$  when the deformation  $\alpha$  passes through the neighborhood of the cross-over,  $\alpha_0$ , (Fig. 33) at the fixed speed  $\dot{\alpha}$  (reference 27).

The probability of a jump is very small when the interaction  $H_{ab}$  between the levels is very weak, or when the rate of deforma-

tion,  $\dot{\alpha}$ , is very large, or both. Then the system, if originally in the state  $\psi_a$  with energy  $E_a$ , will have high probability to be in the same state,  $\psi_a$ , after deformation has carried the system through the region of cross-over. In other words, there will be a high probability for a jump to take place from the lower level,  $E_{low}$ , to the upper level,  $E_{up}$ , as in other familiar cases of nonadiabatic excitation. The opposite will be the case for strong interaction, or slowly varying deformation, or more generally, for large values of the dimensionless "interaction parameter"  $G$ , defined by

$$G^2 = \frac{|H_{ab}|^2}{\hbar \dot{\alpha} d (E_a - E_b) / 2 d \alpha}.$$

The detailed dependence of transition probability upon  $G$  is found by considering the equation

$$i\hbar\dot{\psi} = H(t)\psi,$$

or

$$\begin{aligned} i\hbar\dot{A} &= E_a(t)A + H_{ab}B, \\ i\hbar\dot{B} &= H_{ba}A + E_b(t)B. \end{aligned}$$

To translate into dimensionless variables, write

$$\begin{aligned} A(t) &= f(t) \exp[-i(E_a + E_b)t/2\hbar], \\ B(t) &= g(t) \exp[-i(E_a + E_b)t/2\hbar], \end{aligned}$$

in order to abstract away from the unimportant general slope of the cone, and

$$t^2 = x^2 2\hbar / (a-b)\dot{\alpha},$$

where  $a-b$  represents the difference in slope of the two unperturbed potential energy curves,  $d(E_a - E_b)/d\alpha$ . Also assume  $H_{ab}$  is real and positive, since any complex argument present in  $H_{ab}$  can always be absorbed into the probability amplitudes,  $A$  and  $B$ . The origin of time is chosen as the moment when the deformation arrives at the cross-over point,  $\alpha = \alpha_0$ . The problem is then to find for very large positive times the value of the probabilities  $|f|^2$  and  $|g|^2$  of being in the states  $a$  and  $b$  from the differential equations,

$$\begin{aligned} idf/dx &= xf + Gg, \\ idg/dx &= Gf - xg; \end{aligned}$$

or from the equivalent single second-order equation,

$$d^2 f/dx^2 + (G^2 + x^2 + i)f = 0,$$

subject to the initial condition that at  $t = -\infty$ , or  $x = -\infty$ ,

$$\begin{aligned} f &\sim \exp[-(ix^2/2) - (iG^2/4) \ln 2x^2], \\ g &\sim 0. \end{aligned}$$

The solution is

$$\begin{aligned} f &= (2\pi)^{-1/2} \int_0^\infty dy \exp[ix^2/2 - y^2/2 - (iG^2/2) \ln y] \\ &\quad \times \{ \exp[\pi G^2/8 - (1-i)xy] + \exp[-3\pi G^2/8 + (1-i)xy] \}, \end{aligned}$$

and behaves asymptotically for large positive time ( $x = +\infty$ ) as

$$\exp[-\pi G^2/2 - ix^2/2 - (iG^2/4) \ln 2x^2].$$

The probability of a jump having taken place is evidently

$$J(G) = |f_{final}|^2 / |f_{initial}|^2 = \exp(-\pi G^2).$$

The values of the function are plotted in the figure. It is to be noted that this analysis of the transition probability treats the nucleonic motion in appropriate quantum-mechanical terms: a wave function  $\psi$ , or probability amplitudes  $A$  and  $B$  of being in states  $\psi_a$  and  $\psi_b$ . However, the progress of the deformation itself is treated as a pure classical motion:  $\alpha = \dot{\alpha}t$ . This procedure is ordinarily justifiable because the mass of the individual nucleon is so small compared to the mass of the capillary oscillator.

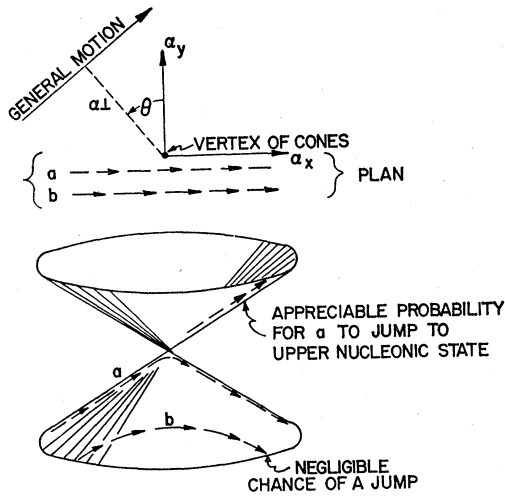


FIG. 35. Transition cross section for energy surfaces in conical contact.

This figure illustrates the concept of effective cross section for the jump from one potential energy surface to another, as first introduced by Teller [reference 24; F. O. Rice and E. Teller, *J. Chem. Phys.* 6, 489 (1938)] in connection with the vibrations of polyatomic molecules. Vertically is plotted the energy. In the two horizontal directions go two of the several coordinates which are required to describe a deformation. The two potential energy surfaces meet in a double cone, which in the present example is supposed to be circular in cross section, for sake of simplicity. Represented here in magnified form is only a very small portion of the two potential energy surfaces (see Fig. 25 for other details). The kinetic energy with which the collective oscillation is endowed is considered to be large in comparison with any of the energies seen here. Consequently, the deformation is idealized as proceeding in a direction and at a rate,  $\dot{\alpha}$ , uninfluenced by this minor local irregularity in the potential energy surface (plan view). When the oscillator coordinates pass close to the vertex of the cone; that is, when the representative point of the system has a small impact parameter,  $\alpha_{\min}$ , there is an appreciable chance for the nucleonic state of the system to jump from the lower surface to the upper surface (case *a*). When the oscillator coordinates stay far from the critical value, the chance of a jump is negligible (case *b*). When the state of the system executes repeated oscillations, the representative point of the system carries out a Lissajous type of motion (not shown) in plan view. In this case the probability of a jump is best stated in statistical form, in terms of the concept of "cross section" for a jump. In the present case this cross section,  $\sigma$ , has the dimensions of the deformation parameter,  $\alpha$ , raised to the first power, for the space of the motion itself is only two dimensional. From dimensional arguments Teller showed that

$$\sigma = \text{const}(\hbar\dot{\alpha}/s)^{\frac{1}{2}},$$

where  $s$  is the slope of the circular cone. The value of the cross section also follows directly from the jump probability,  $J(G)$ , of Fig. 34:

$$\sigma = \int_{-\infty}^{+\infty} J(G) d\alpha_L,$$

where  $\alpha_L$  is the impact parameter or the distance of closest approach. Let the deformation  $\alpha$  be measured away from the center of the circular cone as origin, so that (Fig. 34):

$$\begin{aligned} E_a - E_b &= 2s\alpha_x, \\ H_{ab} &= s\alpha_y, \\ E_{\text{up}} - E_{\text{low}} &= s(\alpha_x^2 + \alpha_y^2)^{\frac{1}{2}} = s\alpha, \\ G^2 &= \alpha_y^2 s / \hbar\dot{\alpha}. \end{aligned}$$

Integration gives for Teller's constant in the expression for the cross section the value

$$\text{const} = \int_{-\infty}^{+\infty} J(G) dG = 1.$$

In the more general case where the two potential energy surfaces

meet in tilted cones, elliptical rather than circular in cross section, the axes  $x$  and  $y$  can still be oriented to lie along the principal axes of the ellipse,

$$\begin{aligned} E_{\text{up}} &= c_1\alpha_x + c_2\alpha_y + (s_x^2\alpha_x^2 + s_y^2\alpha_y^2)^{\frac{1}{2}}, \\ E_{\text{low}} &= c_1\alpha_x + c_2\alpha_y - (s_x^2\alpha_x^2 + s_y^2\alpha_y^2)^{\frac{1}{2}}. \end{aligned}$$

Directions of incidence of the representative point of the collective oscillator are now inequivalent and have to be considered separately:

$$\begin{aligned} \alpha_x &= \dot{\alpha}t \cos\theta - \alpha_L \sin\theta, \\ \alpha_y &= \dot{\alpha}t \sin\theta + \alpha_L \cos\theta. \end{aligned}$$

Then

$$G^2 = \frac{(s_x^2 \sin^2\theta + s_y^2 \cos^2\theta) \alpha_L^2}{\hbar\dot{\alpha}(s_x^2 \cos^2\theta + s_y^2 \sin^2\theta)^{\frac{1}{2}}}$$

the cross section for incidence in the direction  $\theta$  is

$$\sigma_\theta = (\hbar\dot{\alpha})^{\frac{1}{2}} (s_x^2 \cos^2\theta + s_y^2 \sin^2\theta)^{\frac{1}{2}} (s_x^2 \sin^2\theta + s_y^2 \cos^2\theta)^{-\frac{1}{2}},$$

and the effective cross section is found by averaging this expression over all angles of incidence (Lissajous motion).

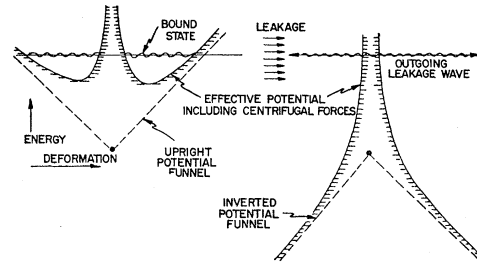


FIG. 36. Probability of a radiationless jump for system bound in cone of intersurface contact.

We consider here the exceptional case where the amount of energy in the collective oscillation is so small, and the potential energy surface is so shaped, that the system oscillates about in the neighborhood of the funnel's mouth with only a few quanta of vibrational energy. In this case both the nucleonic and the collective oscillation have to be treated quantum-mechanically. The system behaves in first approximation as if bound in a stable conical potential, with characteristic energy levels. In next approximation it is necessary to allow for a characteristic probability to switch over to an unstable potential energy surface, without change in total energy, but with great increase in kinetic energy. From the results of the quantum-mechanical analysis can be presumably derived, in the case of large quantum numbers, the same formula for the cross section which is derived and discussed in Fig. 35. Details follow for the case of a right circular cone of slope  $dE/d\alpha = s$ . Here  $\psi_a(\alpha_x, \alpha_y)$  represents the probability amplitude for the oscillator coordinates to have the values  $\alpha_x$  and  $\alpha_y$  and for the nucleonic system to be in the state  $a$ ; similarly for  $\psi_b$ . Then the wave equation for a stationary energy state of the whole system is

$$\begin{aligned} E\psi_a &= -\frac{\hbar^2}{2M_\alpha} \left( \frac{\partial^2 \psi_a}{\partial \alpha_x^2} + \frac{\partial^2 \psi_a}{\partial \alpha_y^2} \right) + s\alpha_x \psi_a + s\alpha_y \psi_b, \\ E\psi_b &= -\frac{\hbar^2}{2M_\alpha} \left( \frac{\partial^2 \psi_b}{\partial \alpha_x^2} + \frac{\partial^2 \psi_b}{\partial \alpha_y^2} \right) + s\alpha_y \psi_a - s\alpha_x \psi_b, \end{aligned}$$

where  $M_\alpha$  is the coefficient in the classical expression,  $\frac{1}{2}M_\alpha\dot{\alpha}^2$ , for the kinetic energy of the oscillator. We write

$$\begin{aligned} \alpha_x &= (\hbar^2/2M_\alpha E)^{\frac{1}{2}} u \cos\theta, \\ \alpha_y &= (\hbar^2/2M_\alpha E)^{\frac{1}{2}} u \sin\theta, \\ \beta &= \hbar s / (2M_\alpha E^{\frac{1}{2}})^{\frac{1}{2}}, \end{aligned}$$

and use the circular symmetry of the system to separate variables:

$$\begin{aligned} \psi_a &= u^{-\frac{1}{2}} [F(u) \cos\frac{1}{2}\theta + G(u) \sin\frac{1}{2}\theta] \exp(im\theta), \\ \psi_b &= u^{-\frac{1}{2}} [F(u) \sin\frac{1}{2}\theta - G(u) \cos\frac{1}{2}\theta] \exp(im\theta), \end{aligned}$$

finding the radial wave equations

$$\begin{aligned} \frac{d^2 F}{du^2} + \left[ 1 - \beta u - \frac{m^2}{u^2} \right] F &= -\frac{im}{u^2} G, \\ \frac{d^2 G}{du^2} + \left[ 1 + \beta u - \frac{m^2}{u^2} \right] G &= \frac{im}{u^2} F. \end{aligned}$$

In absence of the coupling term on the right the first equation describes the motion of a system of the prescribed angular momentum in an upright funnel. The second equation describes the runaway motion of a system of the same energy and angular momentum under the action of the potential of an inverted funnel. The coupling term makes possible transitions from the stable state to the unstable state. The coupling term vanishes for the case  $m=0$ , contrary to what one might have expected from the classical analysis of Fig. 35, where the probability of a jump is the greater the smaller is the impact parameter. However, this classically founded expectation must be confirmed by detailed calculations of the jump probabilities for values of  $m$  greater than 0 from the above coupling terms. Despite the proportionality of these terms with  $m$ , the leakage probabilities fall off fast with  $m$ . These probabilities can in principle be evaluated by perturbation methods. We calculate  $F$  from the first equation neglecting the term in  $G$  on the right hand side. The eigenfunction  $F$  is then inserted on the right-hand side of the second equation to determine  $G$ :

$$G(u) = \left\{ \int_0^u G_1(u)G_2(v) + \int_u^\infty G_2(u)G_1(v) \right\} (im/v^2)F(v)dv,$$

where  $G_1$  and  $G_2$  are two independent solutions of the homogeneous equation for  $G$ , the first behaving as an outgoing plane wave at infinity, but irregular at the origin; and the second regular at the origin. The normalization is chosen so that

$$G_2 dG_1/du - G_1 dG_2/du = 1.$$

For large  $u$  these functions have the form

$$G_1 \doteq - \left(1 + \beta u - \frac{m^2}{u^2}\right)^{-\frac{1}{2}} \exp \left[ i \left\{ \frac{\pi}{4} + \int_{u_{\min}}^u \left(1 + \beta u - \frac{m^2}{u^2}\right)^{\frac{1}{2}} du + \delta \right\} \right],$$

$$G_2 \doteq \left(1 + \beta u - \frac{m^2}{u^2}\right)^{-\frac{1}{2}} \sin \left[ \frac{\pi}{4} + \int_{u_{\min}}^u \left(1 + \beta u - \frac{m^2}{u^2}\right)^{\frac{1}{2}} du + \delta \right],$$

where  $\delta$  is the correction to the phase shift of the J.W.K.B. approximation. The probability per second,  $A$ , for transition from the upper potential energy surface to the lower one is found by comparing the flux of particles outgoing in  $G$  asymptotically at large  $u$  with the number of particles bound in state  $F$ :

$$A = 2\pi [G(u)^2 du/dt]_{u=\infty} / 2\pi \int F^2(u) du,$$

$$= \frac{2E}{\hbar} \left[ \int_0^\infty G_2(v) (m/v^2) F(v) dv \right]^2 / \int_0^\infty F^2(u) du.$$

The dependence of transition probability upon the quantum number  $m$  of rotatory oscillation is derivable by semiclassical arguments in the case of small  $m$  and large energy. Then the transition occurs—if at all—when the representative point in  $\alpha$ -space is near its point of closest approach,  $\alpha = \alpha_{\min}$ . The point is then describing a nearly rectilinear path. Consequently it is appropriate to use the previously derived formula for the probability of a jump in a single pass (Fig. 35):

$$\exp(-\pi G^2) = \exp(-\pi s^2 \alpha_{\min}^2 / \hbar \dot{\alpha} s).$$

The number of passes per unit time in the periodic orbit of the representative point follows from the classical mechanics of a system with energy  $E$ , mass  $M_\alpha$  and angular momentum  $m\hbar$  moving in a conical potential,  $V = s\alpha_r$ :

$$\text{Period} = \oint \frac{d\alpha_r}{\dot{\alpha}_r} = \oint \frac{d\alpha_r}{(2/M_\alpha)^{\frac{1}{2}} (E - s\alpha_r - m^2 \hbar^2 / 2M_\alpha \alpha_r^2)^{\frac{1}{2}}}$$

$$\doteq (8M_\alpha E / s^2)^{\frac{1}{2}}.$$

Inserting in the expression for the transition probability the value

$$\alpha_{\min} \doteq m\hbar / (2M_\alpha E)^{\frac{1}{2}},$$

and

$$\dot{\alpha} = (2E/M_\alpha)^{\frac{1}{2}},$$

and dividing by the period, we find for the chance per second of a jump:

$$A = (E/\hbar) (\hbar s / 2^{\frac{1}{2}} E^{\frac{1}{2}} M_\alpha^{\frac{1}{2}}) \exp(-\pi m^2 \hbar s / 2^{\frac{1}{2}} E^{\frac{1}{2}} M_\alpha^{\frac{1}{2}}),$$

$$A \doteq (E/\hbar) (\beta/2) \exp(-\pi \beta m^2 / 2).$$

As an example, consider a slope of the cone equal to 10 Mev per unit in the magnitude,  $\alpha$ , of ellipsoidal deformations. The kinetic energy is

$$\frac{1}{2} M_\alpha \dot{\alpha}^2 = \frac{1}{2} \rho (4\pi R_0^3 / 3) (3R_0^2 \dot{\alpha}^2 / 10),$$

so that for the case of  $\text{U}^{236}$  the effective "mass" is

$$M_\alpha = 236M (3r_0^2 / 10) (236)^{\frac{1}{2}}.$$

Finally, let the energy  $E$  available for oscillation about the vertex of the cone be 4 Mev. Then the dimensionless quantity  $\beta$ —whose reciprocal is related to the number of states bound in the cone with energy less than  $E$ —has the value

$$\beta = 10 \text{ Mev} (\hbar^2 / 0.6 M r_0^2)^{\frac{1}{2}} / (236)^{\frac{1}{2}} (4 \text{ Mev})^{\frac{1}{2}}$$

$$= 0.0781.$$

The probability for a radiationless jump from a state bound in the upper cone with  $m=1$  to the lower state is

$$A = (4 \text{ Mev} / 0.66 \times 10^{-21} \text{ Mev sec}) 0.039 \exp(-0.123)$$

$$= 2.1 \times 10^{20} \text{ sec}^{-1},$$

corresponding to a level width  $A\hbar$  of 0.14 Mev.

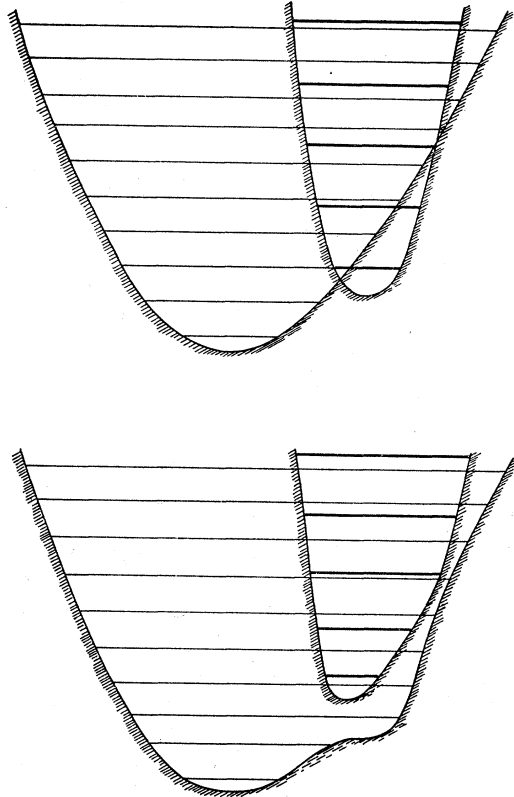


FIG. 37. One-dimensional example of influence of slip-over effect upon energy level pattern.

We shall describe the slippage phenomenon in terms of displacement of stationary energy values rather than in terms of transition probabilities. The latter way of speaking is the more natural in the idealized collective model where these transition probabilities are relatively small. The energy level description is unworkable in practice when the number of ways of dividing the energy between oscillation and nucleonic excitation is very great. In contrast, the figure shows an idealized case—not expected to occur in actual nuclei, but illustrative of the general principles involved—where only two nucleonic states,  $a$  and  $b$ , come into play. The probability amplitude function has two components,  $\psi_a(\alpha)$  and  $\psi_b(\alpha)$ , whose absolute squares give the probabilities for the system to be in one or the other nucleonic states with a wall deformation,  $\alpha$ . We write the Schroedinger equation in the form

$$i\hbar \partial \psi_a / \partial t = -(\hbar^2 / 2M_\alpha) \partial^2 \psi_a / \partial \alpha^2 + V_a(\alpha) \psi_a + H_{ab} \psi_b,$$

$$i\hbar \partial \psi_b / \partial t = -(\hbar^2 / 2M_\alpha) \partial^2 \psi_b / \partial \alpha^2 + V_b(\alpha) \psi_b + H_{ba} \psi_a.$$

In the extreme case of very small coupling  $H_{ab}$ , the problem separates into two eigenvalue equations which will possess characteristic energy values as shown in the upper part of the diagram. In the opposite extreme case of large coupling, the simplest description is obtained when the characteristic level spacings are small

compared to the coupling constant  $H_{ab}$ ; in other words, when the mass  $M_\alpha$  is very large. Then it is reasonable to consider the eigenvalue equations,

$$\begin{aligned} E\psi_a &= V_a\psi_a + H_{ab}\psi_b, \\ E\psi_b &= V_b\psi_b + H_{ba}\psi_a. \end{aligned}$$

The two energy values  $E_1(\alpha)$  and  $E_2(\alpha)$  obtained from these equations give two new potential energy curves with respect to which the oscillation now takes place—at least in so far as those potential curves can be considered to be felt out by a particle of very large mass. In the case of intermediate coupling the ordering of the energy levels will be very complicated. However, in all three cases the total number of energy levels less than any given large energy  $E$  will have the same rate of increase with  $E$ .

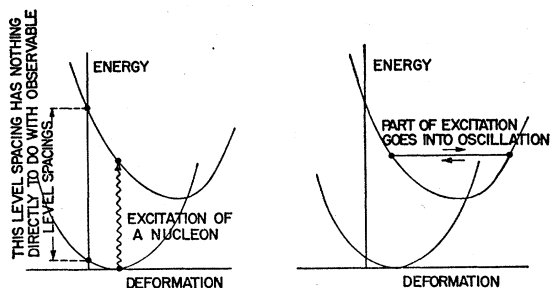


FIG. 38. Franck-Condon principle for nuclear transitions.

In the collective-model idealization of the nucleus as in a molecule, excitation processes (very high energy impact; photoabsorption) which raise a single particle (nucleon; electron) to an excited state can be thought of in first approximation as taking place in such a way that the heavy part of the system (collective oscillator; atomic nuclei) will keep position and velocity coordinates unchanged. The individual particle therefore may be considered to jump from one potential surface to the other at a fixed value of the deformation coordinates. The principle of Franck and Condon indicates that the energy absorbed in the primary act bears a simple relation neither to the energy difference between the minima of the two curves, nor to the separation of the curves for zero deformation, nor to the amount of the absorbed energy which will be available afterwards for vibration (right-hand portion of diagram). In the nuclear case subsequent slippage down from one potential energy surface to another will of course occur after repeated oscillations, and the distribution of energy over the system will finally be randomized, granted time before radiation carries the energy away. From the diagram it is seen that the observed spacing of energy levels may be expected to depend upon the ellipticity of the configuration in which the spacing is measured. It appears reasonable to attribute to this circumstance an appreciable part of the observed anomalies in the spacing of the levels of Pb and Bi [J. A. Harvey, Phys. Rev. 79, 241 (1950)].

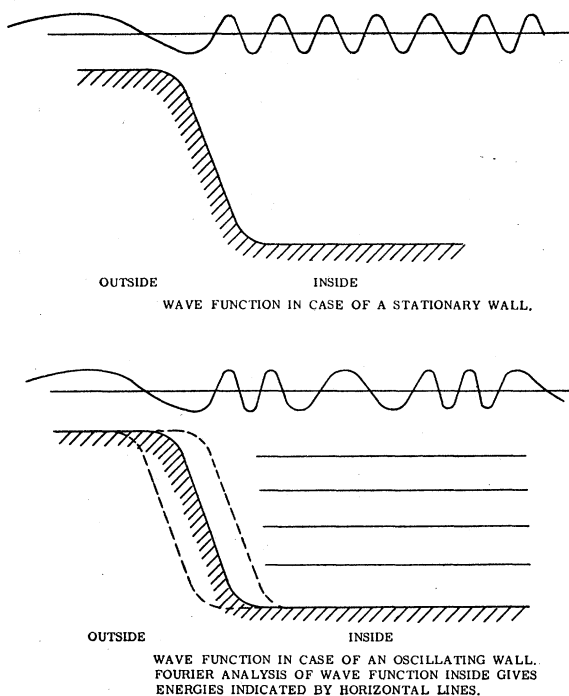


FIG. 39. Phase modulation of nucleon wave function at nuclear surface.

The Doppler change of wavelength of the nucleonic wave function due to wall motion is the elementary mechanism of exchange of energy between nucleonic excitation and collective oscillation. Of this energy exchange *no such analysis as that illustrated in the diagram is permissible*. To observe the phase modulation of the immigrant wave requires freedom from subsequent reflections at the walls. Only then would space and time enough be available to analyze the frequency spectrum with sufficient precision to show up side bands corresponding to exchange of one or more vibrational quanta with the wall. For this purpose the time would have to exceed several periods of collective oscillation. But in fact the time for one traversal of the nucleus is many times *shorter* than the vibrational period. Quite the opposite of a frequency analysis, the proper way to describe the exchange of energy between particle and wall is as adiabatic readjustment of the proper function of the particle to the configuration of the wall. As the boundary changes, the wave function and energy alter, and the energy change can quite properly be attributed to Doppler effect at a moving wall. The important point is that the particle has no way to remember that the wall motion is *periodic*. Thus follows the inappropriateness of a description in terms of phase modulation.

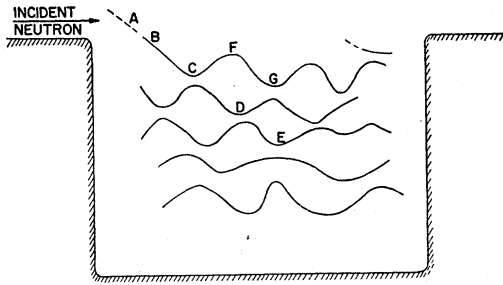


FIG. 40. Schematic representation of neutron capture on the collective model.

The hatched-in potential trough gives an impression of the relative location of the levels of zero kinetic energy inside and outside and has otherwise nothing directly to do with the main part of the diagram: A plot of potential energy surfaces for the compound nucleus as a function of a typical one of the many deformation parameters. The neutron enters and forms a virtual state of the compound nucleus at A. If the oscillational coordinate passes B before the neutron has emerged from the virtual state, then this particle is trapped, at least temporarily. The representative point of the system can then oscillate in principle over the potential energy curve ABCFG, etc. However, the excitation is so high that there can be no well-defined partition of energy between vibration and nucleonic excitation. Otherwise stated, the system jumps from one potential curve to another with a frequency large compared to what would otherwise be the natural oscillation period. Consequently the neutron very rapidly gives up its energy to the rest of the system. The mechanism of transfer is idealized in this discussion as acting entirely through the wall. This wall effect can of course be visualized in terms of Doppler effect, as illustrated in the previous figure.

The neutron is caught, so to speak, because the nodes in its wave function were so oriented relative to the wall motion that the particle lost energy by reflections from the retreating boundaries.

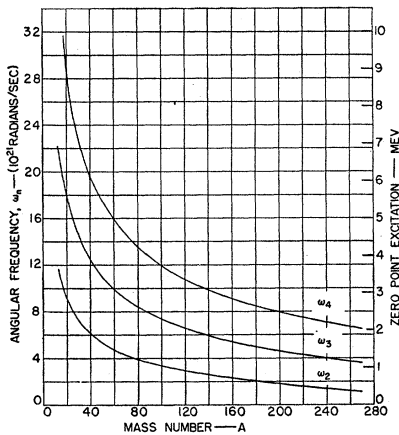


FIG. 41. Nuclear oscillational surface frequencies versus mass number.

Plotted as a function of mass number are the nuclear surface oscillational frequencies,  $\omega_n = 2\pi\nu_n$ , and the associated zero-point excitation values. The values shown follow from the classical analysis of Fig. 1. At small mass numbers the excitation energies rise sharply, but the concept of surface motion loses its validity for low mass numbers. As noted in Fig. 1, the higher the nuclear mass number, the higher the maximum mode of oscillation which may be reasonably defined, but even at mass 240 the highest order acceptable is less than 10.

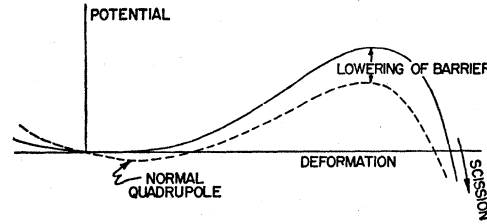


FIG. 42. Fission barrier shift associated with the ground-state quadrupole moment.

This is a schematic representation of the difference in fission threshold between the liquid drop picture and the collective model. The same individualities in potential energy surfaces which are responsible for quadrupole moments also bring about anomalies in fission barrier heights. The order of magnitude of these anomalies can be estimated by comparing the liquid drop potential curve,  $V = V(\alpha)$ , which near the minimum varies about as  $50 \text{ Mev } \alpha^2$ , and at the maximum has a height of the order of  $5 \text{ Mev}$  at a value of  $\alpha$  of the order of 0.7, with another potential curve,

$$V^* = V(\alpha) - c\alpha,$$

where the constant  $c$  is a crude measure of the quadrupole producing force. The minimum of  $V^*$  will lie near  $\alpha_0 = c/100 \text{ Mev}$ , and the shift in the height of the maximum will be of the order

$$\delta E_f \sim c\alpha_{\text{max}} \sim 100 \text{ Mev } \alpha_0 \alpha_{\text{max}} \sim 2 \text{ Mev}$$

for typical quadrupole moments,  $\alpha_0 \sim 0.03$ . Of course the above description is highly schematized; the actual potential energy surface will run much less smoothly as a function of deformation.

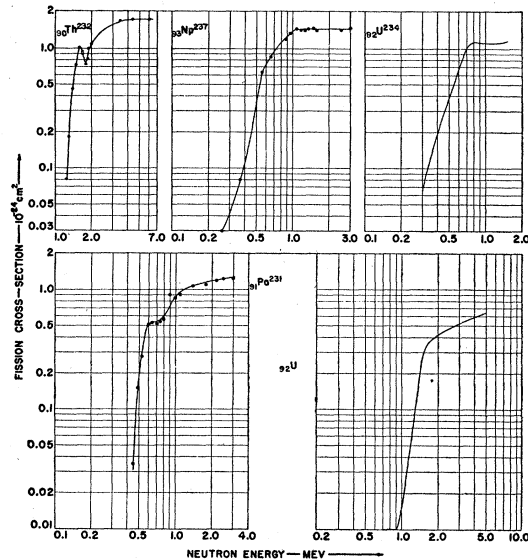


FIG. 43. Neutron fission cross section as a function of neutron energy for five fissile elements. All data are taken from the compilation of reference 29.

The features common to these five cross-sectional curves are in line with the discussion of reference 5. At low energies the probability of fission is inappreciable, until the total excitation of the compound nucleus (neutron binding plus kinetic energy of external neutron motion) approaches the height of the potential barrier to fission, as shown in Figs. 3 and 4. For excitations somewhat less than this value the cross sections show the precipitous rise characteristic of barrier penetration (Fig. 44). Beyond this excitation the cross section increases more slowly, being governed primarily by the competition with neutron emission, as alternative mode for the compound nucleus decay. For excitations several Mev in excess of the barrier height (but less than the binding energy of two

neutrons) the variation of fission cross section with energy is expected to be smooth. The fission cross section may be expected to increase substantially when the excitation becomes sufficiently high for fission still to occur after the compound system emits one or more neutrons [Bohr, reference 31].

A striking example of the possible effect of the internal state of the nucleus upon the fission probability is afforded by the observations of Street, Ghiorso, and Thompson [Phys. Rev. **84**, 135 (1952)] on the formation by neutron capture in  $\text{Am}^{241}$  of two isomers of  $\text{Am}^{242}$ , of which one decays into the other with a 16-hr half-life. They find that the ground-state form is susceptible to fission by thermal neutrons with a 6000 barn cross section, while the fission cross section is 2000 barns for the excited form. Whether this difference comes in the probability of neutron capture and emission, of de-excitation by radiation, or in the differing effects of the different internal states on the fission barrier (Figs. 6 and 42) is apparently an open question.

In studies of the photofission of thorium and uranium, G. C. Baldwin and G. S. Klaiber [Phys. Rev. **71**, 3 (1947)] found the cross sections to be peaked at 17 Mev with a 3-Mev half-width at half-maximum. This result is one of a large number of similar results, as noted by v. H. Steinwedel and J. H. D. Jensen [Z. Naturforsch. **5a**, 413 (1950)].

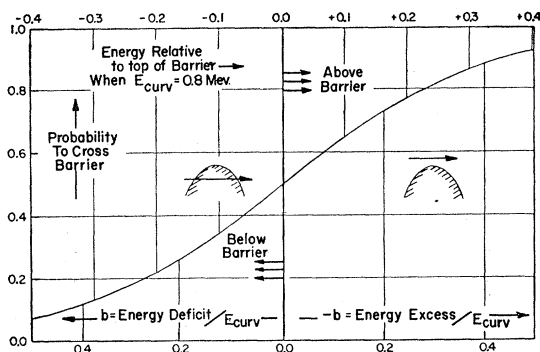


FIG. 44. Probability to cross fission barrier as a function of energy.

The probability to cross the fission barrier as a function of energy, is given by

$$P = 1/(1 + e^{2\pi b}).$$

Here  $b$  is the energy deficit relative to the top of the barrier, divided by a characteristic quantum energy,  $E_{\text{curv}}$ , which is fixed by the curvature of the top of the barrier and by the effective mass associated with the fission mode of deformation. To visualize the meaning of  $E_{\text{curv}}$ , imagine the sign of the potential energy to be reversed, so that the barrier peak becomes a trough. Then the system will behave like a harmonic oscillator in the neighborhood of the critical point, with a natural circular frequency,  $\omega_{\text{imag}}$ , and a characteristic quantum energy,  $\hbar\omega_{\text{imag}}$ . This latter quantity is by definition equal to  $E_{\text{curv}}$ . In a first approximation it is reasonable to take  $\hbar\omega_{\text{imag}}$  to be equal to the characteristic quantum energy,  $\hbar\omega_2$ , of the lowest mode of capillary oscillation of the system about its normal nearly spherical equilibrium form, for the following reason: The potential energy, expressed as a function of deformation, will have for leading terms in its expansion

$$V(\alpha) = A\alpha^2 - B\alpha^3.$$

But this function has at its maximum the same second derivative (except for sign) that it has at its minimum, and therefore the same frequency,  $\omega_{\text{imag}} = \omega_2$ . We conclude that for uranium, where  $\hbar\omega_2$  is estimated to be about 0.8 Mev, the characteristic curvature energy of the barrier will also be of the order of 1 Mev, thus leading to the energy scale shown in the diagram. Note that the probability for crossing the barrier is but 0.5 when the available energy first exceeds the critical energy, and only reaches a value close to unity at considerable distance above the barrier. This result is contrary to the predictions of the usual penetration

formula, which would have given

$$\begin{aligned} P &= \exp\left[-(2/\hbar) \int [2M_\alpha(E_{\text{top}} - \frac{1}{2}V''\alpha^2 - E_{\text{available}})]^{1/2} d\alpha\right] \\ &= \exp[-2\pi(E_{\text{top}} - E_{\text{available}})/\hbar\omega_{\text{imag}}] \\ &= \exp(-2\pi b). \end{aligned}$$

The more complete penetration formula is most easily justified by writing the wave equation for the fission mode in dimensionless variables:

$$d^2\psi/dx^2 + (x^2 - 2b)\psi = 0.$$

The solution we desire represents a wave running to the right on the right-hand side of the barrier, and on the left an incident wave and a reflected wave. In terms of the parabolic cylinder function,

$$\begin{aligned} \psi &= D_{-\frac{1}{2}-ib}[(1-i)x] \\ &= [\Gamma(\frac{1}{2}+ib)]^{-1} \int_0^\infty dt \exp[ix^2/2 - (1-i)xt - t^2/2 - (\frac{1}{2}-ib) \ln t], \end{aligned}$$

with the asymptotic behavior for large positive  $x$ :

$$\approx 2^{-\frac{1}{2}} x^{-\frac{1}{2}} \exp[ix^2/2 - (ib/2) \ln 2x^2 + i\pi/8 - \pi b/4],$$

and for large negative  $x$ :

$$\begin{aligned} \approx 2^{-\frac{1}{2}} |x|^{-\frac{1}{2}} \exp[ix^2/2 - (ib/2) \ln 2x^2 \\ - 3i\pi/8 + 3\pi b/4] \quad (\text{reflected wave}) \\ + (2\pi)^{\frac{1}{2}} [\Gamma(\frac{1}{2}+ib)]^{-1} 2^{-\frac{1}{2}} |x|^{-\frac{1}{2}} \exp[-ix^2/2 \\ + (ib/2) \ln 2x^2 + i\pi/8 + \pi b/4] \quad (\text{incident wave}). \end{aligned}$$

Comparison of strengths of incident and transmitted waves gives the cited penetration formula. It is valid so long as the relevant portion of the potential curve—when plotted against a dynamically uniformized deformation variable—is close to an inverted harmonic oscillator curve.

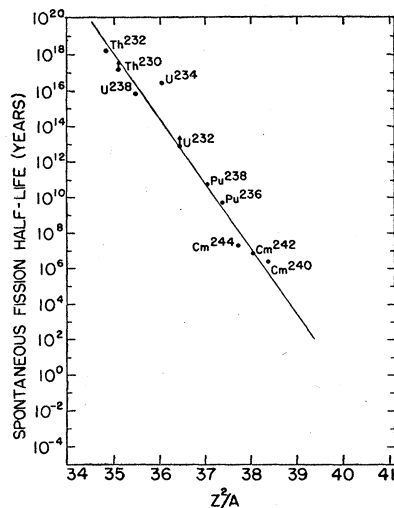


FIG. 45. Relation of spontaneous fission half-life to  $(Z^2/A)$ .

By this plot of spontaneous fission half-life against  $(Z^2/A)$  G. T. Seaborg [Phys. Rev. **85**, 157 (1952)] has demonstrated the neat connection between spontaneous fission rates and the characteristic parameter (Fig. 2, and Table I) to measure fissionability in the liquid drop model. The linear relation shown holds not only for the labeled nuclei but also for the nucleus cosmium (Figs. 2, 51) for which  $(Z^2/A) \approx 47$  and which undergoes spontaneous fission in a time of the order of the period of the lowest order vibration for such a nuclide as  $\text{U}^{238}$  (Fig. 1). Small deviations from the linear relation appear, in line with the expectations (Figs. 6, 26, 42) on the variation of ground-state quadrupole moments, and consequent effects on the fission barrier (Fig. 3). The analogy with the case of alpha-decay (Fig. 30) is evident. Not included on the plot is  $\text{U}^{235}$ , which undergoes spontaneous fission at a rate lower than that of  $\text{U}^{238}$ , despite the higher  $Z^2/A$  [reference 31a].

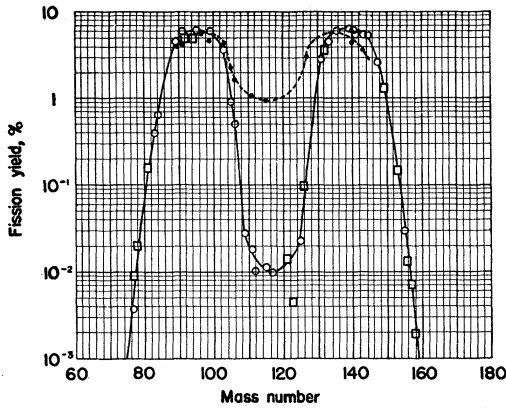


FIG. 46.  $U^{235}$  fragment mass distribution for thermal and 14-Mev neutrons.

Shown are the fragment mass distributions for  $U^{235}$  bombarded by thermal neutrons [Plutonium Project, Revs. Modern Phys. 18, 539 (1946)] and (by the solid points) with 14-Mev neutrons [R. W. Spence, Atomic Energy Commission Unclassified Document BNL-C-9, 1949 (unpublished), Brookhaven Chemistry Conference No. 3]. Evidence that the trend toward symmetrical fission with excitation is completed is afforded by the mass distributions of the heavy elements struck by very high energy particles [P. R. O'Connor and G. T. Seaborg, Phys. Rev. 74, 1259 (1948); R. H. Goeckermann and I. Perlman, Phys. Rev. 73, 1127 (1948)].

A simple hydrodynamic explanation of the mass asymmetry, and its variation with energy, is proposed in Figs. 50 and 51.

Specially interesting is the observation (reference 38) that in  $Cm^{242}$ , with its half-life for spontaneous fission of  $7.2 \times 10^6$  years, spontaneous fission events are sufficiently frequent to enable a study of the distribution in kinetic energy of the fragments. The pattern obtained indicates the same sort of mass distribution as is found for thermal neutron induced fission.

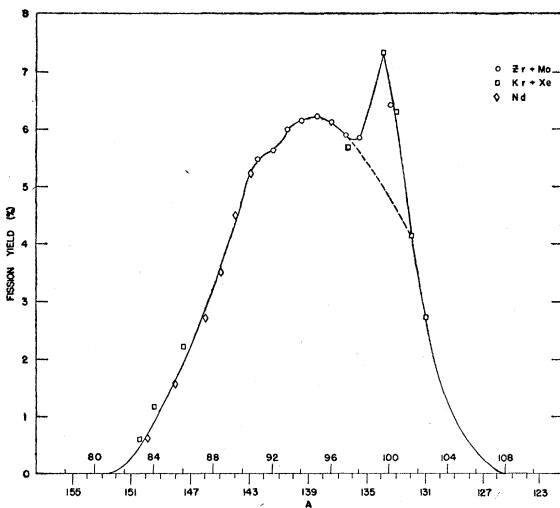


FIG. 47. Fine structure in fission mass yield.

This compilation by Glendenin, Steinberg, Ingraham, and Hess [Phys. Rev. 84, 860 (1951)] of spectrometric measurements on the fission mass yield, plotted with the heavy and light fragment yields folded over one another to produce a common curve, demonstrates a sharp deviation in a limited mass region of the yields from the smooth variation known from earlier work [Plutonium Project, Revs. Modern Phys. 18, 539 (1946)]. The

masses involved in this deviation are consistent with the hypothesis that it follows from the effects of nuclear shells on fission, contrary to the dominant asymmetry of the smooth curve itself.

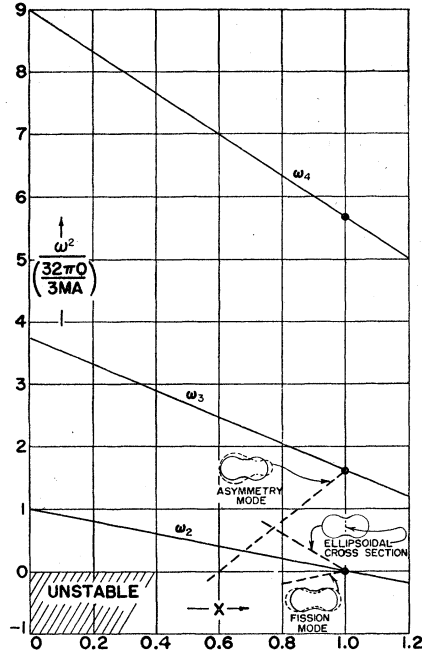


FIG. 48. Characteristic circular frequencies,  $\omega$ , of the lowest modes of oscillation of an incompressible uniformly charged liquid droplet of mass  $AM$  and surface tension  $O$  as a function of the fission instability parameter  $x$  for the spherical form (smooth lines) and for the symmetrical critical form of unstable equilibrium (dashed lines); estimates obtained by calculating limiting slope in neighborhood of  $x=1$ ; i.e., for nuclei differing from the spherical by only a very slight ellipsoidal deformation).

The five independent degenerate modes of vibration of the sphere of order  $n=2$  are describable in terms of radial extensions proportional to the five harmonics  $P_2(\cos\theta)$ ,  $P_2^{(1)}(\cos\theta)[\cos\phi$  or  $\sin\phi]$ ,  $P_2^{(2)}(\cos\theta)[\cos 2\phi$  or  $\sin 2\phi]$ , but these vibrations can also be visualized in terms of revolution of a hump of material over the surface of the sphere (three degrees of freedom) and two types of pure vibration. It is assumed here that the system has no angular momentum, although allowance for rotation would produce a number of complicated and interesting subdivisions of the curves shown here. The two vibration frequencies are distinct for the critical form of unstable equilibrium. The first mode of deviation from the saddle point moves in the direction of decreasing potential energy, either an extension leading to fission or a contraction towards the normal spherical form. The second moves uphill from the saddle point. In it the cross sections of the figure cut normal to the symmetry axis undergo ellipsoidal oscillations about the normal circular form without the length of the dumbbell undergoing change.

Of the subcomponents of the vibration of third order we consider for the forms of unstable equilibrium only that particular one which is of lowest frequency, is axially symmetric, and is the better described by the harmonic  $P_3(\cos\theta)$  the more closely  $x$  approaches 1. This vibration represents a coursing of fluid to and fro through the neck of the dumbbell—an asymmetry oscillation. Its frequency becomes the less the smaller is  $x$ , and vanishes for some value of  $x=x_{crit}$  not yet known, perhaps near  $x=0.65$ . For lower values of  $x$  the symmetric saddle point configuration still exists, but two new and unsymmetric saddle point configurations come into existence which are lower in energy. If  $x$  for uranium is significantly greater than  $x_{crit}$ , as may well be the case, then the asymmetric saddle points should neither exist nor have anything to do with the observed asymmetry of fission for uranium.

W. J. Swiatecki [Phys. Rev. **83**, 178 (1951)] in a brief note has given reasons for believing that the compressibility and polarizability of nuclear matter will favor the development of the asymmetric saddle points; i.e., depress the lowest component of  $\omega_3$ , in the present manner of describing the situation. However, it is not clear that this interesting effect is great enough to make the saddle point of uranium asymmetric.

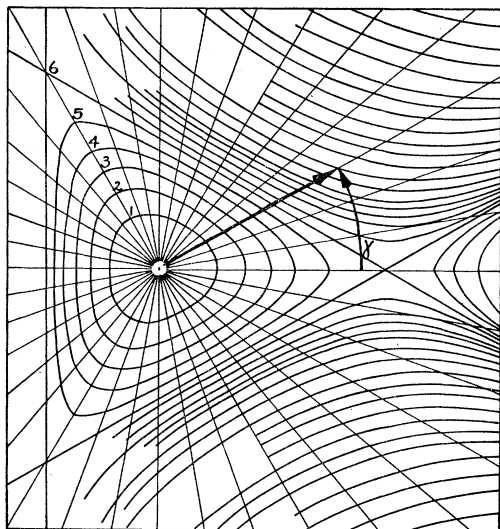


FIG. 49. Contour map of barrier against fission in the idealized limit of a fission criticality parameter close to  $x^* = 1$ .

Only a small deformation is required to carry the system to the saddle point for passage over the barrier. The only deformations considered in the diagram are of ellipsoidal character, as there is no instability in distortions described by spherical harmonics of higher order. The ellipsoidal deformations are measured in terms of polar variables in the diagram: a "deformation magnitude"  $\alpha$  (radius) and a "shape parameter"  $\gamma$  (angle), as defined in Fig. 13. There are three saddle points in the diagram because a prolate extension along any one of the three principal axes of the ellipsoid will result in fission. The present idealized picture is based entirely on the simple liquid drop model. No account is taken of any intrinsic quadrupole moment nor of any angular momentum of the nucleus. The deformation energy in the lowest relevant order of approximation is

$$V(\alpha, \gamma) = 4\pi R_0^2 O \left\{ \frac{2(1-x-z)}{5} \alpha^2 - \frac{[(12x+20z)/105] \alpha^3 \cos 3\gamma}{B} \right\} \\ = B \left[ \frac{u^2}{2} - \frac{u^3}{18} \cos 3\gamma \right] = B f(u, \gamma).$$

Here  $4\pi R_0^2 O = 14 \text{ Mev } A^{2/3}$  is the normal surface tension energy and  $x$  and  $z$  the parameters defined earlier, whose sum,  $x^*$ , is the relevant criticality parameter. In the alternative way of writing deformation energy on the second line,  $B$  is a constant with the units of energy, in terms of which the height of the top of the barrier is 6. The contour diagram gives the dimensionless quantity  $f = V/B$  as a function of  $\gamma$  and the multiple,  $u$ , of  $\alpha$ :

$$u = (18x + 30z)\alpha / 7(1 - x - z).$$

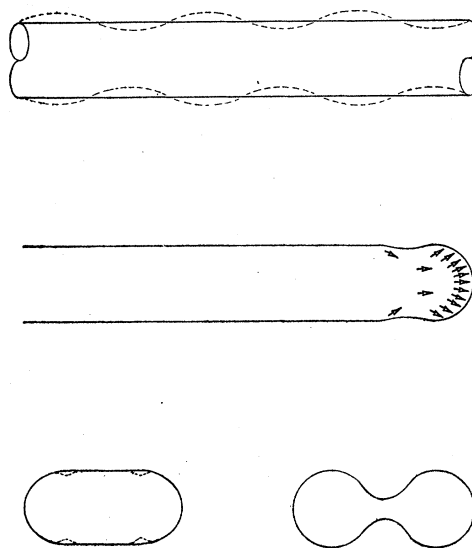


FIG. 50. A qualitative classical hydrodynamical interpretation of the asymmetry of nuclear fission.

The critical form of unstable equilibrium for a nucleus in the vicinity of uranium is so much like an elongated cylinder (Fig. 2) that we are invited to consider the stability of a long jet of incompressible uniformly electrified fluid endowed with a surface tension. Were the charge density zero, the jet would be unstable against small disturbances with wavelength greater than the jet's circumference, as is well known. Such disturbances are the first step in reassembly of the fluid into separated spheres of the same mass but smaller surface. The size of the eventual spheres is the greater the longer the wavelength. The presence of even a small volume electrification makes reassembly of the fluid into very large spheres energetically unfavorable. Consequently, the charge stabilizes the jet against disturbances of long wavelength, just as the surface tension works against deformations of short wavelength. The intermediate zone of wave numbers,  $k$ , of instability becomes the narrower the larger the charge density. Total stability occurs when

$$y = \frac{2(\text{charge per unit length})^2}{\pi(\text{radius})(\text{surface tension})} \geq y_{\text{crit}} \doteq 1.125.$$

This condition is satisfied for  $\text{U}^{235}$  by the critical Metropolis-Frankel forms for the fissionability parameter  $x = 4\pi R_0^3 \rho_e^2 / 30O = 0.74$ . The radius  $R$  of the cylindrical part of the figure is  $0.64R_0$ ; and

$$y = 2\pi R^3 \rho_e^2 / O = 2\pi \times 0.74 \times (30/4\pi)(R/R_0)^3 = 2.92.$$

How can a repulsive force produce such stability? Only by virtue of the ends of the cylinder being at infinity. Consider instead a cylinder of finite length. The capillary force will round off the ends, but be unable to withstand the repulsion of the long column of electric charge. A sizeable drop will break off the end—the elementary act of fission, and of a fission which is very asymmetric indeed. How asymmetric? Let  $L$  represent the distance from the end at which the cylinder starts to neck in, and let  $\epsilon$  represent the diminution in radius at this point. Out of the neck into the incipient drop has been squeezed a volume of fluid of the order

$\epsilon 2\pi RL$ , thus carrying the drop forward and diminishing the electric energy of the system by an amount  $\sim 2\pi^2\epsilon L^2 R^2 \rho_e^2$ , which goes into kinetic energy  $\sim \rho_m (\dot{z}^2 L^2 / R^2) \pi R^2 L$ . Consequently,  $\epsilon/R$ , the fractional necking off, goes in the beginning as  $(t/t_{crit})^2$ , where

$$t_{crit} \sim (L\rho_m/R\rho_e^2)^{1/2}.$$

The shortest growth constant and fastest necking-in is found for a neck length  $L$  of the same order as the radius, for the character of the expression for  $t_{crit}$  changes for smaller  $L$ . We conclude that successive fragments from this machine-gun type of fission will all have roughly the same size.

The following picture suggests itself for the division of a nucleus like  $U^{236}$ , when the available excitation is only little in excess of the threshold requirement. On arrival at the fission barrier the system has so little energy of movement that the nucleus remains for an appreciable time in a form not very different from the elongated shape of unstable equilibrium. This configuration resembles that of a cylinder of electrified fluid. In a crude approximation we may say that, in so far as the behavior of one end of the cylinder is concerned, the other end might as well be indefinitely far away. At each end we will expect the machine-gun type of fission to start. At which end necking-in first starts will be an accident. Once started at one end, however, this type of deformation will grow so rapidly that it will ordinarily soon get far ahead of anything that is happening at the other end, and a fragment will come off with length roughly comparable to its diameter ("light fission fragment").

Moreover, the separation of the two ends is really not large. Between them there is a significant interaction. The start of necking-in near one end will increase the curvature and hence the tightness of the surface near the other end. The effect will inhibit the necking-in which would otherwise have started near the other end, but a little later. Thus there comes about a division into a large and a small fragment. This suggested mechanism for the origin of fission asymmetry is a straightforward application of the most elementary notions of surface tension, electrostatics, and hydrodynamics.

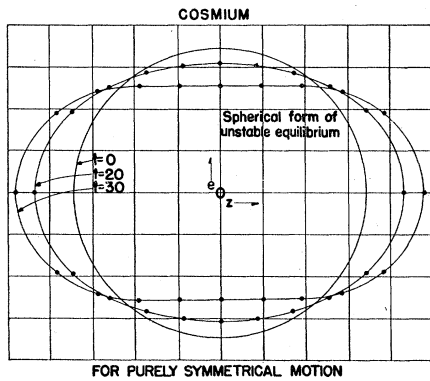
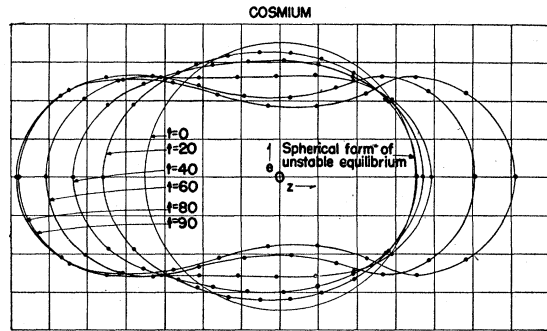
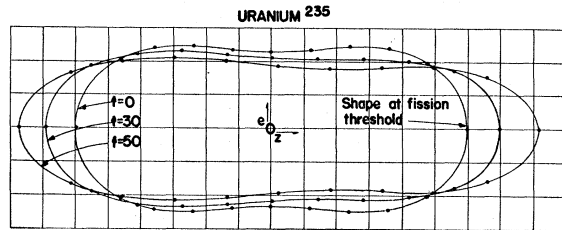


FIG. 51(a)



INITIAL ENERGIES; 2.5 Mev IN LOWEST ORDER SYMMETRICAL MODE, 1.3 Mev IN LOWEST ORDER ASYMMETRICAL MODE.

(b)



INITIAL ENERGIES; 2.5 Mev IN LOWEST ORDER SYMMETRICAL MODE, 1.3 Mev IN LOWEST ORDER ASYMMETRICAL MODE.

(c)

FIG. 51. Results of dynamical analysis of nuclear fission carried out [D. L. Hill, Phys. Rev. 78, 330 (1950); 79, 197 (1950); Ph.D. dissertation, Princeton University, Princeton, New Jersey (unpublished)] on the basis of simple liquid drop model.

These International Business Machine Corporation—endowed electronic computations started with a configuration near the point of unstable equilibrium and followed out the motion by way of the classical hydrodynamic equations for an incompressible fluid with surface tension and uniform volume density of electrification. From the preceding figure the working hypothesis suggests itself that inevitable small asymmetries in the form of the nucleus in the transition state become magnified in the subsequent course of the motion, and lead to a necking-off of the elongated figure near one end or the other in the great majority of the cases. The hydrodynamic phenomena were described by classical mechanics. However, the size and origin of the small initial asymmetries were considered to be connected with the quantal zero-point amplitudes of the various modes of capillary oscillation.

With increasing excitation of the compound nucleus, there will be an increase in the irregularities in the nuclear surface at the moment of passage over the fission barrier, over and above the effect of the zero-point oscillations. These irregularities will increasingly affect the location of the point at which necking-in commences. A sufficiently great displacement of the normal point of necking-in will lead to symmetric fission. The relative probability of symmetric fission will therefore be expected to rise with

increasing excitation energy. Two cases were considered: "cosmium," that unrealizable nucleus for which the fission criticality parameter  $x=(Z^2/A)/(Z^2/A)_{\text{crit}}=1$ ; and a droplet for which  $x=0.74$ , estimated to come close to simulating the case of  $U^{235}$ . Axial symmetry was assumed in all the calculations. Cosmium was started off in the first calculation with a very small deformation of the second order, which remained symmetric as it grew ( $t=20$  signifies a time of  $20 \times 6.66 \times 10^{-23}$  sec). In the second calculation on cosmium a deformation of order three was superposed on the symmetric deformation, with such a magnitude as to correspond to the zero-point energy estimated for the asymmetric mode. In this case the small initial asymmetry multiplied itself in the course of time in such a way as to suggest an eventual division into two fragments of rather different size. This growth of asymmetry arises from the dynamics of the fission process. In this case there cannot be any question of asymmetry in the saddle point configuration, for that is the spherical form itself. In the third case,  $x=0.74$ , a small initial asymmetry superposed on the initial symmetrical Metropolis-Frankel saddle point configuration again multiplies itself in such a way as to appear to favor division into quite unequal parts. The calculations were broken off in all cases well before neck-off because the mesh was not fine enough to treat the narrowing part of the neck accurately. The results cannot be considered to prove, but are at least consistent with, the view that fission asymmetry is a classical hydrodynamic effect.

$\nabla^2\phi=0$ ,  $u_n=-\partial\phi/\partial n$  gives the normal component of the velocity of the fluid surface, and the time rate of change of the velocity potential is

$$\partial\phi/\partial t = \frac{1}{2}(\text{grad}\phi)^2 + V + P = H.$$

The quantity  $H - \frac{1}{2}(\text{grad}\phi)^2$  is the acceleration potential;  $P$  is the pressure divided by the density, taking values at the surface determined only by the local curvature  $\kappa$ ,

$$P_{\text{surf}} = (O\kappa/\rho_m) = (O/\rho_m) \left\{ \rho^{-1} [1 + (d\rho/dz)^2]^{-\frac{1}{2}} - (d^2\rho/dz^2) [1 + (d\rho/dz)^2]^{-\frac{3}{2}} \right\},$$

where  $O$  is specific surface energy and  $\rho_m$  is mass density; and  $V$  is the electrical potential energy of a unit mass element, expressible in cylindrical polar coordinates  $z$  and  $\rho$  as

$$V_1 = (\rho_e^2/\rho_m) \int d\tau_2/r_{12} = 2(\rho_e^2/\rho_m) \int \left\{ dz_2 \rho_2 \frac{[\rho_2 + \rho_1 + (z_1 - z_2)d\rho_2/dz]K - 2\rho_1 D}{[(\rho_1 + \rho_2)^2 + (z_1 - z_2)^2]^{\frac{1}{2}}} \right\},$$

where  $K(k)$  and  $D(k) = [K(k) - E(k)]/k^2$  are defined in terms of complete elliptic integrals of the argument  $k$ ,

$$k^2 = 4\rho_1\rho_2/[(\rho_1 + \rho_2)^2 + (z_1 - z_2)^2],$$

and  $\rho_e$  is the electrical charge density. The actual system with its infinitude of degrees of freedom is replaced by a system with a limited number of degrees of freedom: the location of eleven tracer points which are considered to define the surface. The locations of the two points at the two poles of the figure are specified by coordinates  $z_0$  and  $z_{10}$ . The nine other points have  $z$  coordinates,  $z_j$ , equally spaced between  $z_0$  and  $z_{10}$ . Eleven independent position coordinates  $z_0, \rho_1, \rho_2, \dots, \rho_9, z_{10}$ , and eleven corresponding velocity coordinates thus give the state of the system at one time. At the next instant the new positions follow purely kinematically from the old positions and velocities; while the new velocities follow equally simply as soon as the old accelerations have been found from the acceleration potential:

$$d\mathbf{u}/dt = -\text{grad}(H - u^2/2).$$

The quantity  $H$  has zero Laplacian in the interior, and on the surface a value which is known from the old state of the system. In the calculations the term  $u^2/2$  is neglected, both when it appears in the boundary conditions for  $H$  and when it is subsequently subtracted from  $H$ , as the 170-Mev kinetic energy of fission is small compared with perhaps 540-Mev surface energy and 780-Mev electrostatic energy of the relevant nuclei. In the computations  $H$  was represented as a sum,

$$H(z, \rho, t) = \sum_{n=1}^8 b_n(t) B_n(z, \rho),$$

of eight solid harmonics, with the  $b_n$  chosen at the time interval in question so as to minimize the departure of  $H$  from its proper boundary value:

$$\int (H - V - P)_{\text{surface}} dS = \text{minimum}.$$

From this requirement follows an  $8 \times 8$  system of linear equations for the coefficients  $b_n(t)$ :

$$\sum M_{jn} b_n = f_j,$$

where

$$M_{jn} = \int B_j B_n dS \quad \text{and} \quad f_j = \int B_j (V + P) dS$$

can be found from the state of the system at the old times. Thus the whole cycle of calculations is advanced to the new time.

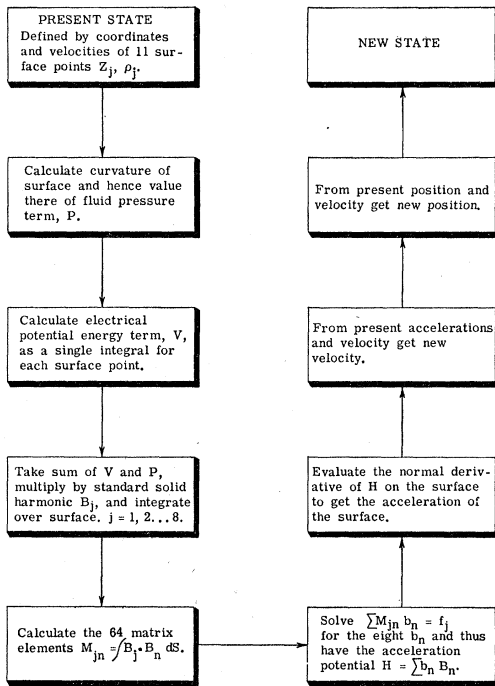


FIG. 52. Schematic flow sheet of hydrodynamic calculations illustrated in the preceding figure.

The motion is taken to be irrotational flow of incompressible fluid, so that the velocity can be expressed as  $\mathbf{u} = -\text{grad}\phi$ , where

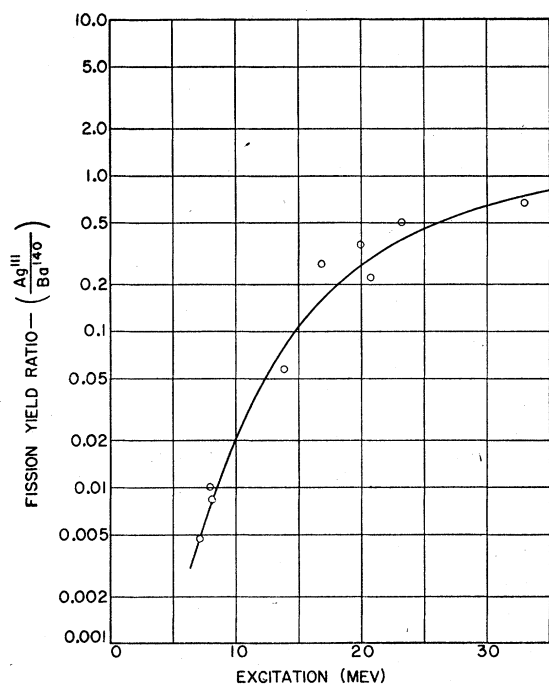


FIG. 53. Fission asymmetry as function of initial excitation.

The fission yield of  $\text{Ag}^{111}$  relative to the yield of  $\text{Ba}^{140}$  provides a measure of the asymmetry of the mass division, for experience indicates (Fig. 46) that the entire yield curve varies in an approximately uniform way with excitation energy. The yields here plotted as a function of the excitation in the original nucleus are obtained (references 36 and 37) from the bombardment of several different fissile elements by several different projectiles. Moreover, for the high excitations indicated, the excited compound nucleus will usually emit several neutrons before splitting. Nevertheless, we note that the mass division which finally occurs shows an over-all trend toward increasing symmetry with increasing excitation of the initial nucleus.

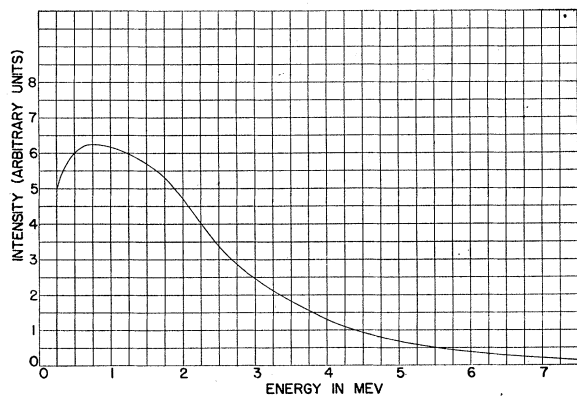


FIG. 54.  $\text{U}^{235}$  fission neutron spectrum.

Recently published papers [Bonner, Ferrell, and Rinehart, Phys. Rev. 87, 1032 (1952); D. L. Hill, Phys. Rev. 87, 1034 (1952); B. E. Watt, Phys. Rev. 87, 1037 (1952)] dealing with the low, medium, and high energy neutrons emitted in the fission of  $\text{U}^{235}$  enable us to draw qualitative conclusions on the manner in which they are released. The three measurements fit nicely together to yield a total distribution-in-energy consistent with the hypothesis that the neutrons are emitted from the excited fragments with distributions-in-energy characteristic of nuclear evaporation [J. M. Blatt and V. F. Weisskopf, *Theoretical Nuclear Physics* (John

Wiley and Sons, Inc., New York, 1952), while the fragments are in rapid motion. The broad spread in excitation of the fission fragments gives a further spread in the number and energy of the neutrons emitted in different fission acts. Finally, the neutrons are emitted, in this hypothesis, at a spread of angles relative to the parent fragment motion which we know according to the work of Brunton, Hanna, and Thompson [Can. J. Research 28A, 190 (1950); 28A, 498 (1950)] to have a spread of kinetic energies of at least 20 Mev for a typical mass division. The resultant energy spectrum observed in the laboratory is thus averaged many times over different sorts of energy spreading effects.

The curve shown is taken from D. L. Hill [Phys. Rev. 87, 1034 (1952)], being deduced from the range spectrum of recoil protons detected with an assembly of proportional counters. The maximum near 0.8 Mev is corroborated by Bonner, Ferrell, and Rinehart [Phys. Rev. 87, 1032 (1952)]; the high energy side of the spectrum falls off exponentially with a 1.6-Mev relaxation energy, in agreement with Watt's result [Phys. Rev. 87, 1037 (1952)].

The fission neutron intensity observed is compatible with the announced value (U. S. Atomic Energy Commission release) of 2.5 neutrons per thermal neutron induced fission of  $\text{U}^{235}$ .

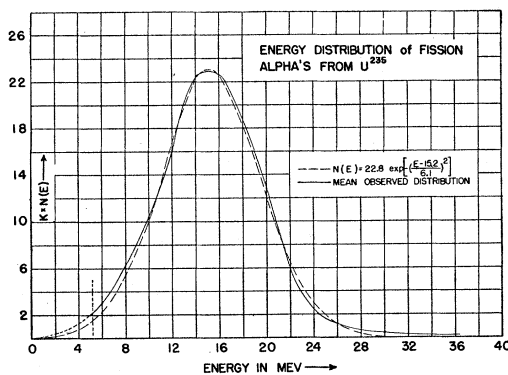


FIG. 55.  $\text{U}^{235}$   $\alpha$ -particle spectrum, coincident with fission.

Of the many different modes of ternary fission listed in Table III, by far the most intensively studied are the long-range alpha particles coincident with fission. Reproduced here is a measurement (reference 54) of the energy distribution of these particles. The close match of this distribution to a Gaussian curve over the high intensity region is indicated by the dashed line.

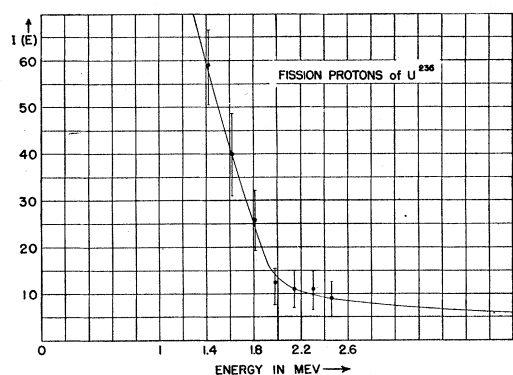


FIG. 56.  $\text{U}^{235}$  fission proton energy distribution.

This curve shows the energy distribution of the protons listed in Table III as being emitted in a rare mode of ternary fission. Although they are somewhat too numerous to be readily explained as arising by  $(n, p)$  or  $(\text{fragment}, p)$  reactions, the energy distribution indicates that they are not associated with the fission mechanism in a manner similar to the particles of the preceding figure. For particles which have penetrated through a potential barrier, one expects a peak at the right side of the graph rather than a monotonic fall. It is unreasonable to believe that these "fission" protons have anything directly to do with the act of fission.